Master's thesis

NTNU
Norwegian University of Science and Technology
Faculty of Engineering
Department of Civil and Environmental Engineering

Sabkeebar Ararsa Erko

Hydraulic model suitability for hydrodynamic analysis based on LiDAR data of steep rivers

Master's thesis in Hydropower Development

Supervisor: Professor Knut Alfredsen and Adina Moraru (PhD student)

August 2020

NTNU
Norwegian University of Science and Technology

Sabkeebar Ararsa Erko

Hydraulic model suitability for hydrodynamic analysis based on LiDAR data of steep rivers

Master's thesis in Hydropower Development
Supervisor: Professor Knut Alfredsen and Adina Moraru (PhD student)
August 2020

Norwegian University of Science and Technology
Faculty of Engineering
Department of Civil and Environmental Engineering

NTNU
Norwegian University of Science and Technology

DECLARATION OF AUTHORSHIP

I, Sabkeebar Ararsa Erko, declare that I am the author of the thesis entitled “Hydraulic model suitability for hydrodynamic analysis based on LiDAR data of steep rivers” that has been submitted to Norwegian University of Science and Technology (NTNU) on 11th of August 2020, in partial fulfillment of the requirements of M.Sc. degree in Hydropower Development.

I have clearly stated the work of any other authors, in accordance with the standard reference management.

ABSTRACT

A hydraulic model is an essential tool to estimate water depth, flow velocity, inundation extent, water surface elevation, and other hydraulic parameters. Different hydrodynamic models have been developed, and some of them have improved in efficiency and become more familiar. In recent decades, various studies have been done to improve the accuracy and reliability of flood mapping. However, the accuracy of the simulate results depends on many factors. For instance: the quality of the topographic data; the river gradient; the river reach length; the complexity of the topography; the consistency of the governing equation; and the numerical scheme can be influencing a selection of the appropriate model. Further, some models can carry out inundation extent estimation, others can execute water depth calculation accuracy, and some models can good perform in mountain rivers modeling.

In this study, two Norwegian rivers were selected to evaluate the performance of the HEC-RAS and TELEMAC-MASCARET models on a mild and a steep-sloped river. For the mild slope modeling, the LiDAR-based digital elevation model with high-resolution digital elevation was applied to simulate the Surna river hydraulics in HEC-RAS 2D and TELEMAC 2D models. The performance of both models was evaluated based on a standard deviation of residuals, particularly the root mean square error (RMSE), which simulated inundation extent was assessed against an observed inundation extent that provided by AHM from their original flight. In addition, the impact of the existence of islands and beds on the accuracy of hydrodynamic models was evaluated.

In regard to evaluating the model's performance on a steep river, digital elevation and digital surface models were applied in both models to examine their functionality and verify the suitability of a LiDAR-based digital surface model, which obtained from https://hoydedata.no/LaserInnsyn/, in hydrodynamic computation. Issues such as the application of finite element and finite volume methods in the TELEMAC-MASCARET simulation for the steep river were assessed.

In both case studies, a comparison of models was based on simulated water depth, velocity, simulation time, and ease of use in the set-up. The results show that both models are performed well with mild slope, and an application of the finite volume method in TELEMAC-2D modeling functioned well for the steep river.

AKNOWLEGDEMNT

In the very beginning, I am truly grateful to the Almighty God for making it all possible and for blessing me with another day of life.

My special gratitude goes to my supervisor Prof. Knut Alfredsen, (NTNU) for his guidance and great support in completing my thesis work.

I would like to thank my Co-supervisor Adina Moraru (PhD candidate), NTNU for her assistances and encouragement in completing my thesis.

My deepest thanks to Michal Pavlícek (PhD candidate), NTNU for his time and countless support with the TELEMAC-MASCARET model. I would like to also thank Ana Juarez for her time and assistance with HEC-RAS model.

My heartfelt acknowledgement to NTNU in cooperation with the Norwegian Agency for Development Cooperation's (NORAD) for the financial support during my master's study.

Warm gratitude to my relatives and friends for your support morally and encouragements all the time.

Table of Contents

1. INTRODUCTION ..... - 1 -

1.1 Problem Investigation ..... - 3 -

1.2 Objectives ..... - 4 -

1.3 Limitation ..... - 4 -

2. LITERATURE REVIEW ..... - 6 -

2.1 Overview of Flood Modelling Methods ..... - 6 -

2.1.1 Empirical Model ..... - 6 -

2.1.2 Hydrodynamic Models ..... - 6 -

2.1.2.1 One-Dimensional Hydrodynamic Models ..... - 7 -

2.1.2.2 Two-Dimensional Hydrodynamic Models ..... - 8 -

2.1.2.3 Three-Dimensional Hydrodynamic Models ..... - 9 -

2.2 Review of Recent Progress in Flood Modelling ..... - 10 -

2.3 Linking Flood Models and Geographical Information Systems; and the Importance of the Quality Topographic Data in Flood Modeling ..... - 12 -

2.3.1 Digital Terrain Model (DTM) ..... - 13 -

2.3.2 Digital Elevation Model (DEM) ..... - 14 -

2.3.3 Triangular Irregular Network (TIN) ..... - 14 -

2.3.4 Digital Surface Model (DSM) ..... - 14 -

3. THE SELECTION OF HEC-RAS 2D AND TELEMAC-2D AS MODELING TOOLS'- 16 -

3.1 HEC-RAS 2D ..... - 16 -

3.1.1 Complications with HEC-RAS 2D Model Stability ..... - 17 -

3.1.1.1 Geometry ..... - 17 -

3.1.1.2 Unsteady Flow ..... - 18 -

3.1.1.3 Roughness Uncertainties ..... - 18 -

3.1.1.4 Model Instability Due to Low Flow ..... - 20 -
3.1.1.5 Time Step ..... - 20 -
3.1.1.6 River Slope ..... - 20 -
3.2 TELEMAC-2D ..... - 21 -
4. CASE STUDIES ..... - 22 -
4.1 Surna River Study Reach ..... - 22 -
4.2 Vekveselva River Study Reach ..... - 24 -
5. MATEIAL AND METHODOLOGY ..... - 28 -
5.1 HEC-RAS 2D and TELEMAC-2D Models Selection ..... - 28 -
5.2 Basic Data Requirements ..... - 29 -
5.3 Surna river Hydrodynamic Simulations ..... - 30 -
5.3.1 Geometry Data ..... - 30 -
5.3.2 Flow Data ..... - 32 -
5.3.3 Comparison Methods ..... - 34 -
5.3.4 HEC-RAS 2D Modeling for Surna river ..... - 34 -
5.3.4.1 Model Set-up ..... - 35 -
5.3.4.2 Terrain creation ..... - 35 -
5.3.4.3 Geometric Data ..... - 37 -
5.3.4.4 Roughness Coefficients ..... - 39 -
5.3.4.5 Boundary Conditions ..... - 40 -
5.3.4.6 Perform Unsteady Flow Simulation ..... - 41 -
5.3.4.7 Simulation Time ..... - 42 -
5.3.4.8 Assumptions and inaccuracy ..... - 43 -
5.3.5 TELEMAC-2D Modeling for Surna River ..... - 43 -
5.3.5.1 Extracting Topographic Data and Creating a Geometry File ..... - 44 -

5.3.5.2 Domain and Grid Characteristics of Geometry File ..... - 44 -
5.3.5.3 Boundary Conditions ..... - 46 -
5.3.5.4 Creating Steering File ..... - 47 -
5.3.5.4.1 Hydrodynamic Simulation ..... - 47 -
5.3.5.4.2 Physical Parameter ..... - 48 -
5.3.5.4.3 Numerical Parameters ..... - 49 -
5.3.5.4.4 Assumptions and Inaccuracy ..... - 51 -
5.4 Vekveselva River Hydrodynamic Simulations ..... - 51 -
5.4.1 Topographic Data ..... - 52 -
5.4.2 Flow Data ..... - 52 -
5.4.3 HEC-RAS 2D Modeling for Vekveselva River ..... - 52 -
5.4.3.1 HEC-RAS 2D simulation for Vekveselva River by Using a Digital Elevation Model (DEM) ..... - 52 -
5.4.3.1.1 Terrain Creation from Digital Elevation Model (DEM) ..... - 53 -
5.4.3.1.2 Geometric Data ..... - 54 -
5.4.3.1.3 Boundary Condition ..... - 57 -
5.4.3.1.4 Manning's Roughness Coefficient ..... - 58 -
5.4.3.1.7 Performing the Computations ..... - 58 -
5.4.3.1.8 Computer Specifications and Model Version ..... - 59 -
5.4.3.2 HEC -RAS 2D Simulation for the Vekveselva River by Using Digital Surface Model (DSM) ..... - 59 -
5.4.3.2.1 Terrain Creation from Digital Surface Model (DSM) ..... - 59 -
5.4.3.2.2 Hydrodynamic Computation ..... - 60 -
5.4.3.2.3 Computer Specifications and Model Version ..... - 62 -
5.4.4 TELEMAC-2D Modeling for the Vekveselva River ..... - 63 -
5.4.4.1 Geometry File ..... - 64 -

5.4.4.1.1 Generating a Geometric File from a Digital Elevation Model (DEM)..... - 64 -
5.4.4.1.2 Generating a Geometric File from Digital Surface Model (DSM)..... - 66 -
5.4.4.2 Boundary Condition File..... - 68 -
5.4.4.3 Creating a Steering File..... - 68 -
5.4.4.4 Computer Specifications and Model Version for Vekveselva River TELEMAC-2D Modeling..... - 70 -
6. RESULTS..... - 71 -
6.1 Surna (mild and shallow) River Simulations' Result..... - 71 -
6.1.1 Inundation Extent Results..... - 71 -
6.1.2 Statistical Comparison..... - 75 -
6.1.3 Influence of Islands on Inundation Extent Prediction..... - 80 -
6.1.4 Comparison of Water Surface Elevation Computed in HEC-RAS 2D and TELEMAC-2D..... - 83 -
6.1.5 Comparison of Velocity Computed in HEC-RAS 2D and TELEMAC-2D..... - 91 -
6.1.6 Models Comparison Based on Simulation Time for Surna River Modeling..... - 94 -
6.2 Vekveselva (steep and shallow) River simulations' Result..... - 95 -
6.2.1 Evaluating of HEC-RAS 2D and TELEMAC-2D computations on Digital Elevation (DEM)..... - 95 -
6.2.1.1 Inundation Extent, Water Depth and Water Surface Elevation Results from HEC-RAS 2D Computations on Digital Elevation Model (DEM)..... - 96 -
6.2.1.2 Inundation extent, Water depth and Water Surface Elevation Results from TELEMAC -2D Computations on Digital Elevation Model (DEM)..... - 107 -
6.2.1.2.1 Inundation Extent Simulated in TELEMAC-2D by Applying Finite Element Method (FEM) and Finite Volume Method (FVM)..... - 107 -
6.2.1.2.2 Water Depth Simulated in TELEMAC-2D by Applying Finite Element Method (FEM) and Finite Volume Method (FVM) and Comparison with Water Depth Simulated in HEC-RAS 2D..... - 109 -

6.2.1.3 Models Comparison Based on Simulated water depth and Velocity Along River Cross-section ..... - 111 -

6.2.1.4 Models Comparison Based on Simulation Time in Vekveselva River Modeling by Applying DEM ..... - 114 -

6.2.2 Evaluating of HEC-RAS 2D and TELEMAC-2D Computations on a Digital Surface Model (DSM) ..... - 115 -

6.2.2.1 Results from HEC-RAS 2D Simulation Based on Digital Surface Model ... - 115 -

6.2.2.2 Results from TELEMAC-2D Simulation Based on a LiDAR Derived Digital Surface Model ..... - 119 -

7. DISCUSSION ..... - 123 -

7.1 Impact of River Steepness in Hydrodynamic Modeling by Using LiDAR Derived DEM… ..... - 125 -

7.2 Application of Digital Surface Model Data Derived from LiDAR in a Hydrodynamic Simulation ..... - 127 -

7.3 Comparison Between Models Related to Inundation Area, Water Depth and Velocity…. ..... - 128 -

7.4 Comparison of Models Based on Simulation Time ..... - 129 -

7.5 Comparison of Models Based on ease to Set Up ..... - 129 -

8. CONCLUSION ..... - 131 -

9. RECOMMONDATION AND FUTURE WORKS ..... - 133 -

REFRERENCE ..... - 135 -

List of Figures

Figure 4-1: Surna river's study reach. ..... - 23 -
Figure 4-2: Elevation profile of the Surna river study area. ..... - 23 -
Figure 4-3: Vekveselva study area. ..... - 25 -
Figure 4-4:Aerial image format captured by Blom AS on16 September2014. ..... - 26 -
Figure 4-5: Elevation profile of Vekveselva river (14 % average slope) ..... - 26 -
Figure 4-6: Land slide and sediment deposits upstream of Vekveselva. ..... - 27 -
Figure 5-1: Stepwise methodology for HEC-RAS 2D and TELEMAC -2D analysis and flood plan mapping ..... - 30 -
Figure 5-2: Surna river with tributaries ..... - 31 -
Figure 5-3: Principle of LiDAR survey. ..... - 35 -
Figure 5-4: TIFF file (left-side)and GeoTIFF file (right side) created by a RASMapper ..... - 36 -
Figure 5-5: Tiled and pyramid data structured by a RAS Mapper ..... - 37 -
Figure 5-6: 2-D flow area of Surna river ..... - 38 -
Figure 5-7: Break line at rapidly changing section (levee) and refinement regions ..... - 38 -
Figure 5-8: Applicable break line at bridge ..... - 39 -
Figure 5-9: Simulated water edge lines and observed water edge line for the 20 August 2016 flow event…. ..... - 40 -
Figure 5-10: Boundary conditions' locations and their ID number/name ..... - 41 -
Figure 5-11: BOTTOM variable geometry (computational grid of the mathematical model) .- 45 -
Figure 5-12:Density (refinement) area of computational grid of the mathematical model ..... - 45 -
Figure 5-13: Finite element mesh and boundaries segments. ..... - 47 -
Figure 5-14: Digital elevation model of TIFF format and new created TIFF format of Digital elevation model..... - 53 -
Figure 5-15: Created terrain in RAS Mapper and terrain profile..... - 54 -
Figure 5-16: Computational mesh with break lines.. ..... - 55 -
Figure 5-17: Terrain elevation profile and black lines surrounding sections indicate a rapidly changing slope ..... - 56 -
Figure 5-18:Refined computational meshes. ..... - 57 -
Figure 5-19:Terrain created by RAS Mapper and orthophoto. ..... - 60 -

Figure 5-20: Computation mesh with 0.5 x 0.5 m default spacing size and break lines.. .....- 61 -
Figure 5-21 Origin and interpolated terrain.. .....- 62 -
Figure 5-22:Contour (isolines).....- 65 -
Figure 5-23: Three-dimensional view of computational domain created from DEM and elevation profile (BLUEKNUE) .....- 66 -
Figure 5-24:Geometry file (selafin) created from DSM data that contains a vegetation canopy….. .....- 68 -
Figure 6-1: Inundation extent form HEC-RAS 2D simulations and observed water cover area….. .....- 72 -
Figure 6-2: Inundation extent computed in HEC-RAS 2D.....- 73 -
Figure 6-3:Inundation extent from TELEMAC 2D simulations and observed water cover.....- 74 -
Figure 6-4: Inundation extent computed in TELEMAC-2D at downstream region. .....- 75 -
Figure 6-5: River sections.....- 76 -
Figure 6-6: Simulated and observed water cover area. .....- 77 -
Figure 6-7: Islands selected for evaluating both hydrodynamic models performance at island sections .....- 81 -
Figure 6-8: Simulated and observed water cover area at island zones. .....- 83 -
Figure 6-9:Selected river cross section for analyzing the influence of river morphology on hydrodynamic models.....- 85 -
Figure 6-10: Water surface elevation at bend 1 .....- 85 -
Figure 6-11: Water depth at bend 1 .....- 86 -
Figure 6-12:Water surface elevation at bend 2 .....- 86 -
Figure 6-13: Water depth at bend 2 .....- 87 -
Figure 6-14: Water surface elevation at island 1 .....- 87 -
Figure 6-15: Water depth at island 1.....- 88 -
Figure 6-16: Water surface elevation at island 2 .....- 88 -
Figure 6-17: Water depth at Island 2 .....- 89 -
Figure 6-18:Water surface elevation at straight river alignment 1 .....- 89 -
Figure 6-19: Water depth at straight river alignment 1.....- 90 -
Figure 6-20: Water surface elevation at river straight alignment 2 .....- 90 -
Figure 6-21: Water depth at straight river alignment 2.....- 91 -

Figure 6-22: velocity at bend 1 .....- 92 -
Figure 6-23: velocity at bend 2 .....- 92 -
Figure 6-24: velocity at island 1 .....- 92 -
Figure 6-25: velocity at island 2 .....- 93 -
Figure 6-26: velocity at river straight alignment 1 .....- 93 -
Figure 6-27: velocity at river straight alignment 2 .....- 94 -
Figure 6-28:Inundation area extracted from simulation1 which was computed in HEC-RAS 2D modeling on a DEM. .....- 96 -
6-29:River sections where inundation area and water surface elevation discontinuities happened in simulation 2... .....- 97 -
Figure 6-30:Water depth profile along with longitudinal river center line (longitudinal profile)…. .....- 97 -
Figure 6-31: Longitudinal water depth profile along river centerline (longitudinal profile)....- 99 -
Figure 6-32:Longitudinal water surface elevation profile along river centerline (longitudinal profile).. .....- 99 -
Figure 6-33:Inundation area extracted from simulation 2 which was computed in HEC-RAS 2D modeling on a DEM.. .....- 100 -
Figure 6-34:Longitudinal water depth profile along river centerline (longitudinal profile)...- 101 -
Figure 6-35: Inundation area extracted from simulation 3 which was computed in HEC-RAS 2D modeling on a DEM. .. ..- 102 -
Figure 6-36:Inundation area extracted from simulation 4 which was computed in HEC-RAS 2D modeling on a DEM.. .....- 104 -
Figure 6-37: Longitudinal water depth profile along the river centerline (longitudinal profile)….. .....- 105 -
Figure 6-38: Water surface elevation and terrain profile.....- 106 -
Figure 6-39:Simulated inundation area estimated by TELEMEMAC- 2D simulation with the finite element method (FEM) algorithm applied .....- 107 -
Figure 6-40: Simulated inundation area estimated by TELEMEMAC- MASCARET simulation with the finite volume method (FVM) algorithm applied .....- 108 -
Figure 6-41: Relationship between water depth simulated in TELEMAC-2D by applying finite element method and finite volume method.. .....- 109 -

Figure 6-42: Relationship between water depth simulated in TELEMAC-2D by applying the finite element method equation and HEC-RAS 2D simulation 4. ..... - 110 -
Figure 6-43: Relationship between water depth simulated in TELEMAC-2D by applying the finite element method equation and HEC-RAS 2D simulation 4 . ..... - 110 -
Figure 6-44: Selected river cross section for analyzing an agreement between velocity and water depth simulated by models ..... - 112 -
Figure 6-45: Water depth profile at cross-section 1..... - 112 -
Figure 6-46: Velocity profile at cross-section 1 ..... - 113 -
Figure 6-47: Water depth profile at cross-section 2..... - 113 -
Figure 6-48: Velocity profile at cross-section 2 ..... - 114 -
Figure 6-49: Inundation area extracted from simulation 1 which was computed in HEC-RAS 2D modeling on a DSM..... - 116 -
Figure 6-50:Inundation area extracted from simulation 2 which was computed in HEC-RAS 2D modeling on a DSM..... - 117 -
Figure 6-51: Cross-sectional river profile at 83 m from upstream boundary.. ..... - 117 -
Figure 6-52: Cross-sectional river profile at 245 m from upstream boundary.. ..... - 118 -
Figure 6-53: Cross sectional river profile at 87.6 m from downstream boundary..... - 118 -
Figure 6-54: Inundation area extracted from simulation 3 which was computed in HEC-RAS 2D modeling on a DSM..... - 119 -
Figure 6-55: Water depth and inundation extent from the Vekveselva river TELEMAC modeling by applying FEM on the DSM. ..... - 120 -
Figure 6-56: Water depth and inundation extent from the Vekveselva river TELEMAC modeling by applying FVM on the DSM. ..... - 120 -
Figure 6-57: Cross-sectional water surface elevation simulated in HEC-RAS 2D and TELEMAC-2D by applying FEM and FVM on DSM ..... - 121 -
Figure 6-58: Cross-sectional water depth simulated in HEC-RAS 2D and TELEMAC-2D by applying FEM and FVM on DSM ..... - 121 -

List of Tables

Table 4-1: Selected river reach for hydrodynamic computations ..... - 27 -
Table 5-1:Measured and estimated flow data for the Surna river ..... - 33 -
Table 5-2: simulations and corresponding roughness coefficients ..... - 49 -
Table 5-3:Computer specification used for Vekveselva HEC -RAS 2D simulation on DEM . - 59 -
Table 5-4: Computer specification used for Vekveselva HEC -RAS 2D simulation on DSM - 62 -
Table 5-5: Simulation scenarios for TELEMAC-2D simulations ..... - 63 -
Table 5-6:Computer specification used for Vekveselva TELEMAC-2D simulation on both DEM and DSM ..... - 70 -
Table 6-1: RMSE values ..... - 76 -
Table 6-2: Inundation area summation of fifty-nine sections ..... - 79 -
Table 6-3:RMSE at islands ..... - 81 -
Table 6-4: Simulation time for the Surna river modeling ..... - 95 -
Table 6-5: Slope value at selected points ..... - 98 -
Table 6-6:Simulation time of TELEMAC-2D modelling for Vekveselva river ..... - 114 -

ABREVIATIONS

1-D	= One-dimensional
2-D	= Two-dimensional
3-D	= Three-dimensional
AHM	= Airborne Hydro mapping
DEM	= Digital Elevation Method
DSM	= Digital Surface Method
DTM	= Digital Terrain Method
FEM	= Finite Element Method
FVM	= Finite Volume Method
GFEM	= Galerkin's Finite Element Method
GPS	=Global Positioning System
IDW	= Inverse Distance Weighted
LiDAR	= Light Detection and Raging
RMSE	= Root mean square error
SAR	= Synthetic Aperture Radar
SRTM	= Shuttle Topography Radar Mission
TIFF	= Tagged Image File Format
TIN	= Triangular Irregular Network

1. INTRODUCTION

Floods is a natural hazard that damges damage infrastructures, lead to loss of human life, and have economic and negative environmental consequences (Pinos & Timbe, 2019). Research indicates thousands of human life mortalities and ten billions of assets are destroyed throughout each fiscal year (Hirabayashi et al., 2013). Flood frequency is likely to increase as a result of population growth rate rises, change of land use, and climate change (Molinari et al., 2020). Such disasters can be handled by different techniques. Effective and efficient flood estimation and result analysis, applying reliable models and risk assessment are key factors for flood management (Molinari et al., 2020). Effective flood mapping and risk analysis is a key tool to use to prevent and decrease the extent of the damages. Depending on flood modeling and further damage analysis, estimated disasters can be mitigated by building structures such as diversion structures, dikes, trenches, storage structures or by removing destructive assets without building any civil structures (ShahiriParsa et al., 2016). Flood mapping is an essential tool to use to estimate hydraulic parameters such as the water cover area, water depth, water velocity, flood extent and wave propagation occurring during a specific time (ShahiriParsa et al., 2016). In addition, spatial planning and flood warning based on flood modeling are scientific and technical approaches used to reduce disaster risks. Consequently, developing effective numerical approaches and efficient hydraulic models is a key issue for mapping the flood extent and determining the magnitude of the hydraulic parameters. Furthermore, the performance of different models on mountain rivers, mildly sloping rivers, vast spatial complex rivers, and the quality of topography data are the core issues needed for carried out successful simulations (Pinos et al., 2019).

The Use of hydraulic models for estimation of flood hydraulic parameters has become more efficient and familiar throughout the world. This progress has come due to various studies which have been carried out for more understanding of hydrodynamics; for improving on numerical methods; for modifying mathematical and physics equations; and for development of computer technology (Bates et al., 1997). For instance, many models were developed with special numerical solutions for analysis of the influence of dynamic phenomena such as wind, oscillation, and diffusing (Bates et al., 1997). Historically, hydraulic calculations such as slope-area methods have been used to performing hydraulic parameters. In contrast, recently, various hydraulic models have been developed to compute one-dimensional, two-dimensional and three-dimensional flows and

high-quality technologies have been invented that can capture dense geographical information (Cooper, 2010). However, these hydraulic models cannot perform in high hydrographic events' computations such as glacial outbreak floods, volcanic flow and ice-dam (Cooper, 2010).

A One-dimensional model (1-D) is a unidirectional simulation of a computer coding system designed to compute specific hydraulic parameters, mostly water surface elevation, along the center line of a river (Teng et al., 2017). This type of simulation considers enormous assumptions and requires fewer input data. Generally, it is applicable when a user is not looking for flow simulation, when the main flow is parallel with river the channel, or ideally one-directional flow such as pipe flow (Cooper, 2010). The main limitation in 1-D simulation is that it could not perform on a multi-direction flow, such as river mountain hydraulics with complex hydrodynamic analysis of the main issues.

A two-dimensional (2-D) hydraulic model is an advanced computer algorithm system that is designed to perform two-dimensional hydraulic analysis of complex flow. Generally, this modelling system was developed for shallow depth computation based on three physics laws: one continuity equation and two conservative momentum equations (Vojinovic et al., 2011). Comparable with 1-D models, 2-D hydraulic models are able to give more accurate and real-world representative simulation results when high-quality topographic and dense digital elevation model dataset is involved in the computation (Pinos et al., 2019). However, an advanced way of using a combination of two models, 1-D, and 2-D models, has been applied for different research, studies and hydraulic design (Vojinovic et al., 2011). Even though, both 1-D and 2-D hydraulic models do not perform in complex riverine systems that three-dimensional velocity variation is considerable (Molinari et al., 2020).

On the other hand, a recent development in hydrodynamic modelling has effectively perform in the three dimensional (3-D) hydraulic flow. In fact, the propagation of flow on the earth's surface is a three-dimensional system where hydraulic parameters vary with dimensional changes. In real flow, flow variables are time dependent, incompressible, and have complex dynamics with a free surface (Teng et al., 2017). In 3-D hydrodynamic computations, Navier-Stokes equations are used to describe dynamic propagation of fluid particles (Teng et al., 2017).Although the turbulence in flow and grid cell size, and the cascade of length and computational time interval are the issues in Navier-Stokes computing in 3-D analysis (Teng et al., 2017).

To sum up, even though a lot of hydrodynamics have been developed, and numerical equations modified, the results obtained from the models' computations have limitations fitting with the real world. In addition, factors such as the quality of topographic data, river geometry, mesh resolution, and mathematical models influence the accuracy of the simulation.

1.1 Problem Investigation

Accurate flooding estimation is critical for preventing economic losses and saving human lives from flood disasters. Various hydraulic models have been developed globally to analyze flood the extent of inundation, water depth, wave propagation, peak velocity, and other hydraulic parameters. Some models have limitation in their analysis of complex topography, deep water, steep slopes, and fluvial flow. While some models have a strange computation in too fine cell size with big river reaches. In addition, some models give good performance in only mild slope river computation and the others may be good with in both mild and steep rivers.

Indeed, the main idea behind this paper is to evaluate the performance of two hydrodynamic models of different sloped rivers, by their implementation to common case studies. The aim is to obtain enhanced information on their ability to compute realistic results, the validity of the models, and their limitations in steep and mild river computations. In a mild slope case study area, common input data is used in both models correspondingly; and the results obtained from the models are evaluated with the observed inundation extent. An observed inundation extent was obtained from LiDAR measurement, which green LiDAR generate efficient mapping of underwater geometry with high detail and promising accuracy (Alfredsen & Lidar, n.d.). Factors such as the influence of the river bend in meandering river, the impact of tidal flow at an island location, and the way of limiting the shore impact in both hydrodynamic models are included in the paper. The consistency of the flow computation on LiDAR-based DSM was evaluated in steep river computations. Issues such as mesh grid sizes and accuracy of flow estimation in hydrodynamic models influence the initial boundary condition in the HEC-RAS 2D simulation, and the effect of initial condition is evaluated in hydrodynamic modeling in a steep river.

1.2 Objectives

The main objective of this study was to evaluate the suitability of two hydrodynamic models for steep and mildly sloping river; and how the model river gradients influence the accuracy of the hydrodynamic modeling: -

To sum up, hydrodynamic computations for HEC-RAS 2D and TELEMAC-2D were carried to achieve the following goals.

- To evaluate the suitability of two-dimensional hydraulic models for a generating inundation extent in mildly sloped meandering river basins
- Evaluating the suitability of both hydrodynamic models' stability in steep river flow modeling
- Evaluating the effectiveness of LiDAR-based digital surface model (DSM) data obtained from https://hoydedata.no/LaserInnsyn/ in flood mapping
- Analyzing the effect of mesh size resolution in hydrodynamic modeling
- Assessing the uncertainty of digital elevation model (DEM) and digital surface model (DSM) in hydrodynamic simulation
- Estimation of representative roughness values for the Surna river

1.3 Limitation

The main limitation for the Surna river (mild slope) study is that the suitability of both models for mild slope modeling was evaluated only by correlating simulated and observed inundation maps in terms of root mean square error (RMSE). However, the global estimating of the RMSE value can only give an overall result. In other words, the river section with a significant error-simulated inundation extent can control the overall result, and the RMSE can biased for large error sections. The models' performance was not evaluated with other flow variables such as velocity, water surface elevation, and cross-sectional discharge.

In the case of the hydrodynamic performance evaluation for the Vekveselva river (steep river), both models evaluated by overlapping simulated inundation results on orthophoto; Such that there was no statistic or numerical assessment of the models' performance.

Although, for the Vekveselva river case study, where digital elevation and digital surface elevation were used for both models, the date that both DEM and DSM obtained was not the same as the data that orthophoto generated. In other words, the river channel profile and river alignment

in orthophoto may not be the same with topographic data used in the hydrodynamic computations. In general, the selection of hydrological data for hydraulic modeling depended on the date that topographic data was available. However, no topographic data available during the day that the flight orthophoto was done.

Another limitation of this paper is that the field measurement was canceled due to the country's lockdown by the COVID-19 pandemic. As a result of this, the initial condition of the models' set-up made by personal assumptions and control sections was not installed in both study areas. In both case studies, the downstream boundary condition was assumed, and the calibration of the representative bed channel roughness was not verified. Also, the results from both models in the modeling of both study cases were not validated. Model validation, which links with model calibration, is used to confirm that the computed flow variables meet the identified flow variables specifications and is applied to adjust the model parameters, assumptions, or equations; and furthermore, to optimize an agreement between simulated by model and observed data (Molinari et al., 2019). On the other hand, the river channel surface in the DSM data applied for the Vekveselva river modeling was not cleaned. Besides this fact, a manual measurement that is mandatory for the filling hole and modifying topography obtained from https://hoydedata.no/LaserInnsyn/ was not made.

2. LITERATURE REVIEW

A general overview of flood computation methods, the historical development of flood modeling, and numerical differences between 1-D, 2-D, and 3-D hydraulic models are all briefly discussed in this chapter. In the next chapters (chapter 3 and chapter 5), current issues related to HEC-RAS 2D and TELEMAC-2D models and their complications with model stability issues, which have been identified in previous researches studies are presented.

2.1 Overview of Flood Modelling Methods

Different methods for hydraulic parameters computation have been developed to understand the flow process in the rivers and/or to estimate extent of water cover area, velocity, wave propagation, peak velocity, water surface depth, and vulnerability assessments. Many scholars have grouped the hydraulic models in different ways (Teng et al., 2017). However, two technically different categories those related to this paper are briefly discussed in next subtopics.

2.1.1 Empirical Model

An empirical model approach is used for flood mapping when high quality technologies used for collecting, analyzing and integrating data do not exist, or when the quality of topographical data, geological data and other data used for flood simulation occur is poor (Teng et al., 2017). The empirical model is developed based on past flood events to predict the flood extent of future events. Indeed, the development of such models includes considering assumptions and uncertainty due to a limited data quantity. Empirical model assessment can be done by using a simple statistical method such as mean, median, or regression, or using approaches with sophisticated mathematical tools (Teng et al., 2017).

An empirical model has a significant limitation: a scientific analysis is an input-out standardization in a specific area and is not applicable in other regions (Amadio et al., 2019). However, they can be used for decision making or further investigation and may be used as other model inputs (Teng et al., 2017).

2.1.2 Hydrodynamic Models

A hydrodynamic model is a set of physics laws, numerical formulas, and computer algorithms used to compute hydraulic parameters. Unlike empirical models, hydrodynamic models consider a lot of input variables for applying the law of physics.(Teng et al., 2017). The purpose of these

models is to compute an accurate simulation by using robust input data and scientifically reasonable assumptions that the model must understand (Dusty Robinson, 2018). Development of technologies such as collecting high-quality topography data, sediment measurements techniques, recording water levels, and flow rate gauging enables water resource managers to develop an advanced model. Such technologies need a user to decrease assumptions and uncertainty, which support model calibration and validation (Molinari et al., 2019). On the other hand, hydraulic models are a set of well-organized tools that help a model that can solve large-sized data.

Depending on the number of parameters solving, hydrodynamic models can be classified as one-dimensional (1-D), two-dimensional (2-D), and three-dimensional (3-D) models.

2.1.2.1 One-Dimensional Hydrodynamic Models

A one-dimensional (1-D) model is a uni-direction computer coding system designed to compute hydraulic variables along the centerline of a river (Molinari et al., 2020). This type of model involves more assumptions than 2-D models. It is mostly applicable when a user does not need a detailed flow simulation result or when the flow is ideally parallel to the river channel (Molinari et al., 2020).

The 1-D models such as HEC-RAS, MIKE 11 and Flood Modeller commonly use 1-D Saint-Venant equation, (Equation 2-1 and Equation 2-2), and the Bernoulli equation (Equation 2-3) to ensure the law of conservative mass (continuity equation), conservation momentum techniques, and energy equation respectively (Kivva et al., 2020):-

$$conservation\ of\ mass \qquad \frac{\partial Q}{\partial x} + \frac{\partial A}{\partial t} = 0 \qquad \textit{Equation 2-1}$$

$$conservation\ of\ momentum \ \frac{1}{A}\frac{\partial Q}{\partial t} + \frac{1}{A}\frac{\partial(\frac{Q^2}{A})}{\partial x} + g\frac{\partial h}{\partial x} - g(So - Sf = 0 \qquad \textit{Equation 2-2}$$

Where Q is a flow discharge; A represents cross-sectional Area; ∂t is the change of time interval between computational interval; ∂x is the distance between consecutive cross-sections; and h is flow depth.

$$Bernoulli \quad y2 + z2 + \alpha 2\,\frac{V2^2}{2g} = y1 + z1 + \alpha 1\frac{V1^2}{2g} + he \qquad \textit{Equation 2-3}$$

where y1 and y2 are water depth at sections 1 and 2, respectively; V1 and V2 are flow velocity at section1 1 and 2; Z1 and Z2 are bottom channel elevation of section1 and 2, respectively. Whereas

he is energy loss between two sections; and $\alpha 1$ and $\alpha 2$ are represent velocity head coefficients at section 1 and 2, respectively (Pinos et al., 2019).

Other 1-D models such as CHArima, InfoWorkers RS (commercial and developed by HR-Wallingford RFSM Innovyze), SOBEK (a commercial developed by CSIRO DELTARES); TUFLOW classic 1-D (a commercial model developed by BMT WBM); FASTER (developed by Cardiff University for research purposes); and MASCARET (a commercial model developed by Electricite de France) are some models those can solve 1-D simulation. (Molinari et al., 2020).

Relative to 2-D and 3-D hydrodynamic models, 1-D simulation is non-time-consuming but less accurate than 2-D and 3-D models (Gharbi et al., 2016). Also, 1-D models are efficient, low cost, and robust for computing one-dimensional water depth. However, such models have limitations such as lateral wave propagation, and diffusion phenomena not considered in simulation; hydraulic parameters computed in the model can be biased by the density of the assigned cross-sections and discontinuous cross-sections (Molinari et al., 2020).

2.1.2.2 Two-Dimensional Hydrodynamic Models

A two-dimensional (2-D) model is a digital representation of a natural river, human-made channel, or other waterway flow that relies on systematic analysis of two-dimension spatial flow. Unlike a 1-D model, a 2-D model avoids many assumptions and uncertainties and is also more potent on graphical visualization of simulated results (Dusty Robinson, 2018). A 2-D model simulation has high-efficiency flow analysis approaches and generally gives more accurate hydraulic variables than a 1-D model (Dusty Robinson, 2018).

A numerical model of a 2-D approach represents the law of mass and momentum conservation on a two-dimensional plane, and neglects flow velocity variation with respect to water depth (Gharbi et al., 2016). This model is mostly applicable for shallow water simulation and can solve by Navier-Stokes equation (Molinari et al.,2020) that were developed for estimation of horizontal hydraulic parameters variation with change in space and time.

Conservative mass and conservative momentum of Navier-Stokes equations are explained as follows: (Molinari et al., 2020)

$$conservative\ \ momentum\ \frac{\partial(hu)}{\partial t}+\frac{\partial}{\partial x}\left(hu^2+\frac{1}{2}gh^2\right)+\frac{\partial(huv)}{\partial y}=0 \qquad \textit{Equation 2-4}$$

$$\frac{\partial(hv)}{\partial t} + \frac{\partial(huv)}{\partial x} + \frac{\partial}{\partial y}(hv^2 + \frac{1}{2}(gh^2) = 0 \qquad \textit{Equation 2-5}$$

Here, x and y are spatial coordinates; u and v are horizontal velocity components on an x and y-axis respectively, and both are perpendicular to the vertical plane.

Some well-known numerical approaches used to solve two-dimensional flow parameters are: TELEMAC-2D; HEC-RAS 2D; FINEL 2-D; MIKE 21; TUFLOW classic 2-D; TUFLOW GPU; TFLOW FV; Flood modeler pro 2-D solvers; and XP2D (Molinari et al., 2020).

In the real world, 2-D hydraulic models are popular and widely applicable for designing and practical implementation. However, they have limitations in the analysis of complex hydraulic analysis. Since hydraulic computations running non-discrete cross-sections, these models can compute more reliable water depth, velocities, inundations areas, and other variables (Matthew Hickox, 2019).

2.1.2.3 Three-Dimensional Hydrodynamic Models

Three-dimensional model approaches are used to solve complex riverine systems, which have significant three-dimensional velocity variation. The 3-D approach can compute hydraulic phenomena such as vertical turbulence flow, rotational flow at bends, dam breaks, and hydraulic jumps (Alcrudo, 2002). The big challenge of such aspects is that nonlinear flow is applied in hydraulic computation and flow parameters are in three-dimensional varies with time and space (Molinari et al., 2020). Such simulation can compute hydraulic variables by using three-dimensional numerical approaches, such as the Eulerian and Lagrangian differential method, with a smooth mesh grid and low computational time interval (Alcrudo, 2002). Navier-Stokes, developed by Harlow and Welch, is a well-known equation for 3-D hydrodynamic simulation (Alcrudo, 2002). The vector component of this equation is described as follows:

$$conservation\ of\ momentum\ \ \frac{\partial u}{\partial t} + u.\nabla u + \frac{1}{\rho}\nabla P = g + \mu\nabla.\nabla u \qquad \textit{Equation 2-6}$$

$$incompressibilty\ condition\ \nabla.u = 0 \qquad \textit{Equation 2-7}$$

where u, ρ, p, g and μ represet flow velocity, density , pressure, gravitation accelaration and kinematic viscosity, respectively.

However, 3-D model simulation is only applicable for small lengths of river reach; being limited by computational feasibility and the problems of accurately representing free surface flows, high-

order turbulence, and a transient flood shoreline. So, most of the 3-D models performance decreases when the river reach scale is higher than 1km (Molinari et al., 2020).

2.2 Review of Recent Progress in Flood Modelling

As a result of many flood events and disasters happening, the level of understanding, assessment, and estimation of flood areas increased over time. Consequently, numerical models and computer algorithms have developed for this purpose (Werner, 2004). However, the reliability and robust simulation of flood inundation areas depends on the availability of hydrology data, the accuracy of topographic data, and meteorological data (Molinari et al., 2020). The continuous development of hydraulic models over the past two decades, with innovation of precise measurement of catchment hydrology and LiDAR technology that gathers high-quality data, have led to achieving sustainable growth of hydrodynamic modeling. Consequently, the performance of hydraulic models has increased due to the increasing number of events and uncertainty associated with the available modeling techniques and precision at the cost of computational expense.

An application of empirical models for flood analysis needs much historical data; even the accuracy of such models depends on the efficiency of the gauging station and the quality of measurement equipment. Also, such input data collection needs manpower and maybe expensive (Molinari et al., 2020). However, recent technology such as the growth of remote sensing and AHM have pushed hydrodynamic models to overcome the limitations in hydraulic modeling (Bates et al., 1997). Active reflectance techniques such as Synthetic Aperture Radar (SAR) provide denser spatial resolution to get detailed information of flooded areas with around 85% efficiency. Also, SAR provides an inundation map for calibration in empirical models (Bates et al., 1997). However, these technologies still have drawbacks in their ability to provide sediment information, detail bed formation information, and the effect of vegetations; these are fundamental parameters for knowing roughness values (Molinari et al., 2020). Such problems can be reduced by using modified technologies such as SWOT, ALOS, and RADARSAT-2, as they provide denser topographical data (Molinari et al., 2020).

Furthermore, improvement in remote sensing technologies can not only provide hydrologic information, but can merge with other technologies such as LiDAR and the Shuttle Topography Radar Mission (SRTM) to create high-quality and cloud point topographic data (Molinari et al., 2020).Such integration of hydrodynamic models and remote sensing is not only limited to

providing and receiving topographic land; their linkages give more progress in model calibration and validation (Bates et al., 1997). However, the many limitations related to remote sensing technologies, errors in water depth reading, errors in gathering sediment information, and inaccuracy in capturing vegetation information in both LiDAR and SRTM have been a significant challenge in recent studies (Bates et al., 1997).

An improvement in hydraulic modeling over two decades has been achieved as result of continuous improvement in understanding mathematical and numerical flow processes. Achievements in hydraulic models and computer programming can save computational time and increase the accuracy of simulation results (Molinari et al., 2020). Such improvements enable the development of high-resolution spatial dimension models such as the 2-D and 3-D models that can compute a hydraulic variable on a non-discrete geometry domain, and allow an algorithm to calculate dynamic movements in flood inundation (Bates et al., 1997). Further, some models, such as HEC-RAS can perform hydraulic computation by combining 1-D and 2-D models (Molinari et al., 2020). So, significant achievements have been made in hydrodynamic models that enable the development of higher dimensions of hydraulic models that can solve the Saint-Venant equation, which is derived from the Navier -stokes equation (Bates et al., 1997).

Another merit of using current hydrodynamic models is the accessibility of advanced numerical methods such as finite element and finite volume methods that enable a computer algorithm to compute flow parameters at each computational node and at each time step (Bates et al., 1997). Also, the finite volume method can perform the hydraulic simulation with flexible geometry, small grid size, and a complex geometry domain, which cannot succeed in the finite element approach (Ata, 2018).

Numerous research studies have been made to address continuous topographic representation in a hydrodynamic simulation that is a common issue in a 1-D model, where hydraulic modeling is computed on discrete geometry (Bates et al., 1997). In contrast, 2-D hydrodynamic models comprise a hyperbolic equation to solve shallow water depth, and they have unphysical oscillation which grows with time steps (Molinari et al., 2020). Currently, a lot of research is being carried out to solve these issues. One action proposed to solve the unphysical oscillations problem is by applying a generalized Riemann problem which encourages a model to use two non-identical initial conditions. Another method proposed is to use a nonlinear equation second-order Godunov

equation. An advantage of second-order Godunov techniques is the ability to solve large gradient solutions that prevent unphysical oscillations (Molinari et al., 2020). Another uncertainty that has been happening in hydrodynamic models is related to fixed time-step computation (G. W. Brunner & CEIWR-HEC, 2016). However, a fixed time-step reduces the accuracy of the simulation. Nevertheless, using a courant number that applies a variable time-step provides more accurate model simulation (G. W. Brunner, 2008).

Advanced models such as MIKE FM, TUFLOW FV, DELF 3D, and FINEL 2D comprise a numerical algorithm that was developed to solve uncertainty associated with a discretization of space (Molinari et al., 2020). Such models have a program for refining the mesh around complex topography and applying coarser meshes in the rest of the areas (Molinari et al., 2020); consequently, the program decreases simulation time and increases model performance.

Other factors, such as developments in computer software technology are more influential in hydrodynamic computation. Modern computers hold special programs known as an application program interface (API) to enable parallel computing hydrodynamic models to decrease simulation time (Ata, 2018). While some hydrodynamic models such as HEC-RAS, TUFLOW, and MIKE FLOOD increase computation performance because of the models being incorporated the with graphical user interface (GUI).

3-D hydrodynamic models have a limitation in modeling long-reach rivers:- for instance, HEC-RAS's performance decreases as the grid number increases (G. W. Brunner & CEIWR-HEC, 2016). Also, feedbacks has indicated that 3-D hydrodynamic models' users need computer graphics which enable them to visualize computation results in animation, video, and movie type (Molinari et al., 2020).

2.3 Linking Flood Models and Geographical Information Systems; and the Importance of the Quality Topographic Data in Flood Modeling

Globally, the application of hydraulic models has been increased, as a result of recent technologies which are able to generate high-quality and dense topographic data (Molinari et al., 2020). The quality of the topographic data and the extent of the resolution are critical issues in hydrodynamic modeling. Using dense and high-resolution terrain data is essential in flood risk assessment, flood management, and the design of hydraulic structures (Casas et al., 2006). Digital terrain model

(DTM) with low quality can force the model to either overestimate or underestimate(Casas et al., 2006).Related to this, implementing underestimated flow data for civil engineering can address a significant flood disaster in flood protection work. On the other hand, overestimated hydrologic event can lead to an exaggerated hydraulic structure construction.

Topographic data collection depends on the quality needed; the availability of the measured data; economic factors (if data available for free and noncommercial); the resolution required; and the extent of area required. For hydraulic analysis on small areas, topographic information is obtained from global positioning system the (GPS) and conventional survey techniques. The precision and accuracy of the data gathered from GPS and conventional survey techniques depends mainly on the quality of the instruments used for measurement, the number of selected points, the space between the points, and homogeneity of the space between points (Casas et al., 2006). The main limitation of these techniques is that they give lower resolution due to implementing interpolated elevation values between the points. On the other hand, elevation information can be extracted from satellite images, aerial photos, radar and LiDAR group points. Accuracy of such data can be achieved by integrating with GPS or other survey techniques.

Terrain information use in hydrodynamic models can be categorized as a digital terrain model (DEM), digital surface model (DSM), and triangular irregular networks (TIN).

2.3.1 Digital Terrain Model (DTM)

A digital terrain model (DTM) can be described as a three–dimensional representation of a terrain surface consisting of x, y, and z coordinates stored in digital form (Saurabh Singh, 2013). The DTM is a digital visualization of the earth surface that can describe spatial attributes such as slopes between points and topographic aspects. It is a digital format of the earth surface that defines terrain height (Casas et al., 2006).

The DTM data can be collected by LiDAR, photogrammetry, contour line digitizing and radar measurements. Basically, the spatial resolution of the DTM is a key parameter in a hydraulic model. Moreover, the quality of the hydrodynamic modeling output is influenced by terrain factors such as terrain roughness, sampling point distribution, elevation points density, grid size, slope break lines, and an algorithm used for DEM/DTM analysis (Saurabh Singh, 2013).

2.3.2 Digital Elevation Model (DEM)

A digital elevation model is one type of digital terrain model representing a 3-D spatial value of bare earth that is referenced from known horizontal coordinates and vertical datum. Related to this, the DEM has an equivalent meaning with the bare-earth DTM (Julzarika & Harintaka, 2019). Interpolation points can create a DEM by inverse distance weight (IDW) from irregular base points. Also, the DEM can prepared by Stereo, LiDAR, Videogrammetery and interferometry (Meneses et al., 2017). In Principle, the quality of this DEM depends on the size of the surface area represented by a single elevation value (Geography, n.d.).

The integration of a digital elevation model and a hydrodynamic model well-suited in flood mapping. Combined with supplementary flow channel stage data and removal objects on earth surface, DEM have been used to improve hydraulic computation for regions that have no access to high resolution alternatives (Ettritch et al., 2018). A coarser resolution influences the accuracy of hydrodynamic results. Recent improvements in hydraulic models ,such as LISFLOOD-FP, have been developed especially in relation to large-scale hydrodynamic modeling at a resolution below the narrative grid spacing of the DEM (Ettritch et al., 2018).

2.3.3 Triangular Irregular Network (TIN)

TIN is a Delaunay triangulation of a continuous surface, vector-based on a combination of interlocked triangular faces that are associated with elevation data of the earth surface. The vertex of triangles is associated by spatial three-dimensional coordinates x, y and z values; where x and y are horizontal coordinates and z is the vertical coordinate form defined datum, gathered by GPS, digital aerial photography, and some other methods(Cone, 1998) .The TIN is un-overlapped triangle networks that can be generated from original base points by the Delaunay triangulation method. The TIN is preferable for hydraulic modelling because a user can add more important geometry features such as break lines, bridges, levees, minimum and maximum elevation points, a barrage, points at elevation changes and other elements that can be influenced by hydraulic properties of flow channels (Casas et al., 2006).

2.3.4 Digital Surface Model (DSM)

DSM is a 3-D spatial dataset arrangement describing the elevation of the earth surface, including objects on it. In other words, the DSM is a continuous terrain surface elevation from a common reference datum that reflects the actual earth surface (Hirt, 2016). In general, a DSM visualizes the

height of objects elevated above bare land. However, features such as a vegetation canopy can be the reason for a false flow blockage in hydraulic modelling. This problem occurs when the DSM data is from LiDAR and the river channel is covered by a tree canopy. Therefore, in such a situation, it better to transform the DSM to a DTM; unless the vertical uncertainty in light detection gives errors of topographic values and then can provide an inaccurate vertical coordinate value (Meneses et al., 2017).

3. THE SELECTION OF HEC-RAS 2D AND TELEMAC-2D AS MODELING TOOLS'

As indicated in the previous topic, the main goal of this paper is to examine the suitability of HEC-RAS-2D and TELEMAC-2D for the modeling of the Surna river (mild slope and calm flow) and the Vekveselva river (steep slope and rapid flow). The selection of both models was due to their popularity and open source. Moreover, HEC-RAS and TELEMAC-MASCARET can perform 2-D dimensional modeling, and both models recognized as good for flood mapping (Mino et al., 2006).

3.1 HEC-RAS 2D

The Hydrologic Engineering Center- River Analysis System (HEC-RAS) is a river hydraulics model developed by the United States Army Corps of Engineers. The model was designed to analyze subcritical, supercritical and mixed flow types. The HEC-RAS has an algorithm to perform a steady flow simulation, 1-D and 2-D unsteady simulation, quasi unsteady, and water quality computation (G. W. Brunner & CEIWR-HEC, 2016). It comprises a graphical user interface (GUI) that is used for file management, inputting data, river simulation, input and output data visualization and parameter mapping (G. W. Brunner & CEIWR-HEC, 2016). As stated above, HEC-RAS is a non-commercial and popular model which is widely used for calculation hydraulic parameters. This recognition as being well-known in hydrodynamic simulations is due to its high-performance for modeling natural river simulations, its free access, and user-friendly software (Theses & Sharkey, 2014).

A numerical model for HEC-RAS 2D is based on Saint-Venant equations and 2-D diffusion wave equations. In contrast, a diffusion equation can decrease simulation time and inherently more stable than Saint-Venant equations (G. W. Brunner, 2016).

The HEC-RAS solving 2-D unsteady open channel flow based on mass conservation and momentum equations, which are described as follows: -

Mass conservation equation: is also known as a continuity equation that relies on Newton's law, which states a principle of energy is neither created nor destroyed. This equation is stated as follows (G. W. Brunner & CEIWR-HEC, 2016):

$$\frac{\partial H}{\partial t} + \frac{\partial (hu)}{\partial x} + \frac{\partial (hv)}{\partial y} + q = 0 \qquad \textit{Equation 3-1}$$

here, t represents time; u and v are horizontal flow velocity on x direction and y direction; and q is a source or sink term (Kayyun & Dagher, 2018).

Momentum conservation: this equation is formed from a Navier-Stokes equation based on neglect vertical velocity variation. The horizontal length scales are much higher than the vertical water length in shallow water depth; such that there is no vertical velocity derivation in respect to the vertical axis, and the momentum conservation equation comprises two terms. The left-hand side equations contain acceleration terms that imply Newton's 2nd law of motion and the right-hand side terms describe internal and external forces acting on fluid particles(G. W. Brunner & CEIWR-HEC, 2016).

$$\frac{\partial u}{\partial t} + u\,\frac{\partial u}{\partial x} + v\frac{\partial u}{\partial y} = -g\,\frac{\partial H}{\partial x} + v_t\left(\frac{\partial^2 u}{\partial x^2} + \frac{\partial^2 u}{\partial y^2}\right) - c_f u + fv \qquad \textit{Equation 3-2}$$

$$\frac{\partial v}{\partial t} + u\frac{\partial v}{\partial x} + v\frac{\partial v}{\partial y} = -g\,\frac{\partial H}{\partial y} + v_t\left(\frac{\partial^2 v}{\partial x^2} + \frac{\partial^2 v}{\partial y^2}\right) - c_f v + fu \qquad \textit{Equation 3-3}$$

where u and v are horizontal velocities on perpendicular directions; v_t ad c_f are an eddy viscosity and bottom roughness coefficient, respectively; R is commonly known as a hydraulic radius, which represents a ratio of cross-sectional channel area and wetted perimeter of a flow channel. f represents Coriolis parameters of a flow.

3.1.1 Complications with HEC-RAS 2D Model Stability

This subsection provides important compilation of important information found from researches which has been done on the stability of HEC-RAS 2D.

3.1.1.1 Geometry

HEC-RAS user manual indicates that incorrect topography of a river can disturb model stability and gives wrong results(G. W. Brunner & CEIWR-HEC, 2016). A HEC-RAS experienced user mentioned that more complexity is added into a model when the parameters have little influence on the hydraulic computation, and that creates a more accurate model (Theses & Sharkey, 2014); and coarser cross-sections can cause model instability. Brunner (Senior Hydraulic Engineer, Hydrologic Engineering Center, Institute for Water Resources, U.S. Army Corps of Engineers)

mentioned that numerical diffusion will be an issue when hydraulic computation on coarse geometry, and smooth mesh size can provide an overestimated flood wave (Theses & Sharkey, 2014). To solve this issue Dr. Fread (1988 and 1993) and P.G. Samuel (1989) mentioned equations for control of this issue (Theses & Sharkey, 2014).

$$Fread: \Delta X \leq C\ Tr\ /20 \qquad \textit{Equation 3-4}$$

$$Samuel' :\ \Delta X \leq 0.20\ D\ /So \qquad \textit{Equation 3-5}$$

where ΔX represents spacing in feet; Tr is a time rise of a flood wave; C represents wave speed (feet/second), D represents in feet, average water depth; and So is the mean average of the channel slope.

However, interpolation processing tools in RASMapper can interpolate and decrease inaccuracy caused by coarse geometry (G. W. Brunner & CEIWR-HEC, 2016).

3.1.1.2 Unsteady Flow

HEC-RAS can solve hydraulic computations based on finite element methods (G. W. Brunner & CEIWR-HEC, 2016). The user manual states that model instability can be caused by numerous aspects that involve inflow calculation. In a practical application, factors such as abrupt change of bed slope, cross-sectional areas, and complex hydraulic structure changes can cause model instability (Theses & Sharkey, 2014).

3.1.1.3 Roughness Uncertainties

Knowing the proper roughness coefficient values is the challenging thing aspect of flow computation for natural rivers (Shamkhi & Attab, 2018). Many researchers have found various formulas for estimating flow-resistance, but no one has achieved a standard equation (Shamkhi & Attab, 2018). This issue has been challenging due to flow resistance being dependent on a river morphology and hydraulic parameters: such as bed slopes; the grain size of bed elements; irregularity of grains elements; bedforms; flow velocity; water depth; Froude and other factors are affecting flow resistance (Aberle & Smart, 2003). The influence of bed slope on flow resistance, such that weight is less in steep mountain flow due to high velocity (Aberle & Smart, 2003). In fact, many studies have been done on the determination of an effect of roughness on a flat channel, and Aberle & Smart, (2003) carried out an efficient study on mountain rivers to get an appropriate technique to estimate the roughness value. So far, both authors obtained a shear stress concept,

which had calculated the roughness by using log-law and power-law resistance before, and the authors decline these approaches. They got a modified technique that determines a representative roughness value of the flow channel based on a standard deviation of the bed elevations (Theses & Sharkey, 2014). In general, these researchers summarized that roughness parameter values depend on the river reach, slope, bed materials, and other river morphology parameter. Moreover, their study recommends more studies to reduce uncertainty in the roughness parameters (Aberle & Smart, 2003).

For the HEC-RAS simulation, Manning's coefficient is a mandatory parameter which represents the roughness of the riverbed and side channel. Estimation of this parameter is a controversial subject which may give many uncertainties and is subjective to users. Another research study done by (Rickenmann & Recking, 2011) shows that Manning's coefficient values for shallow water are more agreeable with the flow rate than the velocity and the water depth. They evaluated flow resistance in different gravel beds and observed that Manning's roughness coefficient values are low, relative to water depth and have a more positive proportion with grain diameter (Rickenmann & Recking, 2011). Likewise, the study relies that Manning's coefficient being effective for a deep mildly sloping river, but using this equation on shallow and sedimented rivers is unreliable and may give a large error in using HEC-RAS computations (Theses & Sharkey, 2014).

Further model instability can be caused when hydraulic computation of the HEC-RAS simulation is computed with too low a Manning's coefficient on the shallow the river, rapid flow, and supercritical flow. The following equation (Dr. Robert Jarrett's equation) is commonly used for a steep river reach where Manning's coefficient is in direct proportion with the energy slope (s_f) and has an inverse relation with hydraulic radius (R in feet) (Theses & Sharkey, 2014).

$$n = 0.39 s_f^{0.38} R^{-0.16} \qquad \textit{Equation 3-6}$$

Additionally, Brunner declared more ways of finding Manning's 'n' estimation, such as field observation photos of calibrated streams and calibration of observed profiles (G. W. Brunner, 2008). However, he specified that an observation-calibration method is the best method for an experienced water resource engineer (G. W. Brunner, 2008), even though there are many uncertainties when try to obtain proper roughness in each river section (G. W. Brunner, 2008).

3.1.1.4 Model Instability Due to Low Flow

Generally, hydraulic models are not desired to compute low flow events. The HEC-RAS instability can be caused by low flow computation in pool and riffle river arrangements. Brunner stated that hydraulic simulation of a steeply sloped river with low flows can be stable when the roughness coefficient is increased and the model run as a mixed flow regime (Theses & Sharkey, 2014).

3.1.1.5 Time Step

The HEC-RAS solves hydraulic parameters based on the Saint-Venant equation, in which flow parameters are a function of a change of time. Correspondingly, the magnitude of the time step influences the quality of the simulated hydrography shape and can give rough velocity values (G. W. Brunner & CEIWR-HEC, 2016). The HEC-RAS computation carried out by applying too long time steps leads to incorrect model results and could decrease simulation time (Theses & Sharkey, 2014). Applying the Courant number, where variable time step value depends on the change of wave velocity and grid size, can stabilize model, and give more precise computation results. However, such time steps can increase simulation time (G. W. Brunner & CEIWR-HEC, 2016).

Research done by G. W. Brunner, (2008) shows that using a large Courant number can cause model instability. Further, Burner identified model instability due to a Courant number being more sensitive on a middle big river reach than in a short reach. Consequently, computational time step (△t) can be appraised from the flood wave rise time (Tr) (Theses & Sharkey, 2014).

$$\Delta t \leq \frac{Tr}{20} \qquad \textit{Equation 3-7}$$

3.1.1.6 River Slope

In fact, one goal of this paper is to evaluate the suitability of the HEC-RAS simulation in a steep river. However, some issues which were raised from previous research studies are included in this s ection. A stream classification analysis, rivers with more than ten percent slope are classified as very steep rivers. Those with a four- to ten – percent slope are classified as a steep slope (Rosgen, 1994). Sturm defined a river section with approximately five to six percent of gradually varied flow as a steeply sloped river (Sturm et al., 2010). Also, a user's manual mentions that HEC-RAS computation on greater than ten percent of bed slope can cause model instability.

3.2 TELEMAC-2D

TELEMAC is a noncommercial computer program and it is mainly applicable in a river, marine, fluvial, coastal, estuarial, and lacustrine to computational water flows in 1-D,2-D and 3-D (Cooper, 2010). In this paper, a 2-D modeling package river simulation was used to compute the inundation area and other hydraulic variables for both case studies. The TELEMAC-2D software was founded by the National Hydraulics and Environmental Laboratory (Laboratoire National d'Hydraulique et Environnement - L9NHE) of the Research and Development Directorate of the French Electricity Board (EDF-R&D). Depending on a Saint-Venant equation of surface water flow, which came from the Navier-Stokes flow equation, TELEMAC-2D can solve shallow unsteady flow (Cooper, 2010; Mino et al., 2006).

$$\frac{\partial v}{\partial t} + (v.\nabla)v + g\nabla(z_0 + h) + \frac{n^2 g v|v|}{h^{4/3}} = 0 \qquad \textit{Equation 3-8}$$

$$\frac{\partial h}{\partial t} + \nabla(hv) = 0 \qquad \textit{Equation 3-9}$$

here, v represents 2-D water depth along cartesian coordinates, h is flow depth; Z_0 represents a flow channel bed elevation; g is acceleration due to gravity; n represents Manning coefficient values; and t is time.

The above equations, which the applicable for TELEMAC- 2D computations in this study, are not included phenomena such as turbulence: Coriolis force; the effect of atmospheric pressure such as rain; wind and evaporation; effects of temperature and salinity gradients; tracer diffusion; and porosity occurrence.

Moreover, more discussion of TELEMAC-2D was involved in the next chapter.

4. CASE STUDIES

As described in the introduction, the main objective of this study was to evaluate the suitability of two hydraulic models for a mildly sloping and a steep river, along with discovering how the river gradient influences the accuracy of the hydrodynamic modeling. To achieve this goal, two Norwegian rivers, namely the Surna river which has a mild slope, and the Vekveselva which has a steep slope, were selected.

4.1 Surna River Study Reach

The Surna river has a mild slope calm flow, and it is 45 km in length starting from Rindal municipality (Trøndelag county) to an outlet in Surnadalsöra, Møre og Romsdal county, in central Norway. It is a regulated river due to the Brandåå, Kysinga, Gryta, Gråsjø, and Trollheim hydropower plants which were developed on it (Anonnser.nu, n.d.; Neachell, 2014).

Hydraulic modeling in the Surna river was carried out on the approximately 17.17-km river reach. The Vs-Skjermo gauging station was selected for the upstream limit, and the Øye bridge was selected for the downstream limit. The upstream river reach was selected to include water flow from the Trollheim power plant in simulations, and the downstream reach location was assigned to prevent a tidal influence from the ocean, which may disturb hydraulic conditions of a downstream reach. Additionally, this study's outcome might be helpful for considering the further study environmental impact of the Trollheim power plant. Due to the environmental impact of developed hydropower pants on the demolishing of the Atlantic Salmon, where Salmon can migrate up to 56-km from the ocean, the Norwegian Parliament selects the Surna river for the national Salmon watercourse (Neachell, 2014). Hydrodynamic modeling for the Surna river carried out on the flow data form the Vs-skjermo gauge station (upstream limit)(Figure 4-1) and 14 tributaries: orange circled indicates the location at which estimated tributaries' flow data applied). For selected river reach, the mildly sloping with a 0.12% average slope rages from 0.03 to 0.34%; and the water depth is shallow for the scenarios tested; with 26.1 m.a.s.l. elevation at the upstream reach and 1.5m.a.s.l at the downstream reach.

Hydrological information obtained from http://nevina.nve.no/ indicates the Surna river is a perennial river, and Vs-Skjermo gauge station's (upstream study reach) catchment area covers 925

km^2 with 44.8 l/s km^2 annual specific run-off (Avrenning 1961-90 (Q_N); which is able to generate 41.44 m^3/s yearly mean flow. Air temperatures equal to 1.3 ^{0}c, 7.2 ^{0}c, and -2.9 ^{0}c were recorded for mean annual, summer, and winter air temperatures, respectively. Indeed, the water temperature in the river channel is a function of the turbine water temperature.

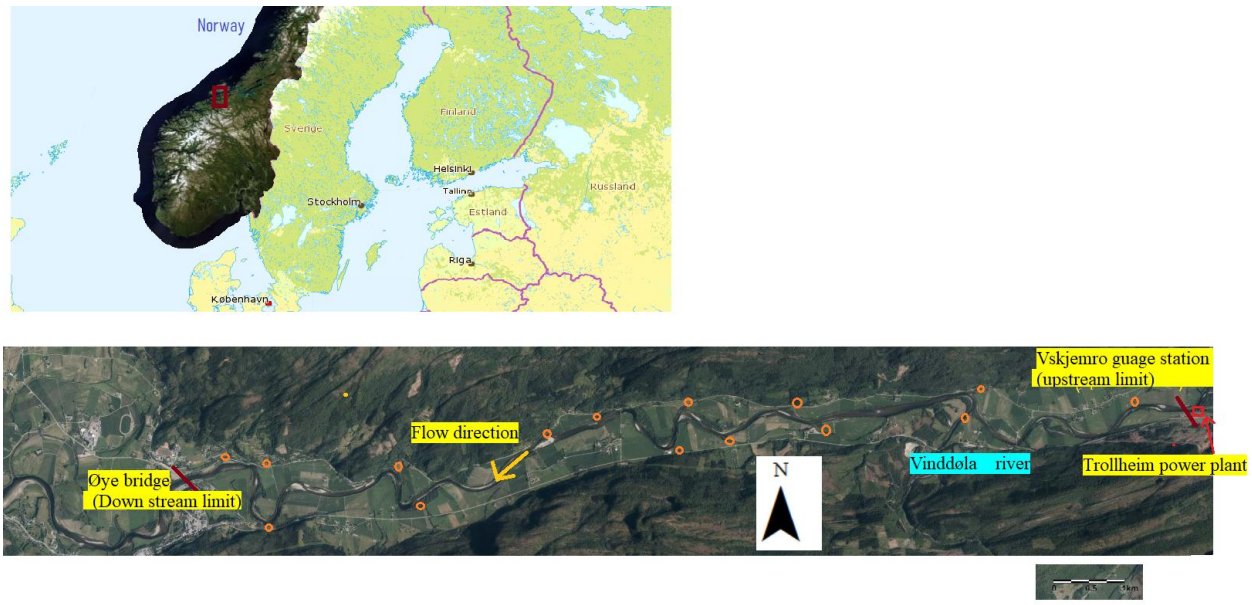

Figure 4-1: Surna river's study reach. As well as the boundary conditions, gauging stations providing the hydrologic data and surveyed areas for the model comparison are shown. Orange circle indicate the location of 14tributaries, dark-red line indicates the location of upstream and downstream limit and red rectangle indicate the location of Trollheim power plant. (Source https://www.norgeibilder.no/)

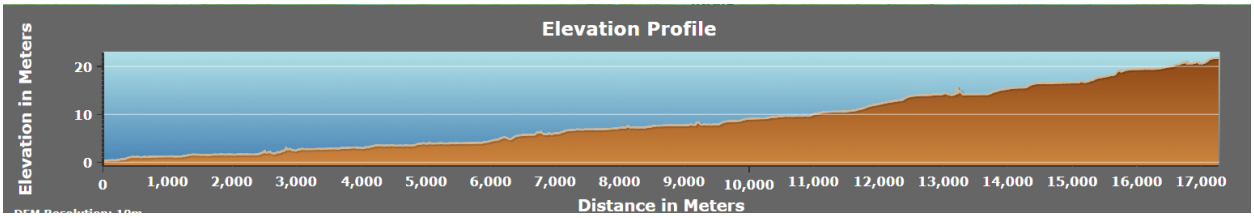

Figure 4-2: Elevation profile of the Surna river study area. Elevation profile of study area (source: https://hoydedata.no/LaserInnsyn/). The river reach slope varies from 0.03 to 0.34%.

4.2 Vekveselva River Study Reach

Vekveselva is a steep river starting from EU89 UTM33 6961067 N and 224278 E to EU89 UTM33 6953343 N and 222139 E. The highest elevation of the river is 1154.4 m.a.s.l. and lowest is 448.8 m.a.s.l. Vekveselva river is a Norwegian mountain river with steeped slope and sedimented with different materials (Engvik, 2011). Vekveselva river is a 12.8-km long river located in central Norway, particularly in the Oppdal municipality of Sør-Trødelag county (Sulebakk, 2017). The catchment area of the Vekveselva river covers 33km^2, which approximately generates an annual run-off 28.4 million m^3 runoff (Norwegian Water Resources and Energy Directorate 2016). The river Vekveselva is in a catchment area dominated by snow activity, and the river subjected to a significant flood event during snowmelt seasons (Sulebakk, 2017). The metrological data obtained from the Norwegian metrological Institute (2017) indicates that a mean 670 mm annual rainfall was measured in between 1971 -1990 (Sulebakk, 2017). The Vekveselva river is flow in between two hills that affected by glacial activity, and sediment materials starts from the hills (Sulebakk, 2017).

Extreme rainfall happened in 2003 caused massive slide and sediment materials eroded by this event clogged tunnel that transfer water to hydropower plant (Sulebakk, 2017). In 2007, Trønderenergi, the local power plant owner, constructed a sediment dam in the Vekveselva river, which has been grabbing sediments during the spring season and removed the deposits in means of excavation methods (AS, n.d.). The sedimentation dam built at 750 m.a.s.l.

In June 2011, large event, which is 100 -year flood event, was happened for over 8 hours. Due to this event, 2800 m^3 of sediments was transported to Vekveselva sediment dam. Furthermore, the event destructed Drive drainage network(Sulebakk, 2017).

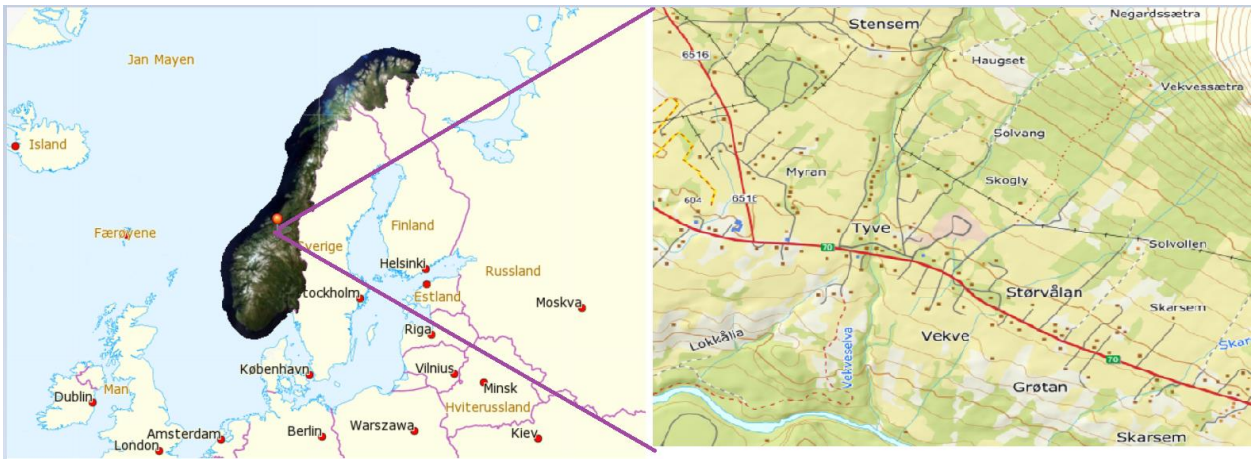

Figure 4-3: Vekveselva study area. Norway map (left-side) obtained from https://www.norgeibilder.no/ and Vekveselva river (right-side) map obtained from https://norgeskart.no/

High rainfall and snowmelt that delivers sediments from hill slopes and landslide events that changes river morphology Different river channel modifications were made to catch sediment and decreasing flow velocity during massive flow event (Sulebakk, 2017). These structures created ponds in the river section, which can influence hydrodynamic computation. Unfortunately, storage data such as volume, discharge coefficient, storage area, and other hydraulic data was not provided for this study, and storage locations were excluded from the hydrodynamic computation performed here.

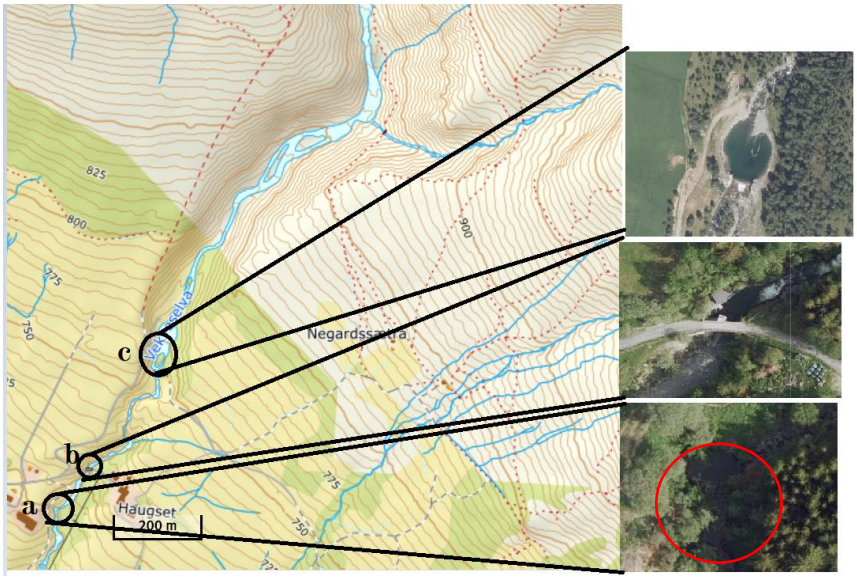

Figure 4-4: Aerial image format captured by Blom AS on16 September2014. a) pool water at EUREF89_UTM33_6955634N 222372E; b) river ponds at EUREF89_ UTM33_6955726N 222450E;and c) weir at EUREF89_UTM33_6956002N 222620E (source: https://www.norgeibilder.no/) (andhttps://norgeskart.no/)

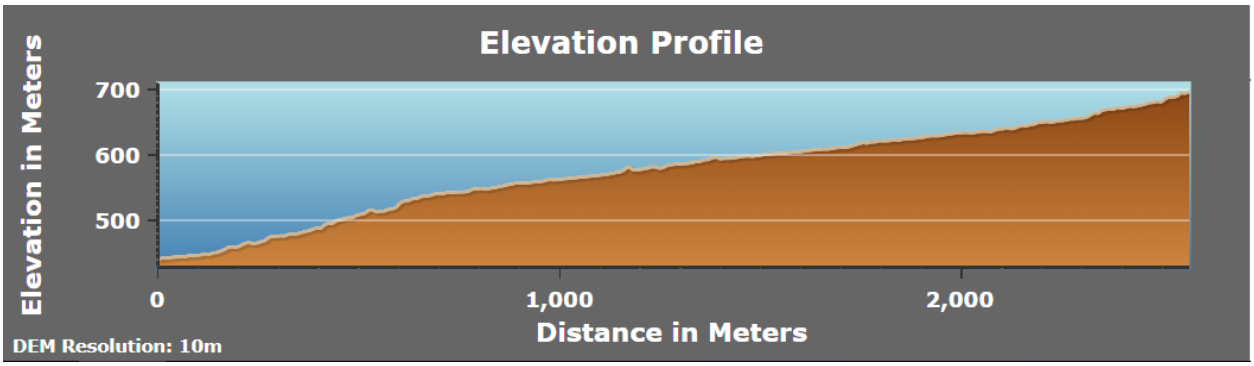

Figure 4-5: Elevation profile of Vekveselva river (14 % average slope)

On the other hand, an upstream section of the Vekveselva river was excluded from a hydrodynamic simulation due to a frequent landslide that occurred in this section which can reduce the accuracy of topographic data generated by LiDAR. Moreover, topographic data which is available at https://hoydedata.no/LaserInnsyn/ does not cover middle and downstream segments of the Velveselva river.

Figure 4-6: Land slide and sediment deposits upstream of Vekveselva. (source : https://www.norgeibilder.no/ and image on 16th September2016)

To sum up, the following river reach was selected for this study.

Table 4-1: Selected river reach for hydrodynamic computations

River reach name	**X and Y coordinates system: ETRS_1989_UTM_Zone_32N**		**Z coordinate system: NN 2000**
	Latitude	Longitudinal	Elevation
Upstream boundary	6944103N	529926E	680.55m
Downstream boundary	6943546N	529822E	624.54m

5. MATEIAL AND METHODOLOGY

Various hydraulic models have been developed globally to estimate flood events which will thus enhance decision-making, damage protection, and mitigation measurement (Bhandari et al., 2017). Some models can perform for 1-D,2-D, and 3-D hydraulic analysis, while some of them can only-compute for 1-D and 2-D. The one-dimensional (1-D) approach has been used for more than three decades (Seyoum et al., 2012), and many researchers use 1-D for research work and practical applications. Even nowadays, different 1-D models are still being developed. Some reasons behind using these 1-D models are that they are easy to set up, easy to use, and calibrate (Seyoum et al., 2012). For instance, 1-D models ignore some fundamental aspects of hydraulic computation, such as flow parameters, which vary only in one direction; and lateral diffusion is not included in numerical approaches. Also, the discretization of topography depends on the number of cross-sections rather than as a surface, and it is subjective to cross-section location and orientation (Abdullah et al., 2012). Researches studies have indicated that 1-D/2-D combination models can be more efficient than using 1D or 2D models for flood simulation (Abdullah et al., 2012).

The development of the 2-D approaches has decreased the application of 1-D approaches for flow computation (Bhandari et al., 2017). However, 2-D modeling contains more realistic numerical approaches with fewer assumptions than 1-D simulation (Usman, 2019). On the other hand, 3-D models are more complex and mostly used for short river reaches and consider flow waves.

Moreover, we select 2-D hydrodynamic models to evaluate hydrodynamic models' suitability for steep and mild slope rivers.

5.1 HEC-RAS 2D and TELEMAC-2D Models Selection

In general, river characteristics such as those which are topographical, morphological, and hydrological vary between rivers. Such conditions need to be improved in hydrodynamic models to get better simulated conditions at different points in time. Different users such as researchers, students, and designers want relevant and reliable models to determine hydraulic parameters such as flow, velocity, wave propagation, energy gradient and water cover area of a stream at specific flow event. Some of these models are uncommercial, while others may be user friendly. Such factors strongly influence the acceptance of models. The Hydrologic Engineering Center’s River Analysis System, or HEC-RAS, is a noncommercial and graphic user interface, or GUI model,

widely used in 2-D steady, unsteady, and fixed flow simulation(G. W. Brunner & CEIWR-HEC, 2016). F.E. Hicks and T. Peacock indicated that HEC-RAS has been widely used for unsteady flow regimes. Also, research made on the Peace River in Alberta, Canada verified that HEC-RAS is viable for unsteady flow simulation when compared with more advanced and sophisticated hydraulic models (Hicks & Peacock, 2005). In addition to the above benefits of using HEC-RAS, the model is widely used because it is accurate in flood risk forecasting and easy to use for new users (Theses & Sharkey, 2014). The TELEMAC is another model selected to compute a two-dimensional hydraulic variable for an unsteady flood regime.

This paper focuses on comparing two hydrodynamic models, HEC RAS 2D (version 5.0.7) and TELEMAC-2D (V8P0 parallel), for generating the extent of flood inundations and related hydraulic parameters. Moreover, the computation of hydraulic parameters, such as water depth and water surface elevation, is included in this paper. The selection of both models was based on the free availability of models, the familiarity of both models in practical use, and the vast difference of the computational configuration and algorithm between them.

5.2 Basic Data Requirements

Like other hydraulic models, HEC-RAS 2D and TELEMAC-2D also require four basic data inputs for computing hydraulic parameters and validating a result. These key data are: 1) topographic data that is used to build a geometry grid and connect river systems such as cross-section data, river reach length, water pond area, and its extent, and 2-D flow area and hydraulic structures in 2-D flow area rivers' junctions, contractions, and expansion locations that are the main issues in computing energy losses; 2) flow data that describes inflow discharge values and the hydraulic parameter condition at prescribed boundary conditions of a model; 3) channel roughness which is a subset parameter in a governing hydraulic equation; 4) validation data for evaluation reliability of a simulation.

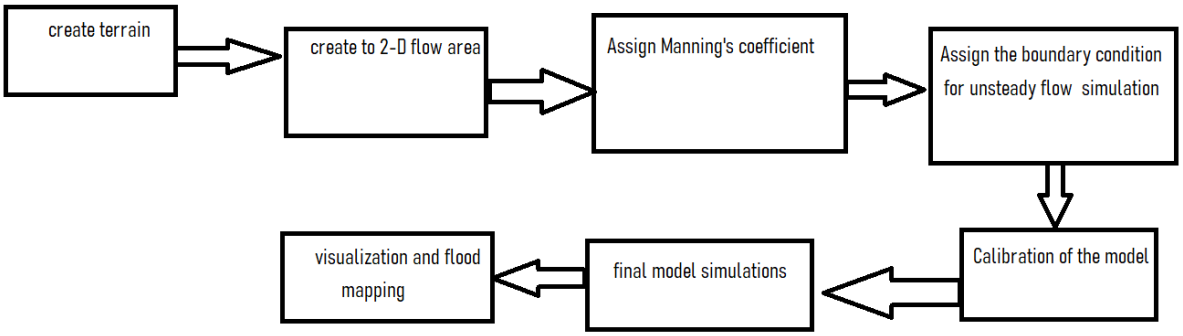

Figure 5-1: Stepwise methodology for HEC-RAS 2D and TELEMAC -2D analysis and flood plan mapping

However, due to the lack of data and the countrywide lockdown due to COVID-19, a calibration of the model based on observed data was not done, and this paper is missing a model calibration step.

5.3 Surna river Hydrodynamic Simulations

The goal of the hydrodynamic computations for the Surna river was to evaluate the hydrodynamic models' suitability for a mildly sloping river. This analysis was performed on unsteady flow simulation in HEC-RAS 2D using the wave diffusion equation and finite volume method. In the same way, TELEMAC-2D simulations of the same geometry and input data were computed based the numerical equation of the finite element method. Further, both models' performance was evaluated based on comparing inundation extent results extracted from both models with observed data. In addition, factors such as simulation time, complexity, user friendliness of the models and input data needed were considered for comparing both models.

5.3.1 Geometry Data

The Surna is a calmly flowing and mildly slope river. Two hydrodynamic models, HEC-RAS 2D and TELEMAC-2D were chosen to evaluate a suitable model for this river. Both hydraulic models' simulation of the Surna river starts from the Vs-skjermo flow gauge station to Øye bridge. The study area starts from a flow gauge station in order to obtain measured discharge values. Another reason for fixing an upstream boundary location is to include a flow from the Trollheim power plant outlet, and the downstream reach is selected to prevent backflow from the ocean. Both the

HEC-RAS 2D and Telemac-2D simulations of the Surna river are based on two basic input data: 1) geometric data that provides topographic information. This spatial data type is used to define the bottom river channel elevation, a flood plain area, the location of bridges, levees, riverside roads. 2) Topographic data is used to identify junction points of river tributaries and a main river.

Three 1x1m green LiDAR datasets were collected on the 20, 26 and 28 August 2016. These files contained both the water surface and the dry terrain for all three flights independently. The green LiDAR dataset contained 601,934,091 ".las" points, out of which 80.68% of the points were classified as ground, 17.40% as buildings and similar, and 1.92% as reserved; only ca. 0.001% of the points were never classified. The points were converted to a raster data format of 0.5x0.5m grid size.

However, the bathymetric data did not fully cover all river sections in any of the cases. The 20 August dataset was the most completed, and that for the 28th was the least completed, which made us exclude the data from 28 August from this study. The topographic datasets consist of the river reach locations, river section profile, bridge levee and bridge location, refinement areas, and other related objects that can influence the flow. On the other hand, the attribute data of the field observed inundation water edge and the corresponding water-covered area in each section of the river reach were described and mapped.

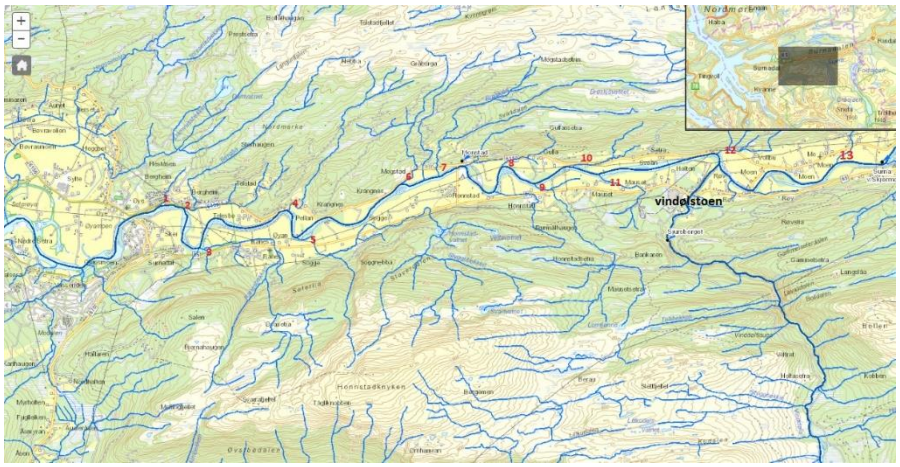

Figure 5-2: Surna river with tributaries

5.3.2 Flow Data

The preliminary hydraulic simulations were carried out on HEC-RAS 2D based on hydrologic data for both 20 and 26 August 2016. This enabled the analysis of the suitability of both datasets for further study. However, the inundation extent simulated in HEC-RAS 2D based on the 26 August event was better fit on observed inundation extent. However, insufficient observed inundation data availability for a further analysis on the 26 August (no observed inundation extent available except downstream zones). Subsequently, the study focused on the modeling the Surna river by applying an event on 20 August. Since the observed water-covered area collected during normal flow conditions and the flow area only covered the river channel, and estimated roughness values may not represent the flood plain characteristics.

The constant discharge measured at Vs-Skjermo flow gauging station used as upstream boundary condition. Moreover, the flow rates of 14 ungauged tributaries were used for additional boundary conditions. In the case of neither manual hydraulic measurement nor hydrological data given at the downstream boundary, personal judgment was taken in the simulation in both models. The tributaries discharge was transformed from Rina gauged station by using scaling method as follows:

$$scaling = \frac{q_u \, x \, A_u}{q_g \, x \, A_u} \qquad \textit{Equation 5-1}$$

$Q_u = Q_g$* scaling factor

Q_u = daily flow rate of targeted tributary

q_u = mean annual discharge of targeted tributary

A_u = catchment area of target tributary

q_g = mean annual discharge of gauged station

A_g = catchment area of gauged station

The annual flow rate of the Rina station was 1.3 and 2.37 m^3/s for 20 August 2016 and 26 August 2016, respectively.

Table 5-1:Measured and estimated flow data for the Surna river

Name or number of Boundary condition	**Discharge for a simulation of 20 Aug 2016 (m^3/s)**	**Discharge for a simulation of 26 Aug 2016 (m^3/s)**	**Remark**
Upstream/ vs_skjermo	21.06	22.64	gauged
1	0.005006034	0.009126	calculated
2	0.047219168	0.086084	calculated
3	0.372036148	0.678251	calculated
4	0.046131506	0.084101	calculated
5	0.173206672	0.315769	calculated
6	0.034533265	0.062957	calculated
7	0.117303639	0.213854	calculated
8	0.010887077	0.019848	calculated
9	0.081072645	0.147802	calculated
10	0.012236196	0.022308	calculated
11	0.011190368	0.020401	calculated
Vindølstoen tributary	4.09837977	7.471662	calculated
12	0.028070044	0.051174	calculated
13	0.096543938	0.176007	calculated
Rina gauged station	1.3(annual flow rate used for 20 August scaling)	2.37 (annual flow rate used for 26 August scaling)	gauged

In this study, a model calibration and validation based on measured velocity, water depth, or water surface elevation was not done due to the non-existence of measured data for calibration and validation. Uncertainty of roughness was handled by trial and error in HEC-RAS 2D and TELEMAC-2D simulation and the result was evaluated with observed inundation extent. The TELEMAC simulation was based on the Strickler equation by using equivalent roughness values

used for the HEC-RAS simulation. Another limitation of the Surna river simulations is that the observed inundation extents did not cover all river sections. In comparison, the 20 August observed inundation extent covers a large area, and 28 August covers a small area.

5.3.3 Comparison Methods

The performance of both methods was evaluated by comparing their precision against observed data. To do so, the same input data and model set-up was used for both HEC-RAS and TELEMAC-MASCARET.

The examination of the accuracy of models was carried out based on water cover area simulated in both HEC-RAS 2D and TELEMAC-2D models, and evaluation was made based on the Root Mean Square Error (RMSE) and Mean Absolute Error (MAE). To compute RMSE values, modeled river sections were divided into 59 zones, and the corresponding inundation area of each section was calculated.

5.3.4 HEC-RAS 2D Modeling for Surna river

Analysis in the Surna river was carried out by using an unsteady flow modeling and constant flow discharges at each boundary condition except the downstream point. The main goal of this task was to find representative roughness coefficient values of the Surna river and evaluate simulated water edges with bathymetry data (observed water cover area). Five single Manning's coefficients were used to compute five simulations to find the precise inundation area with the observed inundation extent. The inundation plain area obtained from the simulation was compared with the observed water cover edges that were observed at the same flow rate.

Some topographic data used in this simulation and the evaluation of the result files consist of two groups called spatial data, which are georeferenced with the UTM 1984-zone 32 XY coordinate system and NN2000_height vertical coordinates system. This data includes spatial data that indicates river reach locations, river section profiles, bridge levees, and bridge locations, refined areas, and other related objects that can affect flow. On the other hand, attributed data of the bathymetry inundation water edge was described and represented with spatial data and corresponding water cover area in each section of the river reach.

5.3.4.1 Model Set-up

A two-dimensional analysis and unsteady hydrodynamic simulation were set up in HEC-RAS (v.5.0.7), recent version with the following procedures: early, two simulations computed on a gauged flow rate.

5.3.4.2 Terrain creation

Topographic data was based on the green LiDAR dataset and manual measured spatial 3-D values. LiDAR technology collects elevation information of an earth surface by illuminating a pulse from a laser light to the earth surface, measuring the reflected light based on the wavelength and return period (Arc Map, 2020). A 1x1m LiDAR dataset (LAZ dataset), projected with WGS 1984-32 North coordinates, were collected on 20 August 2016, 26 August 2016, and 28 August 2016. These files comprise a water line edge and dry terrain edge for all three days. Manually measured latitude, longitude, and elevation were merged with LiDAR data to fill a hole in the geometry. This ASCII file was also projected with the WGS 1984_32 North coordinate to keep the same projection with the LiDAR point cloud data.

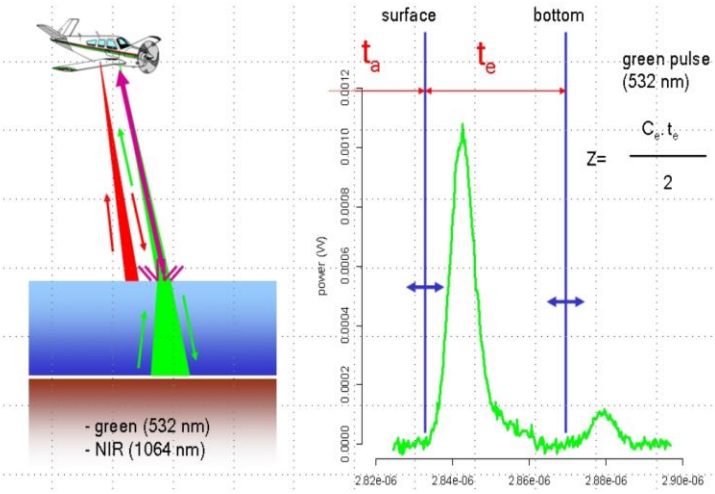

Figure 5-3: Principle of LiDAR survey (Populus, 2019)

The cloud LiDAR points were initially zipped by LAZ format, which was unzipped by LAS tools. La2las.ex is a bin subset of LAS tools used to transform the 20 August2016, 26 August 2016, and 28 August 2016 LAZ files to LAS data before being processed in ArcMap. Similarly, a manually measured ASCII (XYZ text) file was converted to LAS file format by a txt2las bin. A LAS (LASer) is a binary format developed by the American Society for Photogrammetry and Remote Sensing (ASPRS) for managing, collecting, and storing airborne LiDAR data. The LAZ format is a

compression algorithm which is used to compress and til LiDAR data (*LAS Point Cloud Format*, n.d.). All LAS transformed from LAZ files, and text files were stored in 'lasdataset' by using an Arc catalog spatial program. A LAS dataset file was converted to a raster data format with a 0.5 x 0.5 m grid size format using a spatial conservation tool called Arc toolbox, which was converted to a tagged image file format(tiff) before it could be processed in hydraulic models.

After adjusting the System International unit system (SI units), the first step in HEC-RAS was importing and loading a tagged image file format (TIFF) file to a RAS mapper. A RAS Mapper is a GIS tool used to convert raster grid format to GeoTIFF format with a specific spatial coordinate system. This coordinate system adjustment by tools called spatial reference projection. A created GeoTIFF file format is an automatic zipped file format that holds less storage than the original imported file due to a removable no data value. The consequences of tiling a file are that GeoTIFF helps a model to decrease a simulation time and increasing computation speed. Another advantage of the GeoTIFF file format is having a pyramid data storage format containing multiple terrain layers with varying resolutions (G. W. Brunner & CEIWR-HEC, 2016).

However, a developed terrain model by a RAS Mapper has a limitation on reflecting actual topography underwater. In the case of the Surna river, this problem decreased due to representing underwater topography data mapped by high-quality techniques called LiDAR surveying with green infrared. This problem can also be handled in RASMapper by modifying a terrain by interpolating a surface (G. W. Brunner & CEIWR-HEC, 2016). This method is also useful for removing a flow blockage from the flow channel.

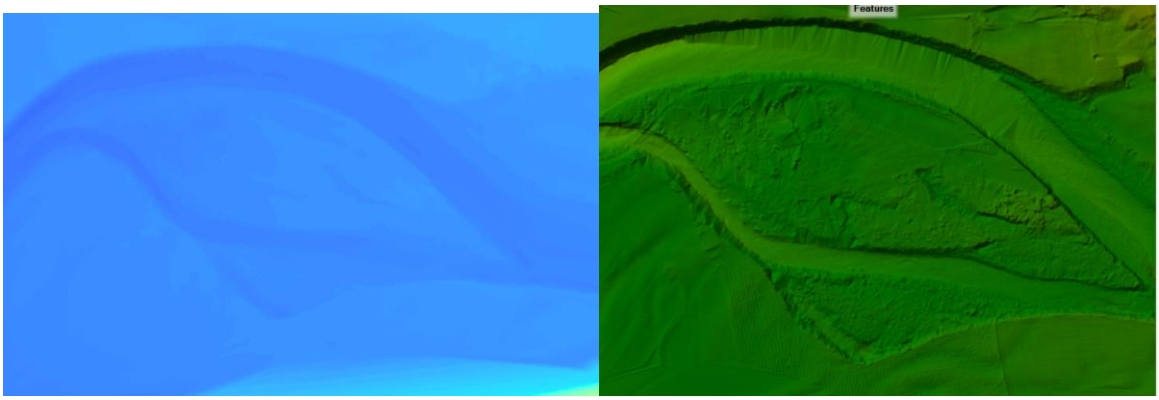

Figure 5-4: TIFF file (left-side)and GeoTIFF file (right side) created by a RASMapper

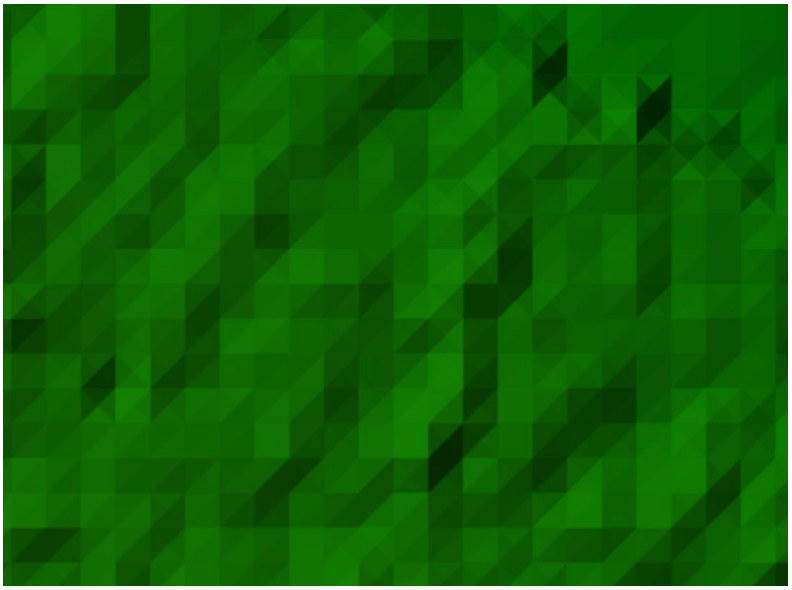

Figure 5-5: Tiled and pyramid data structured by a RAS Mapper

5.3.4.3 Geometric Data

The HEC-RAS comprises a geometric data tool which is used to create a structured and unstructured computation mesh. These non-overlapping polygons are sets of three to eight side cells. Further, the creation of a mesh enables the model algorithm for finite volume simulation. However, the accuracy of the computation results depends on the mesh resolution extent due to the HEC-RAS simulation being based on a finite volume method, which is influenced by cell size (Pinos & Timbe, 2019). This challenge can be managed by using break lines and refinements in essential sections (G. W. Brunner & CEIWR-HEC, 2016).

Relatively, hydraulic computation done on smooth mesh can achieve more accurate results than that performed on a coarser grid size. Around 1.9 million cell numbers are generated for a defined flow area created from a 1.05 x 1.05 m grid cell size along the 2-D flow area, and a 0.8 x 0.8 m refinements mesh size. Also, the performance of the finite volume algorithm was increased by applying break lines. A refinement mesh was used place on islands in the river and riverside, where there was a rapidly changed bed slope. Increasing the mesh resolution helps a finite volume algorithm to compute a hydraulic parameter on a small grid volume.

Furthermore, break lines were placed along the levee, the shores of islands, roads, and bridges. The main purpose of applying break lines was to keep a flow in the channel until it got high enough to overlap any ground berm along the pathway. However, HEC-RAS does not perform well when

the total mesh number in the 2-D flow area is more than two million. Moreover, coarser mesh sizes tend to reduce simulation time, but the results generated from these mesh size computations can decrease accuracy.

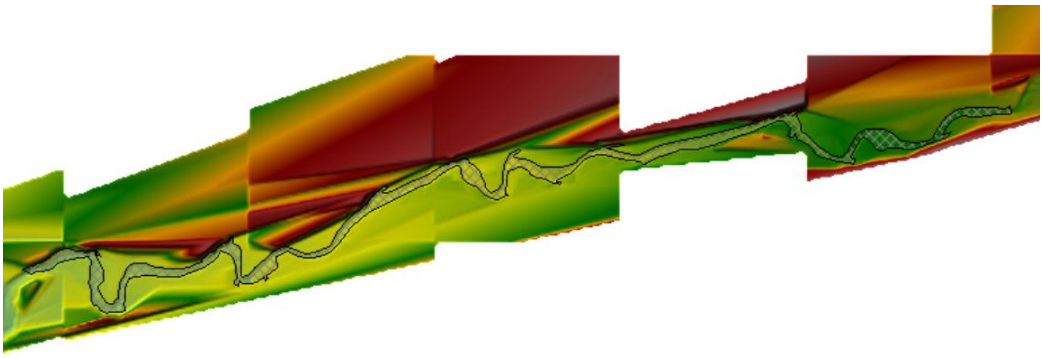

Figure 5-6: 2-D flow area of Surna river

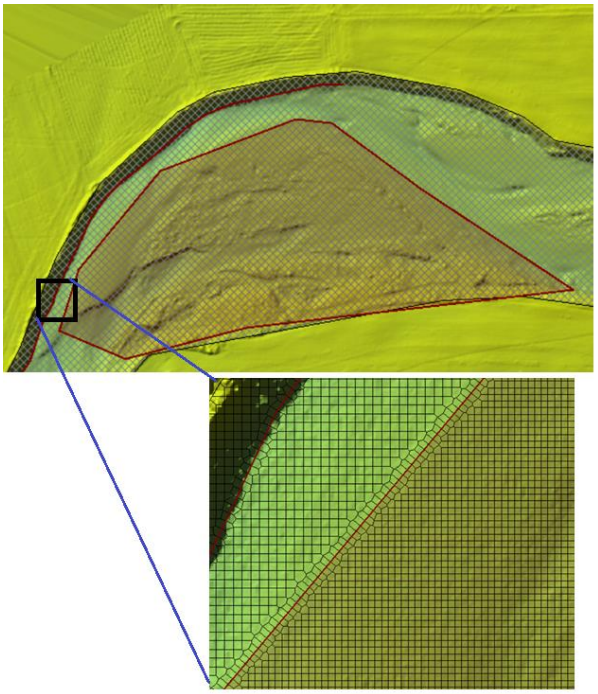

Figure 5-7: Break line at rapidly changing section (levee) and refinement regions

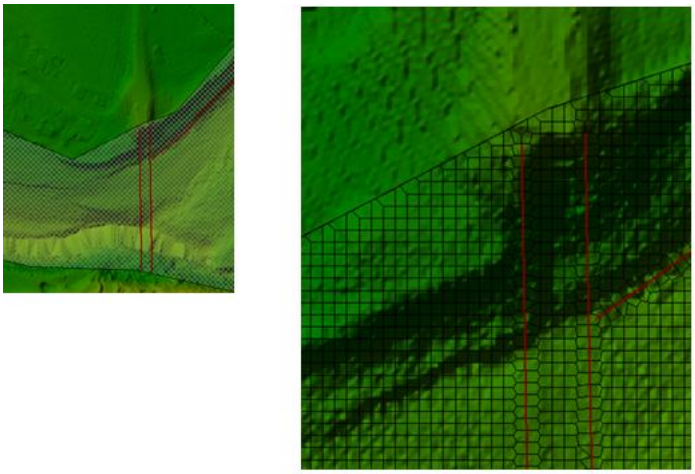

Figure 5-8: Applicable break line at bridge

5.3.4.4 Roughness Coefficients

Hydraulic computations comprise two ways of energy losses: 1) friction loss which is associated with velocity head and roughness bed channel; 2) single losses that are related to contraction and expansion of flow channel, bridge, and culvert's energy losses coefficients, shape and types of structures built in the river, energy losses at river bend, energy losses at the entrance and exit conditions. The selection of appropriate coefficients related to these factors plays an essential role in various flow applications and hydraulic models. Chow indicates that flow condition and channel types are affecting roughness coefficients values, and these values are not constant through river cross-section and change of spaces. So, predicting and evaluating representative roughness coefficients is a creative and complex task (Shamkhi & Attab, 2018). Whereas Manning's coefficient 'n' is a parameter used to reflect a flow resistance coefficient in the HEC-RAS model. However, the roughness coefficient value is highly variable. It depends on channel roughness, cleanliness of the channel bottom, availability of sediments and deposit materials, types of vegetation on a flood plain, and density of brush on flood plain and alignment of channels (Chow, 1959).

For the Surna river, HEC-RAS 2D computation involves a diffusion-wave equation. River channel river roughness is considered in the form of a diffusion-wave moment equation and can be defined in the continuity equation: -

$$\frac{\partial H}{\partial t} - \nabla \left(\frac{(R(H))^{\frac{2}{3}}}{n\,(\nabla H)^{\frac{1}{2}}}\,\nabla H + q = 0\right) \qquad \textit{Equation 5-2}$$

where V is a vector flow velocity, n represents Manning's coefficient; ▽H is partial differential of water surface level; R is a hydraulic radius; and q represents flow source or sink.

The HEC-RAS reference manual advises using a 0.025 to 0.06 for the Surna river because it is characterized by a clean bottom, a mild slope, a flat cross-section, and shallow water depth. After five simulations were done by using 0.025, 0.03, 0.045, 0.05, and 0.06 of Manning's coefficient, the best fit was statistically evaluated by using the RMSE method.

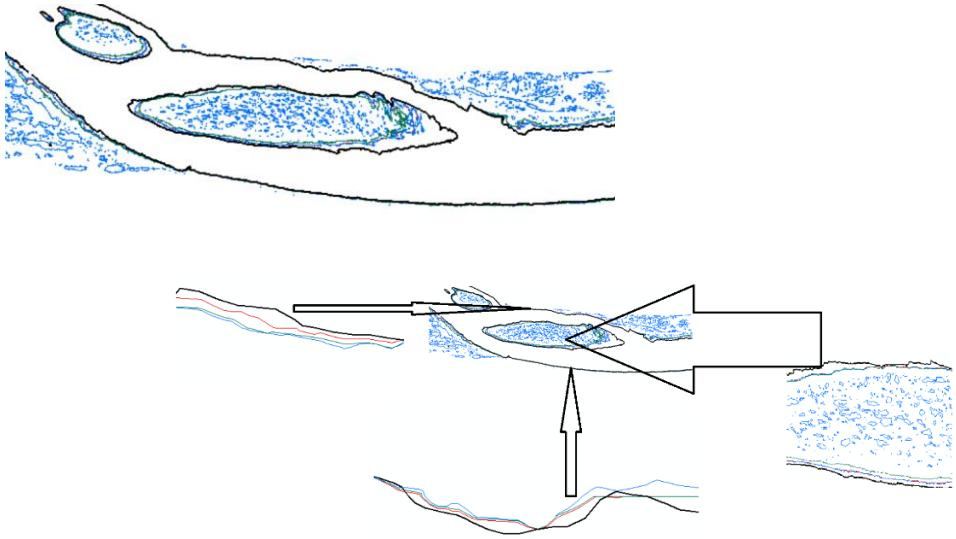

Figure 5-9: Simulated water edge lines and observed water edge line for the 20 August 2016 flow event. Black line represents observed water line; green line represents simulated water edge line by using n=0.045; red line is simulated water edge line by using n=0.05; blue line is simulated water edge line by using n=0.06; n represents Manning's coefficient value.

5.3.4.5 Boundary Conditions

Since the Surna river is a long-reach length and dynamic flow occurrence, unsteady flow simulation was selected to calculate the hydraulic parameters. Flow hydrography upstream and at the tributaries and normal depth downstream was defined in the unsteady flow data tool. Normal depth was assumed at the downstream boundary conditions due to no flow parameter measured or identified at downstream river reach. A 0.01 friction slope was considered to access the Manning equation to compute normal depth. In principle, steady flow implies that the bed slope is equal with a slope so that a user can use a bed slope as a boundary condition. However, this principle is

not valid for unsteady flow due to the energy grid line that varies with the change of time not being parallel with the bed slope (G. W. Brunner & CEIWR-HEC, 2016).

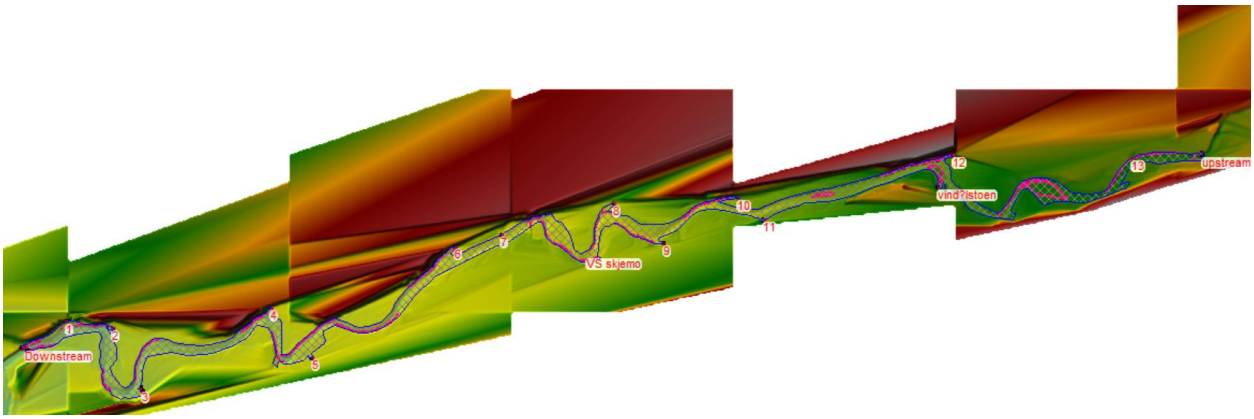

Figure 5-10: Boundary conditions' locations and their ID number/name

5.3.4.6 Perform Unsteady Flow Simulation

HEC-RAS comprises mass conservative (Equation 3-1)and the diffusion -waveform of the moment equation to compute hydraulic variables (Kayyun & Dagher, 2018). The unsteady form of 2-D computation is described by a differential form of a continuity equation with respect to change of time and two directions. For the Surna river, the diffusion wave equation set was chosen since a diffusion equation can decrease simulation time and has more stable properties than Saint-Venant equations. The diffusion-wave moment equations is defined as following: -

$$g_{\nabla H} = c_f v \qquad \textit{Equation 5-3}$$

where g is an acceleration gravity; c_f represents channel bed roughness friction; and ∇H is the vertical partial differential of the water surface level; -g∇H is equivalent with Manning's formula: -

$$-g_{\nabla H} = \frac{\{n^2 g|V|}{R^{\frac{4}{3}}})V \qquad \textit{Equation 5-4}$$

n is Manning's coefficient; R is a hydraulic radius that is the ratio of a cross-sectional area and wet perimeter and V is velocity.

Indeed HEC-2D can compute either steady or unsteady simulations. However, the unsteady flow type was selected for this study because one of the study goals was to calculate variable velocity, water depth, discharge, and other hydraulic variables values along an x and y-direction. The HEC-RAS 2D unsteady simulation comprises three interdependent programs for running targeted simulations. All Surna river simulations contain a set of the programs for the geometry preprocessor, unsteady flow simulation, and post-processor.

5.3.4.7 Simulation Time

As described in the previous sections, the Surna river simulations were computed on 17.17-km-long section and with more than 1.8 million cells with an average 1.05x1.05 grid cell size and 0.8 x 0.8 m average mesh size in the refinement regions. Indeed, noisy cell numbers and smooth cell grid sizes increase computational time. Also, the computational time is the most crucial parameter which can affect result quality. Small computation time interval and smooth grid size simulations give more accurate results than those of computing by using long time intervals and rough grid sizes (G. W. Brunner & CEIWR-HEC, 2016). Further, using a fixed time step could decrease result accuracy(G. W. Brunner & CEIWR-HEC, 2016). Thus, all HEC-RAS simulations in this paper were performed based on numerical criteria called the Courant condition. The HEC-RAS user manual describes using the Courant number time step as giving the best numerical condition due to the variable time step magnitude depending on cross-section spacing (grid cell size) and flood wave velocity. However, using the Courant number for a simulation can force a model to run longer. The Courant condition equation is defined as the below equation (G. W. Brunner & CEIWR-HEC, 2016):

$$c = \frac{v\Delta T}{\Delta X} \leq 1 \qquad \textit{Equation 5-5}$$

where, C is a Courant number; V is flood wave velocity; $\triangle$T is computational time and $\triangle$x is an average cell grid size. A study indicates that less or equal to one (=<1 with maximum 3) Courant number is applicable for a full momentum equation (Saint-Venant equation) .One can use up to 2 with a maximum 5 for a diffusion wave equation (G. W. Brunner, 2016).

Thus, the following computation time settings were used for all simulations.

- ✓ Computational time interval =5 sec
- ✓ Maximum Courant = 0.5 sec

- ✓ Minimum Courant = 0.2 sec
- ✓ Number of steps below minimum before doubling = 2
- ✓ Maximum number of doubling base time steps = 2
- ✓ Maximum number of halving base time step = 2

In addition, a 30-minutes time interval was assigned for a detailed output interval, hydrograph output interval, and mapping output interval to, write out the water surface profile and flow at a specific range, define the flow hydrography result, and the visualize output result which is displayed on a RAS Mapper, respectively.

5.3.4.8 Assumptions and inaccuracy

The following assumption were made in the computing HEC-RAS 2D for the Surna river: -

- All simulation was done by using the single Manning's values throughout each grid cell.
- Vertical velocity and other flow parameters' derivation was neglected (2-D flow computation)
- Energy head computation was computed at the cell center
- The correctness of the tributaries discharge transformed from the gauged station to the ungauged station by runoff map, and correlation relation methods are in doubt.

5.3.5 TELEMAC-2D Modeling for Surna River

As explained earlier, the primary goal of the hydrodynamic computation for the Surna river was to evaluate the performance of HEC-RAS 2D and TELEMAC -2D in a shallow and mildly sloped river. The same river reach, corresponding flow data, and identical boundary conditions were allocated for both HEC-RAS 2D and TELEMAC-2D. The same as for HEC-RAS 2D simulations for the Surna river, five TELEMAC-2D simulations were computed based on 16.67, 20, 22.22, 33.33, and 40 Strickler roughness values that are equivalent with Manning's coefficient 0.06,0.05, 0.045,0.03 and 0.025, respectively.

A finite element method was applied to solve a partial differential equation of TELEMAC-2D, also known as a Saint-Venant equation (Sauvaget et al., 2000), which commonly used to solve shallow water equations, applies to compute hydraulic parameters on an unstructured grid.

5.3.5.1 Extracting Topographic Data and Creating a Geometry File

In order to get a similar riverbed elevation profile, the topographic data utilized for hydrodynamic computation in TELEMAC -2D was obtained from the terrain data that was generated by RAS Mapper of the HEC-RAS. The TIFF formatted file was exported from a terrain, which was created by the RAS Mapper, and further converted to an ASCII file by using a conservation tool of QGIS. The ASCII (American Standard Code for Information Interchange) is a formatted text file that contains the XYZ point set that represents topographic data of the selected domain. Likewise, the XYZ file is a tabular formatted point set file containing x, y, and z coordinates of a node (Selméus, 2018).

Further, the XYZ file was imported to BLUEKENUE to create the geometric file domain of the selected river reach. The BLUEKENUE advanced tool was created by the Canadian Hydraulics Centre of the National Research Council Canada. It is an advanced program which is used for pre- and post-processing of hydraulic models (Selméus, 2018). In this study, the program was used to prepare geometry data, boundary condition files, and visualization of TELEMAC results.

5.3.5.2 Domain and Grid Characteristics of Geometry File

The same as in the simulation in HEC-2D, an upstream limit of the TELEMAC 2D simulations was at Vs-skjermo and the downstream boundary was located at the Øye bridge. The geometry file was created by using hydraulic analysis software called BLUEKENUE. This tool uses a mesh generator algorithm to generate a non-structured grid that has 1230781 nodes and 2445124 triangular elements. For a selected domain, a default edge length of 1.5 m and 1.2 edge growth ratio, 1 m edge length of density object (the same as refinement region in HEC-RAS), and 0.5 m edge length of soft lines were utilized. Four density areas with a 1-m element length were applied to refine the mesh at the shore area of the islands and four soft lines were applied to the smooth mesh size at roads. A created mesh was interpolated by XYZ file to generate the BOTTOM variable of the SELAFIN file. An advantage of decreasing mesh size is to refine numerical computation at complicated topography, and this decreases computation time.

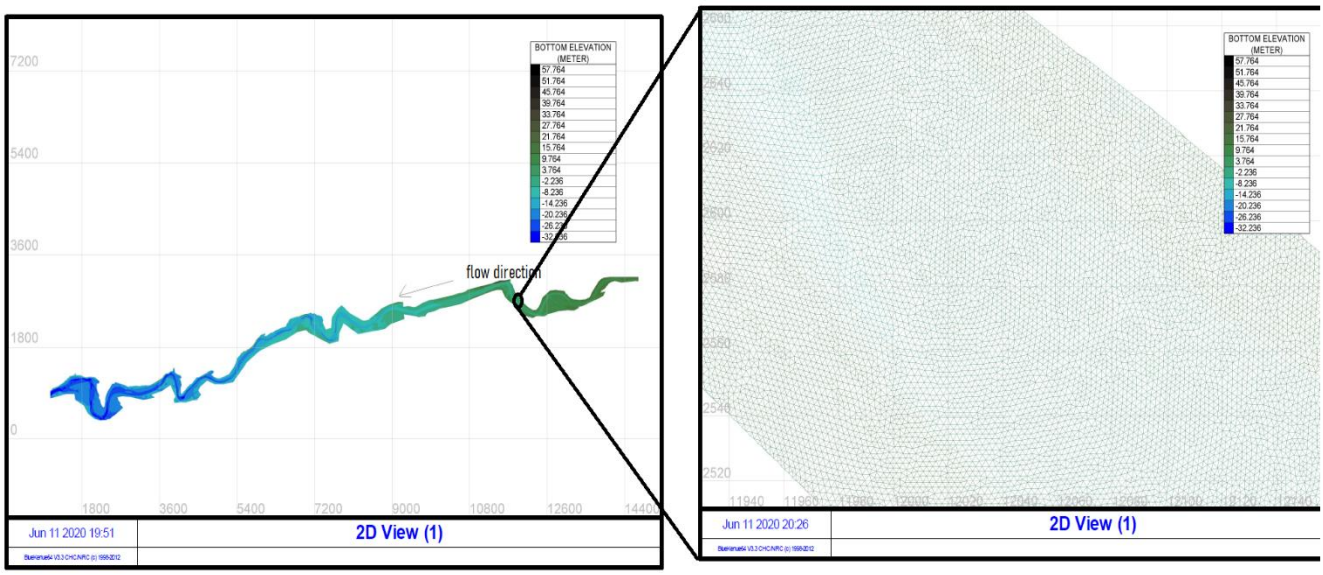

Figure 5-11: BOTTOM variable geometry (computational grid of the mathematical model)

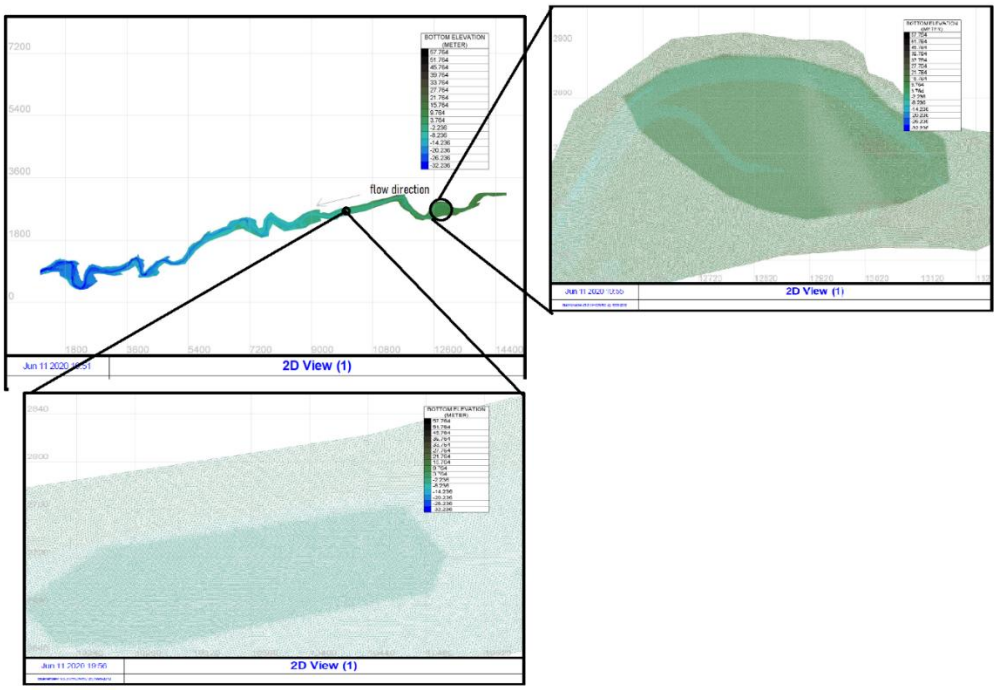

Figure 5-12:Density (refinement) area of computational grid of the mathematical model

5.3.5.3 Boundary Conditions

The boundary condition file was also created in BLUEKENUE. BLUEKENUE has a special program that uses to generate a finite element mesh of boundary conditions (CONLIM), creating a boundary segment and defining the type of boundary code(Alta, 2018).

In the Surna river, the boundary conditions were imposed in 15 inflow data, including upstream and the tributaries' inflow (Table 5-1) along with downstream boundary conditions. These boundary segments were created at the same location as those defined in the 2-D flow area of HEC-RAS. Moreover, an open boundary with prescribed flow was applied for upstream boundary limit and tributaries, and constant ordinate hydrography and the same flow data used for HEC-RAS 2D simulations (Figure 5-10) were assigned. At the downstream limit boundary condition, an open boundary with prescribed elevations was applied to define the bottom elevation at the lower limit section. A synthetic downstream boundary condition was considered based on the bottom elevation at selected boundary segments. Thus, selected open boundary prescribed elevations were reflecting an elevation of a selected boundary segment and preventing unnecessary constraint of the models. However, better simulations can be applied if the field measurement of the flow parameters is taken and used for downstream boundary conditions. In addition, field measurements of the stage-discharge curve, velocity, and other hydraulic paraments at different river sections can be used as a control section that improves model performance, increases simulation stability, and gives more accurate results.

In general, BLUEKENUE creates two different format files, namely cli and bc2, whereas the cli file is further used for input values of 'BOUNDARY CONDITIONS FILE' keyword.

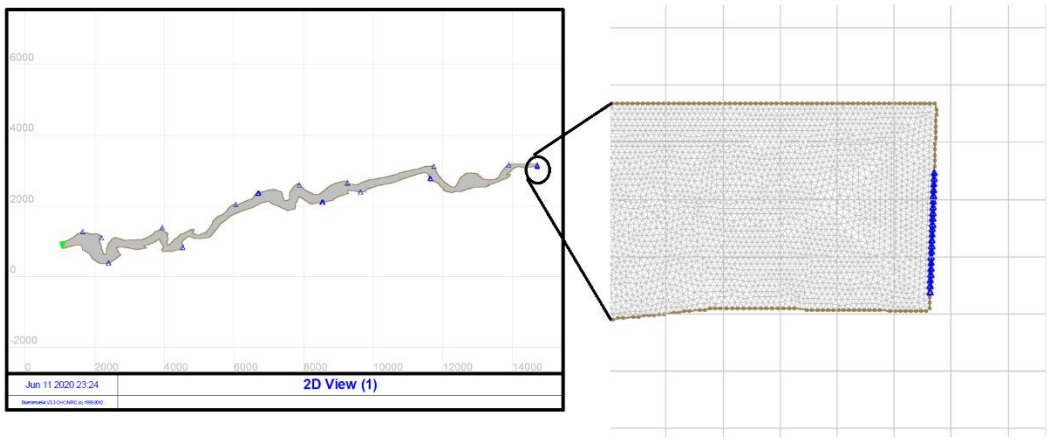

Figure 5-13: Finite element mesh and boundaries segments; green line is an open boundary with prescribed depth of downstream boundary; and blue lines imply an open boundary with prescribed flow of upstream and tributaries boundary conditions

5.3.5.4 Creating Steering File

The steering file is mandatory in a TELEMAC simulation. It contains the computational configuration, such as input directory, numerical equations, physical parameters, solver types, and other computational parameters (Ata, 2018). Steering file is a text file with 'cas' format that can be created by EDAMOX, FUDAA PRE PRO, or directly by a text editor; it represents the control panel of the hydrodynamic in domain computation (Telemac, 1999). This text file contains keywords with assigned values and directory input files (Telemac, 1999).

5.3.5.4.1 Hydrodynamic Simulation

The TELEMAC-2D user V8P0 manual declares that the initial state, from which the model starts a computation, must be defined by the user. In the Surna river simulation, constant water depth was assigned to describe the initial condition. A 0.001m is systematically chosen to describe the initial water depth and linked to 'INITIAL DEPTH' keywords. A small initial water depth is used to decrease the computation time. The suggested initial condition can be improved by modifying the initial water depth (0.001 m) at each iteration. It can be done by applying the 'INITIAL GUESS FOR H' (depth) and 'INITIAL GUESS FOR U' (velocity) equation. In the Surna river simulations, the initial value of the change of depth and velocity was defined as follows (Ata, 2018):

$$DH = Hn + 1 - Hn \qquad \textit{Equation 5-6}$$

$$DU = Un + 1 - Un \qquad \textit{Equation 5-7}$$

where DH and DU represent change of water depth and velocity, respectively; Hn+1 and Hn represent water depth computation values at consecutive time steps. Likewise, Un+1 is a velocity at 't +1' time and Un is a velocity value at the previous time step.

The constant hydrographs from the discharge value (Table 5-1) were defined boundary conditions of upstream and the tributaries. Whereas a -26.6 m (bottom elevation at a downstream boundary) segment was defined a 'PRESCRIBED ELEVATIONS' of the downstream boundary condition. Furthermore, the 'VELOCITY PROFILES' launched with the velocity vector are normal to the boundary conditions where flowrate value is set to 1 and multiplied by a constant to get nominated discharge (Ata, 2018).

5.3.5.4.2 Physical Parameter

The TELEMAC 2D user manual implies that a number of physical parameters are mandatory for most simulations. These parameters may be space-dependent, sometimes they can defined with a mesh, and then the parameter is also defined with a function of zone number (Ata, 2018). Frictional law, which uses to compute hydraulic variables, is a mandatory equation in hydraulic computation, and various equations have been developed to estimate hydraulic parameters. For the Surna river, Strickler's law was assigned to perform hydraulic computations. This equation was explained by a keyword, namely 'LAW OF BOTTOM FRICTION' and the roughness value was defined by the 'FRICTION COEFFICIENT' keyword. Generally, Strickler's law is equivalent to Manning's equation (Equation 5-8) (Olivier et al., n.d.). The only difference between them is that manning's coefficient value is reciprocal with Strickler's relation coefficients.

$$U = \frac{1}{n} J^{\frac{1}{2}} \; R_h^{\frac{2}{3}} \qquad \textit{Equation 5-8}$$

$$k = \frac{1}{n} \qquad \textit{Equation 5-9}$$

where U is a flow velocity; n is Manning's roughness coefficient; J is river slope; R_h is the hydraulic radius; and k represents Strickler's relation coefficients.

Like HEC-RAS 2D modeling for the Surna river, a single roughness coefficient, which was constant in time and space, was assigned in TELEMAC-2D computations. Since the goals of the Surna river hydrodynamic modeling was to evaluate the performance of two models and to find

the representative roughness coefficient value of a selected domain, the same as in the HEC-RAS 2D computations, five simulations of the 20 August 2016 flowrate were performed by using 16.67, 20, 22.22, 33.33 and 40 Strickler's roughness coefficient.

Table 5-2: simulations and corresponding roughness coefficients

Name	**Flow event date**	**Manning coefficient value used in HEC-RAS 2D computations**	**Strickler's relation coefficients value used in TELEMAC-2Dcomputations**
Simulation 1	20 August 2016	0.06	16.67
Simulation 2	20 August 2016	0.05	20
Simulation 3	20 August 2016	0.045	22.22
Simulation 4	20 August 2016	0.033	33.333
Simulation 5	20 August 2026	0.025	40

5.3.5.4.3 Numerical Parameters

TELEMAC comprises three numerical parameters and the user can choose one among them using the 'EQUATIONS' keyword. These equations are namely (Ata, 2018):

- 'SAINT-VENANT FE'
- 'SAINT-VENANT FV',
- 'BOUSSINESQ'.

SAINT-VENANT FE' and SAINT-VENANT FV' are desired options in environmental numerical modeling of Saint-Venant equations and represent the finite element and finite volume method, respectively. Also, anyone who wants to compute hydraulic variables in the Boussinesq equation can utilize the TELEMAC program by means of 'BOUSSINESQ'(Ata, 2018).

As previously described, Galerkin's finite element method (GFEM), which solves the depth-average of shallow water equations, was selected to solve the hydraulic variables. Also, linear velocity and linear depth were used to specify discretization in space. In the case of a wave equation associated with free surface gradient compatibility, the TELEMAC-2D user manual advises that the value of the keywords 'FREE SURFACE GRADIENT COMPATIBILITY' is less than one for reducing suppression of spurious oscillations(Ata, 2018). This technique decreases

simulation time, but it reduces result accuracy(Ata, 2018). However, this limitation was handled by using smooth computations smooth sizes and applying wave equation; but is a technique recommendable for shallow and mildly sloping rivers with high-quality topographic data and refined grid sizes (Edf, 2000). A wave equation can optimize model stability and CPU time (Ata, 2018). A wave equation also includes a mass of lumping on depth and velocities; and applies explicit velocity diffusion. Both a mass of lumping on depth and velocities is suggested as diagonal mass matrices. In addition, the method of characteristics and conservative PSI-scheme, mass-conservative methods were applied in the 'TYPE OF ADVECTION' keyword. These methods are used to satisfy model stability conditions. An explicit scheme of advection velocity was applied to limit time-dependent problems in the PSI distribution scheme (Ata, 2018). Galerkin's finite element method (GFEM) encourages the domain to subdivide into finite elements(Edf, 2000) (Values, n.d.). A streamline-upwind-Petrov-Galerkin (SUPG) was applied to fix the scheme and adjust the correct Courant number for the simulation. For the Surna river simulations, four dimensions of SUPG were used. Namely, one of the no upwind scheme and three of an upwind scheme with modified SUPG. These techniques used advection of flow depth to decrease the spurious spatial oscillation in-depth to which Galarkin's methods are predisposed and no upwind scheme that eliminates advection of velocity, depth, and turbulence (Ata, 2018; Edf, 2000; Horritt & Bates, 2001). On the other hand, the maximum number of iterations computed by the solver was controlled by steady-state development. Whereas residual errors can be introduced at the downstream boundary with imposed water depth, this was handled by allowing CONTINUITY CORRECTION which enables in velocity correction at these points.

As discussed in above section (section 3.1.1.5) , an accurate result can be achieved by applying a low Courant value in numerical schemes and allowing a model to upgrade the computational time step at each iteration(Ata, 2018; Edf, 2000). However, this study contains big geometry: the computational domain covers 17.17 km with a smooth mesh size (1.5 m x 1.5 m), which contains 1230781 nodes and 2445124 elements, and the hydrodynamic simulation based on variable time took a long time. For instance, three weeks was needed to finish a TELEMAC-2D simulation by using a 0.5 Courant number. Further, a constant time step of 1 second, was assigned for all simulations.

For the Surna river simulation, the following options were applied for tidal treatment: 1) an option that tidal flats detect, and the correct free surface slope was applied. In this case, a movable boundary in nature (tidal) was detected with a drying and wetting algorithm, eliminating spurious surface slopes at shorelines (Horritt & Bates, 2001). 2) Treatment of negative depths was done by flux control that strictly ensured positive depths (Ata, 2018), which computer software considers zero for a threshold of negative depths. Likewise, the formation of radial acceleration and centrifugal forces act in a tilted radial water surface, where pressure force lower than centrifugal force in the shallow river was prevented. Therefore, there was no formation of secondary currents in Surna river simulations.

5.3.5.4.4 Assumptions and Inaccuracy

The following assumptions were made during the TELEMAC-2D computation for the Surna river:

-

- All simulation was done by using the single Manning's values throughout each grid cells.
- Vertical velocity and other flow variables' derivation was neglected (2-D flow computation).
- Energy head computation was computed at the cell center.
- A constant time step was applied. However, a variable time step used for the HEC-RAS 2D simulations.
- The correctness of the tributaries discharge transformed from the gauged station to the ungauged station by the run-off map, and correlation relation methods are in doubt.

5.4 Vekveselva River Hydrodynamic Simulations

This section evaluates the suitability of hydrodynamic models for steep river. Therefore, the Vekveselva study area was selected to examine both models (HEC-RAS 2D and TELEMAC-2D) by using mandatory input data, namely: topographic data generated from and measured flow data. The performance of a digital elevation model (DEM) and digital surface model (DSM), obtained from https://hoydedata.no/LaserInnsyn/, was evaluated in both models.

Also, the effect of smoothing the mesh size in HEC-RAS simulation, and the performance of both a finite element method and finite volume method in TELEMAC2D were assessed.

5.4.1 Topographic Data

Topographic data of the Vekveselva river was interpolated from three airborne LiDAR datasets obtained from https://hoydedata.no/LaserInnsyn/. The performance of a digital surface model of 0.5 m resolution that was acquired on 1 January 2014 and mapped by an aerial company called BlomAS (*Hoydedata.No,* n.d.)was evaluated in both hydrodynamic models. In the same way, a digital elevation model (DEM) observed on 24 October 2011 taken by Terratec AS aerial company and a 25 October 2016 Light Detection and Ranging (LiDAR) dataset collected by COWI AS company were used for the models' simulations. Both the DEM remote sensing measurements were recorded with 0.5 m resolution and FKB-laser 2.0 object catalog (*Hoydedata.No,* n.d.).

5.4.2 Flow Data

The selection of the flow data for hydrodynamic computation on the Vekvesleva river was based on matching an available historical orthophoto that was authorized by KartVerket.no, which is accessible at https://www.norgeibilder.no/, and with the available flow data. Therefore, an average daily flow rate on 16 September 2014 (0.898 m^3/s) was selected to analyze the suitability of hydrodynamic models on a steep river and the performance of topographic data, a DEM and DSM, originated from https://hoydedata.no/LaserInnsyn/.

5.4.3 HEC-RAS 2D Modeling for Vekveselva River

As per defined in section 5.1, unsteady flow of two spatial dimensions of the HEC-RAS modeling were computed by using DSM and DEM; so that two different terrains were created to the compute unsteady simulation.

The following, subsection discuss the methods that the terrains created, and the hydrodynamics computation performed for the DEM and DSM scenarios.

5.4.3.1 HEC-RAS 2D simulation for Vekveselva River by Using a Digital Elevation Model (DEM)

A big challenge of the hydrodynamic simulations for the selected river was obtained corresponding relevant data: namely, orthophoto data from https://www.norgeibilder.no/ and topographic data from https://høydedata.no/. As discussed in previous section (section 4.2*)*, the suitability of the hydrodynamic simulation of the Vekveselva river was evaluated on an orthophoto that originated from norgeibilder.no. A TIFF that was generated on16 September 2014 was selected for hourly resolution of the given flow data starting from 23 December 2012 to 18

September 2014 and was provided for this study. However, the availability of representative DEM data for the provided flow data was a big challenge in this river reach. Further, LiDAR dataset measurements taken on 24 October 2011 and 25 October 2016 do not cover all the selected river section. Even though a combination of both LiDAR datasets can be a representative topographic profile for the chosen river reach. The following procedures were applied to create a representative Vekveselva terrain profile.

5.4.3.1.1 Terrain Creation from Digital Elevation Model (DEM)

A LiDAR dataset is high-quality data that truly represents earth's features compared to topographic data taken from satellite imagery and radar data. However, LiDAR data has limitations. LiDAR has a movable part, which can create more errors. LiDAR measurement is expensive, and it is not easy to get seasonally captured data for an interesting area (*Lidar vs Radar*, n.d.). Also, LiDAR not penetrate water; it may obtain inches of a water body but cannot penetrate the bottom channel profile(*Lidar vs Radar*, n.d.). The same limitation was occurred in DEM of the Vekveselva study. The DEM data obtained 24 October 2011 and 25 October 2016 from høydedata.no imported to ArcGIS, which further processed in ArcMap. All raster files were merged in 'mosaic to new raster of Arc toolbox was done based on 32-bit float pixel, one band, and 0.5 x 0.5 m cell size.

Conservation from raster to TIFF was done, which further is used in HEC-RAS 2D to illustrate a topographic and geometric property of a selected river reach. These TIFF of the merged files were imported to RAS Mapper of HEC-RAS to create terrain.

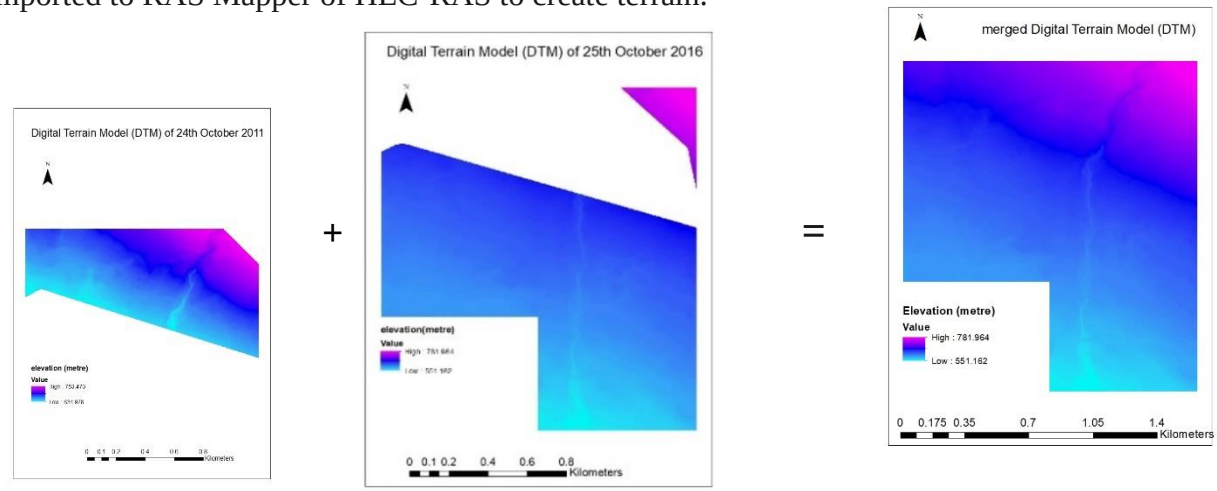

Figure 5-14: Digital elevation model of TIFF format and new created TIFF format of Digital elevation model

A new terrain model of the GeoTIFF, hierarchical data format (*hdf), Virtual Raster Translator (* vrt) files are created in RAS Mapper along with 1/128 elevation precision. RASMAPPER was convert TIFF file to pyramid and tiled data which removes no data values and store multiple terrain layers (G. W. Brunner, 2016).

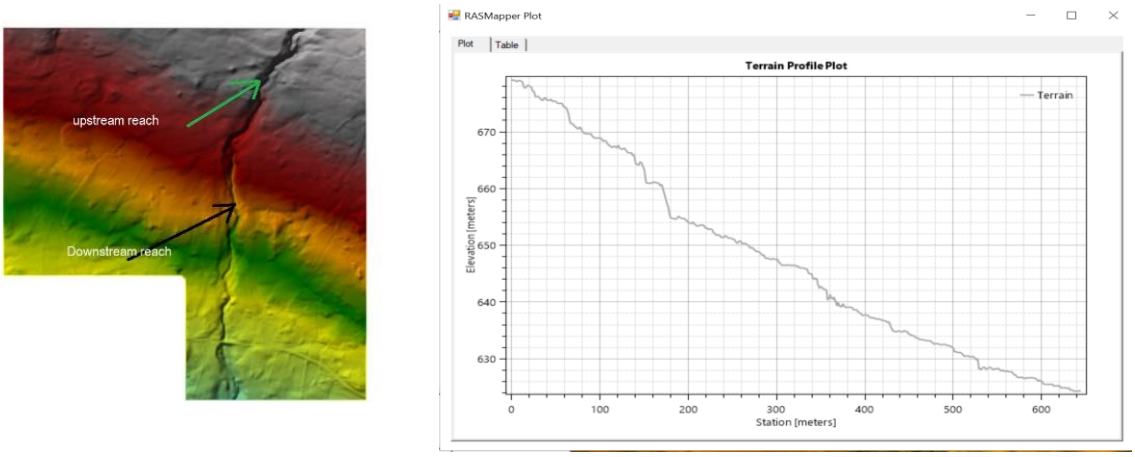

Figure 5-15: Created terrain in RAS Mapper and terrain profile

5.4.3.1.2 Geometric Data

A finite volume technique was assigned to computation meshes of a minimum of three-sides to maximum eight sides (G. W. Brunner, 2016). A 2-D flow area of the selected river reach was drawn along with five break lines. The advantage of break lines is to enforce the mesh generation to align the computation cell mesh along the break lines (G. W. Brunner, 2016). Break lines are represented along natural embankments, roads and erupted changes of elevation. The grid size of a 2-D flow area is must be small to increase the accuracy of simulations. A minimum 0.12 m^2, an average 0.25 m^2 and a maximum 0.43 m^2 grid areas were formed from the applied 0.5 m x 0.5 m mesh size.

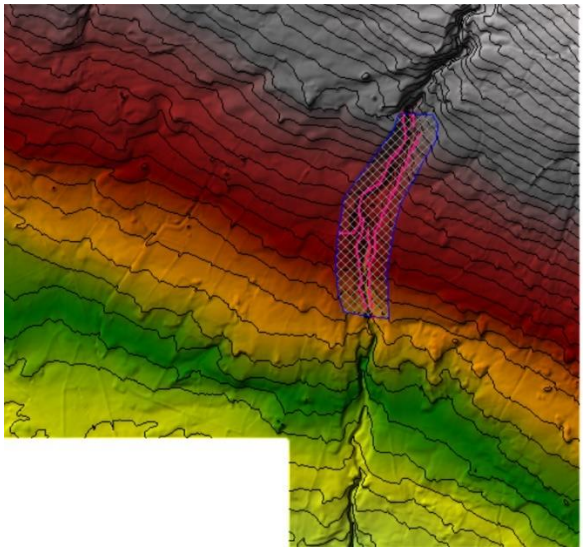

Figure 5-16: Computational mesh with break lines: blue lines represent 2D flow area; redline represents the break lines; and black lines are contour lines of 5m intervals.

However, hydraulic computations performed on this geometry could not be stable on areas that have a steep slope (section 6.2.1.1). In general, the HEC-RAS user manual recommends a flat and not rapidly changing slope, with coarser grid cell sizes(G. W. Brunner & CEIWR-HEC, 2016). A steep terrain, with an elevation rapidly changing over small length, requires a small grid cell size to decrease the gradient between consecutive cell faces to give stable numerical equation in HEC -RAS (G. W. Brunner & CEIWR-HEC, 2016).

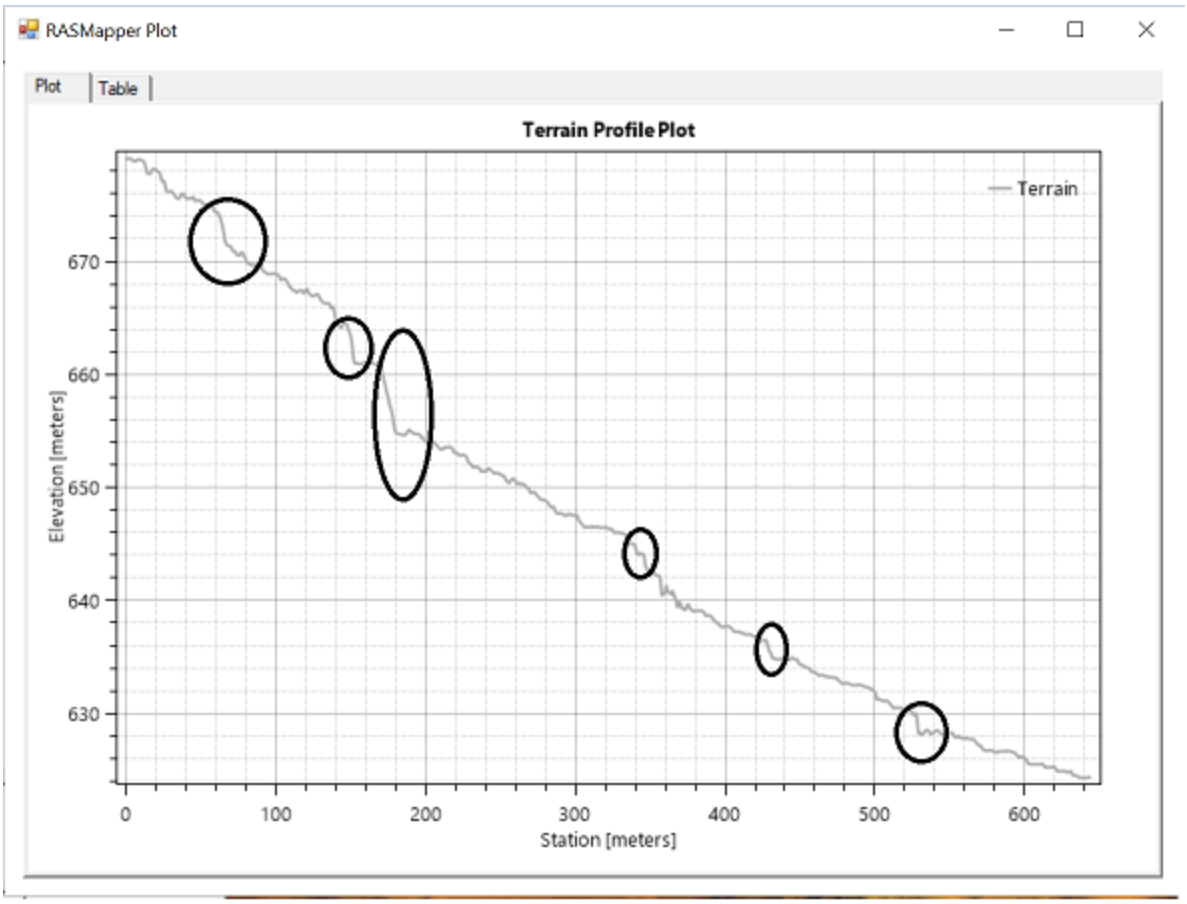

Figure 5-17: Terrain elevation profile and black lines surrounding sections indicate a rapidly changing slope

Therefore, the above geometric data was updated by modifying the computation mesh via applying 0.2 x 0.2 m at the steep slope location and 0.5 x 0.5 m. In contrast, the smoothing of the grid sizes increases computation time.

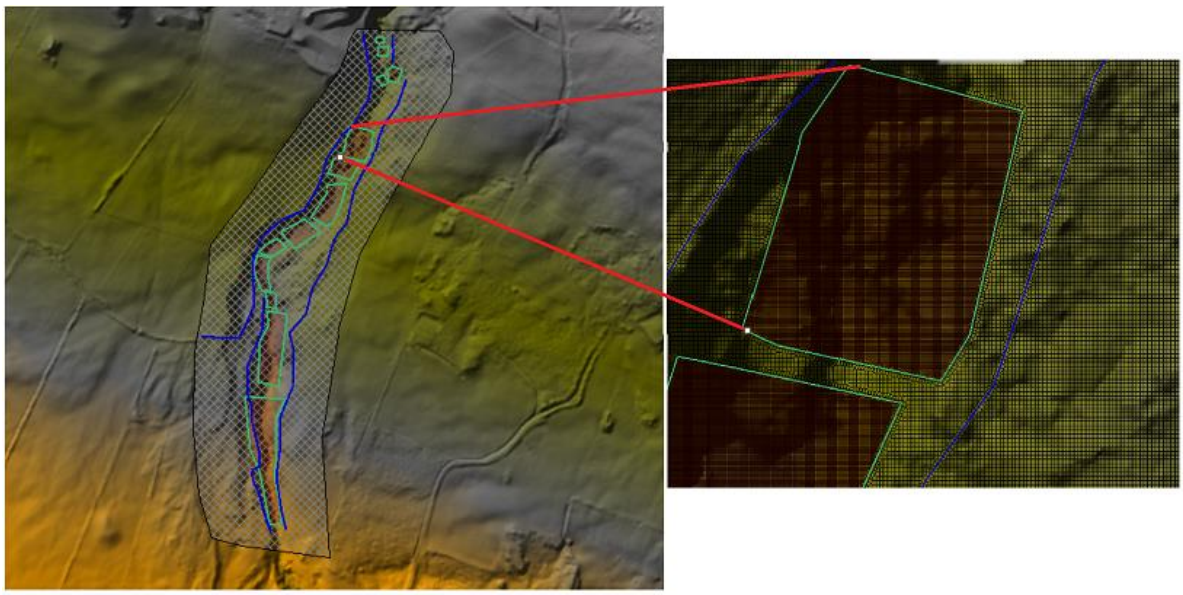

Figure 5-18:Refined computational meshes: blue line represents break lines and green polygons represent refinement

5.4.3.1.3 Boundary Condition

Generally, constant flow hydrography of an average daily flow event on 16 September 2014 was applied to refer to the upstream boundary condition, while normal depth at the downstream condition was used to define the hydraulic parameters. An initial condition of the friction slope uses in Manning's equation to calculate the normal water depth boundary line; whereas an energy grid line was applied at the flow hydrograph boundary condition to compute normal depth.

In Vekveselva 0.03 and 0.001 frictional slope at downstream boundary condition, and 5- and 24-hours flow hydrograph were used to create a continuous surface water profile indicated as follows:

1. **simulation 1**: 5-hour simulation on 0.5x0.5m mesh size with 0.898 m^3/s of constant hydrography with 0.03 energy grid line and 0.03 friction slope.
2. **simulation 2**: 24-hour simulation on the 0.5 x0.5m mesh size with 0.898 m^3/s of constant hydrograph with 0.03 energy grid line and 0.03 friction slope. The object of the simulation was to analyse the water surface profile by extending the simulation time.
3. **Simulation 3:** 5-hour simulation on 0.5 x0.5m mesh size with 0.898 m^3/s of constant hydrograph with 0.001 energy grid line and 0.001 fraction slope. This simulation was applied

to analyse the effect of the initial friction and energy grid line slope that was used at downstream and upstream boundary conditions, respectively.

4. **Simulation 4:** 5-hour simulation on 0.5 x0.5 m mesh size with 0.898 m^3/s of constant hydrograph with 0.001 energy grid line and 0.001 friction slope. In addition, 0.2 x 0.2 m refinement grid cells were drawn at the steep slope location. The aim of this simulation was to decrease slope between consecutive grid cells which may create a continuous water surface profile.

5.4.3.1.4 Manning's Roughness Coefficient

Since field measurement was not done, which is used to setup manning's coefficient values and no river roughness data was provided, all hydraulic computations were performed based on an assumed coefficient value for all computational meshes. In principle, Manning's coefficient depends on roughness, slope flow rate, and related factors. Vekveselva is a steep river that carries sediment and large boulder during high-flow season. Consequently, 0.05 Manning's coefficient value was selected due to a stony bottom channel and vegetation on the riverbank.

5.4.3.1.7 Performing the Computations

As mentioned earlier, a hydrodynamic computation of Vekveselva was based on unsteady flow simulation, which uses a diffusion wave equation to determine hydraulic variables at each cell face.

Since the Vekveselva river is a steep slope and a smoothing computation time step was obligated to achieve stable simulation with continuous water surface profile, courant methodology where a function of flow velocity, time interval and flow length was applied.

- ✓ Computational time interval =1 sec
- ✓ Mapping output interval = 1 minute
- ✓ Hydrography output interval = 1 minute
- ✓ Detailed output interval = 1 minute
- ✓ Maximum courant = 0.5 sec
- ✓ Minimum courant = 0.2 sec
- ✓ Number of steps below minimum before doubling = 2
- ✓ Maximum number of doubling base time step = 2
- ✓ Maximum number of halving base time step = 2

5.4.3.1.8 Computer Specifications and Model Version

The hydrodynamic simulations of the Vekveselva river in the DEM were performed in HEC-RAS version 5.0.7 and a multi-processor.

Table 5-3:Computer specification used for Vekveselva HEC -RAS 2D simulation on DEM

Component	**Information**
OS	64-bit Operating System, x64-based processor
Processor	Inter® Core ™ i7-7700 CPU @ 3.60GHz
RAM	32 GB
Number of cores to use in 2-D computation	All Available

5.4.3.2 HEC -RAS 2D Simulation for the Vekveselva River by Using Digital Surface Model (DSM)

The DSM data used for the Vekveselva study comprehends airborne LiDAR technology. A DSM of the Vekveselva river, which has 0.5 x 0.5 m resolution and was generated on 1st January 2014 by Blom AS aerial company, was extracted from https://hoydedata.no/LaserInnsyn/.

5.4.3.2.1 Terrain Creation from Digital Surface Model (DSM)

Interpolation and creation of LAS and raster data were done by using Lastools and ArcMap. LAZ zipped data of 1st January 2014 was obtained from https://hoydedata.no/LaserInnsyn/ and converted to las format by using the las2las tool. Of these LAS points, 99.41 % are classified as ground (class 2), and 0.59 % are classified as water (class 9) as a classification code statistic appears in the Arc catalog of ArcGIS. However, the classification did not consider vegetation classes that represent vegetation that exists in the study area and are mandatory in DSM classification. Further, conversion from Lasdataset to raster format was done by using conversion tools of the Arc toolbox. This spatial conversion was carried out based on an elevation value field. Binning interpolation was assigned, where average method techniques were used to interpolate raster cell values from Lasdataset and voids interpolated by the linear method. Consequently, 0.5 x 0.5 m cell dimension of float type raster was processed from a Lasdataset to raster conversion, and further exported to TIFF format.

Lastools is the high-speed software used to classify tiles, convert one file format to another format, filter, raster, triangulate, contour, clip, and polygonise LiDAR data. A Las2las tool is multi-purpose tools that can processes LiDAR data (*Las2las*, n.d.). It is an open tool that can convert, transform, compress, filter, subset, repair, and scale a LiDAR file (*Las2las*, n.d.).

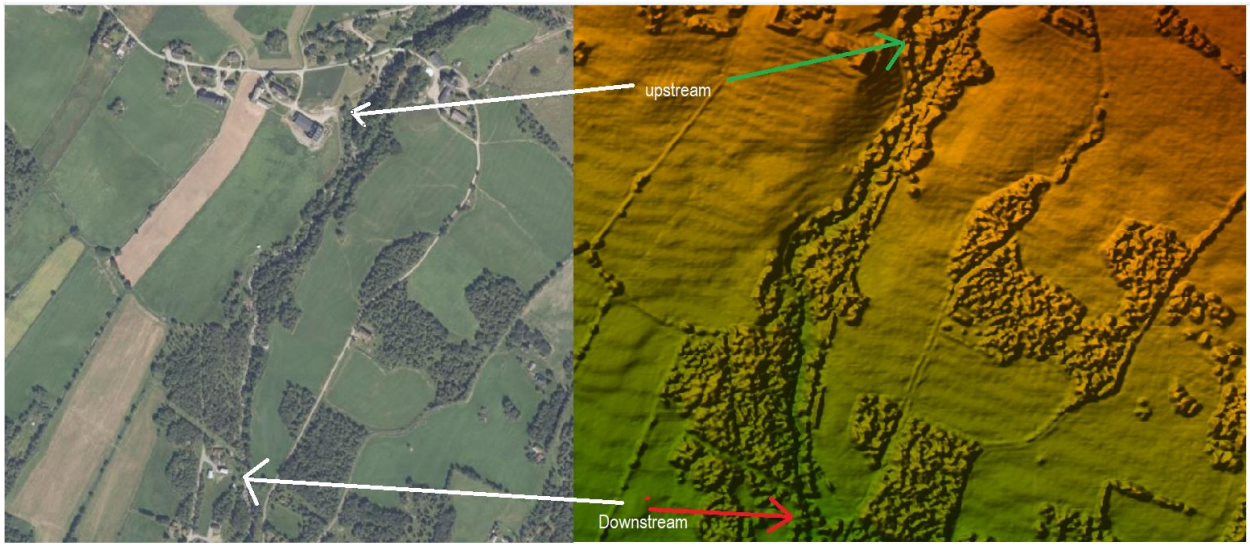

Figure 5-19:Terrain created by RAS Mapper and orthophoto: Left side :aerial image of study area (https://www.norgeibilder.no/); Right Terrain created by RAS MAPPER

5.4.3.2.2 Hydrodynamic Computation

As discussed in the previous (section 5.4.3), of the accuracy HEC-RAS 2D simulation of the DSM of the Vekveselva river was evaluated by simulated overlaying of the inundation extent on the orthophoto. Three simulations were done to get a good-fit inundation extent. All simulations were computed by using a diffusion wave. An advantage of using the diffusion equation is that it decreases simulation time and is inherently stable (G. W. Brunner & CEIWR-HEC, 2016). To achieve accurate simulation, a Courant methodology where the Courant number is the ratio of velocity change and length was applied. The following computational time sets are applied in all simulations.

- Computational time interval =1 sec
- Mapping output interval = 1 minute
- Hydrography output interval = 1 minute

- Detailed output interval = 1 minute
- Maximum Courant number =0.5 sec
- Minimum = 2 sec
- Number of steps below minimum before doubling = 2 sec,
- Maximum number of doubling base time step = 2 sec
- Maximum number of halving base time step = 2 sec

Like the hydrodynamic computation on the DEM, a single Manning's coefficient equal to 0.05 was assigned.

I. **Simulation 1**: The first simulation was performed based on a 5-hour simulation time and 0.5x0.5m mesh size. A 0.898 m3/s of constant hydrography was applied at the upstream boundary condition with 0.03 energy grid line, and 0.03 friction slope applied at the downstream boundary condition. The break line was assigned along with the river center line and road to create significant computational meshes that increase the accuracy of outcome results.

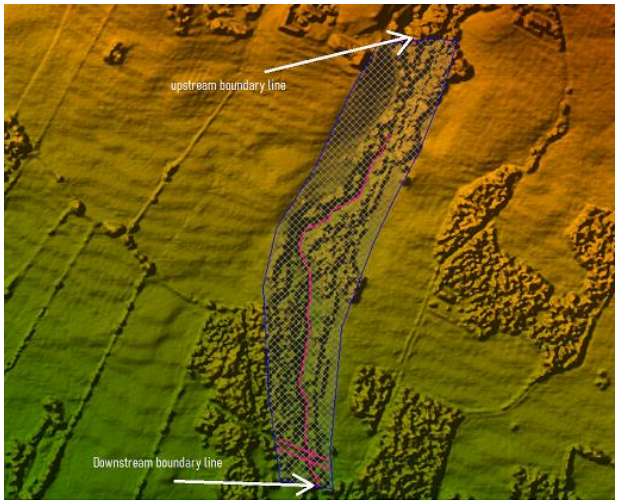

Figure 5-20: Computation mesh with 0.5 x 0.5 m default spacing size and break lines. The red line represents a break line and the blue line represent the 2-D flow area

II. **Simulation 2:** The 24-hr simulation time was adjusted on the same geometry, mesh size, and boundary lines. However, 0.001 sloped energy grid lines and friction slope were applied at upstream and downstream boundary conditions. A flattened energy and friction line can build

up a stable hydrodynamic computation at the initial state. This simulation aimed to fix a gapped inundation extent that estimated in simulation 1.

However, gapped, and unrealistic inundation areas were estimated in both simulation1 and 2 (section 6.2.2.1).

III. **Simulation 3:** At this stage, a terrain was modified by removing a false blockage that exists in the river channel. A false blockage is common in hydrodynamic modeling when the DSM is generated from LiDAR (Julzarika & Harintaka, 2019). A new terrain was created by interpolating river cross-section and new geometric data that contains a 0.5 x 0.5 grid size assigned in a selected 2-D flow area. Also, a refinement region with a 0.2 x 0.2 m cell size was drawn at an interpolated region. The same as for simulation 2, the energy grid line and friction line sloped by 0.01 percent assigned for the initial condition and a 24-hr simulation time was applied to compute hydraulic parameters.

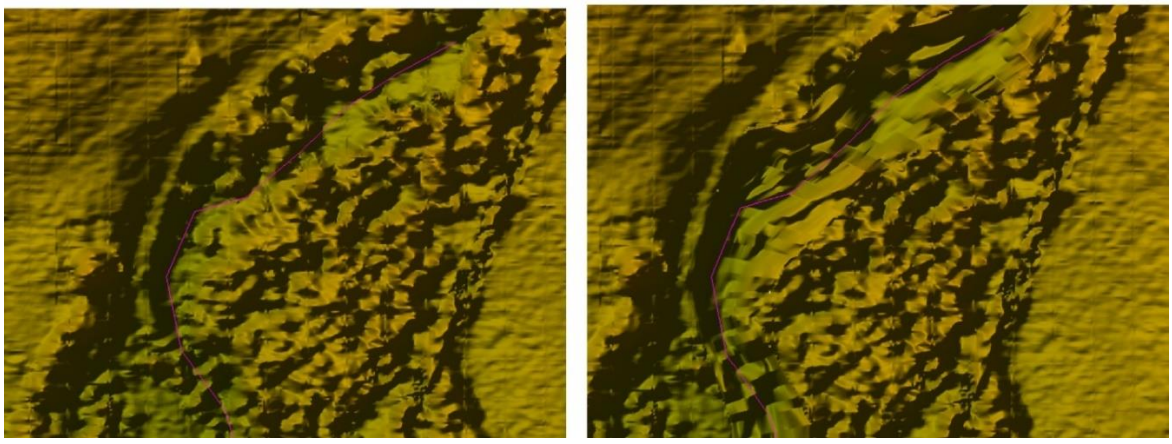

Figure 5-21 Origin and interpolated terrain. The left-hand figure is an original terrain and the right-hand terrain represents an interpolated terrain. The red line represents a river centerline.

5.4.3.2.3 Computer Specifications and Model Version

This hydrodynamic simulations of Vekveselva river in DSM topography profile was performed in HEC-RAS version of 5.0.7 and multi-processor.

Table 5-4: Computer specification used for Vekveselva HEC -RAS 2D simulation on DSM

component	Information
OS	64-bit Operating System, x64-based processor
Processor	Inter® Core ™ i7-7700 CPU @ 3.60GHz
RAM	32 GB

5.4.4 TELEMAC-2D Modeling for the Vekveselva River

As explained in previous (section 5.4) section the goal of hydrodynamic modeling for the Vekvekselva river was to assess the suitability of two hydrodynamic models, namely HEC-RAS 2D and TELEMAC-2D, for a steep river modeling; and to evaluate the consistency of DEM and DSM those extracted from https://hoydedata.no/LaserInnsyn/. The same with as with the hydrodynamic simulations performed in HEC-RAS 2D, two scenarios were applied. The first scenario is that a geometric file was generated from the DEM. In contrast, the second scenario is that a DSM was applied to create a geometric file that is further used for hydrodynamic computation. In both scenarios, a common upstream and downstream stream location was selected. Moreover, equal computational mesh size and the same boundary conditions file were applied. Such that, 0.898 m3/s constant hydrography of a liquid boundary was applied at an upstream boundary segment, and the prescribed elevation, which presents the bottom elevation, was assigned at a downstream boundary segment.

In order to get healthy results from both scenarios, finite element and finite volume methods were carried out.

Table 5-5: Simulation scenarios for TELEMAC-2D simulations

Name of scenario	**Manning's coefficient value (n) HEC-RAS 2D**	**Strickler's relation coefficients value (k =1/n) used in TELEMAC 2D**	**Topographic data**
Scenario 1	0.05	20	DEM
Scenario 2	0.05	20	DSM

Related to this, two hydrodynamic computations: one hydrodynamic simulation by applying finite element and one hydrodynamic simulation by using the finite volume method, were computed in both scenarios. Since both scenarios aim to perform parallel simulations, the same boundary condition options, the same initial conditions, the same numerical parameters and the same mathematical equations were applied. The following subsections, subtopics describe how a geometry file, boundary condition, and steering files are created.

5.4.4.1 Geometry File

A geometry file is a set of computational mesh and a mandatory file that contains bottom topography information, which can reflect an elevation profile of the domain (Ata, 2018). This file contains all information related to computation mesh, such as number of mesh points (NPOIN variable), number of elements (NELEM variable), number of nodes per element (NDPNDP variable), and x and y coordinates of each node (Ata, 2018). For the TELEMAC simulation, a geometry file was created by a hydraulic tool called BLUEKENUE. This is a tool that can read an *XYZ formatted file and produce a computational mesh generator, which is used to interpolate bathymetry data and create a geometry file to Selafin (slf) standard format. A geometric file is further linked in the steering file to provide a geometry profile for TELEMAC- MASCARET simulations (Telemac, 1999; (Manual, 2010).

5.4.4.1.1 Generating a Geometric File from a Digital Elevation Model (DEM)

As explained in the above section and **Error! Reference source not found.**, the first scenario indicates that the geometric file was generated from the DEM that was obtained from hoydedata.no. The same with terrain preparation procedures implemented for HEC-RAS 2D simulation, DEM data of 24t^{h} October 2011 and 25th October 2016 were extracted from https://hoydedata.no/LaserInnsyn/ and merged in ArcMap software to create a single terrain file which covers the selected study area (section 5.4.3.1.1 and Figure 5-14). Further, created raster data was converted to contour lines of 0.4 m intervals. Conversion from tools to points data was held in the Arc toolbox, namely known as 'feature vertical to points.' Also, XY coordinates were added to points data by applying a 'Add XY coordinates' features program. Moreover, a table format file was converted to dBase (database management program) and the dBase format file edited and changed to the *XYZ format file by using Excel.

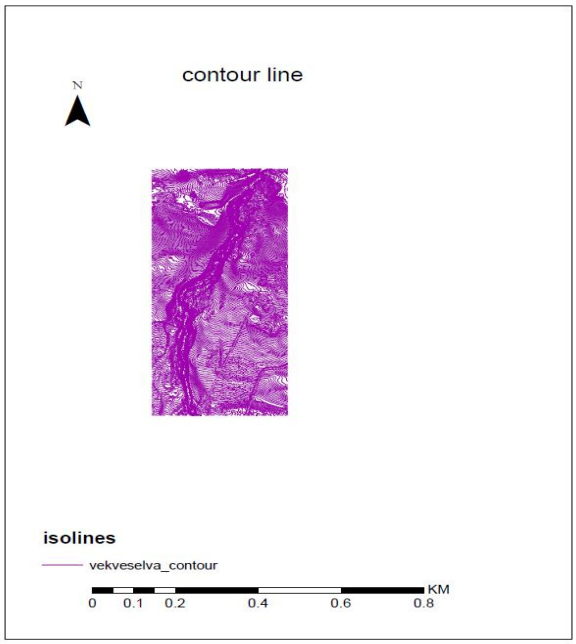

Figure 5-22:Contour (isolines)

Furthermore, the ASCII (*XYZ) format file created in Arc Map was imported to BLUEKENUE to form a geometry file. Initially, bathymetry data was imported to BLUEKNUE, and a computational mesh was generated for a selected domain region. Additionally, a Serafin format file was created based on generated computational mesh and interpolated with a bathymetry file. The Serafin file is a binary format file that TELEMAC-MASCARET can process(Ata, 2018). Then, a Serafin file was mapped with a BOTTOM variable created from 1 m default edge length and 1.2 edge growth ratio. For the selected bathymetry domain, 64253 nodes and 127133 elements of the geometry file of the BOTTOM attribute were created in BLUEKENUE and further provided bottom topography and mesh information for numerical computation that performed in TELEMAC 2D.

Figure 5-23: Three-dimensional view of computational domain created from DEM and elevation profile (BLUEKNUE)

5.4.4.1.2 Generating a Geometric File from Digital Surface Model (DSM)

Accuracy of topographic data is one major problem causing uncertainties in simulations' result (Podhorányi et al., 2013) (Rahman et al., 2006). In the real world, topography is a crucial factor governing flow variables such as dimensional velocities, water depth, storage, wave propagation, inundation extent, and other variables (Tamiru & Rientjes, 2005). Many investigations have been done on the influence of topographic data in hydrodynamic modeling, indicating that the quality of topographic data and their resolutions are significantly influencing the accuracy of results (Horritt & Bates, 2001); (Merwade, 2009). The DEM, which is widely used for hydrodynamic modeling, removes existing objects on the earth surface. In other words, the DEM has equivalent meaning with a representation of 3D spatial value on bare earth (Meneses et al., 2017). Indeed, objects existing on the earth surface can control flood parameters and change flood behavior. For instance, vegetation, stones, and other human-made objects are not handle in the DEM (Meneses et al., 2017).Even though the DSM is a model it generally reflects actual earth surface. However, earth features such as a vegetation canopy can be a reason for a false flow blockage in hydraulic modeling. A false flow blockage occurs when the DSM data is from LiDAR and the river channel

is covered by a tree canopy. Therefore, it better to transform the DSM to a DEM (DEM is a subset of DTM) or manually scan of features and collect mass points and break lines; editing geometric input can decrease modeling uncertainty (Meneses et al., 2017).

In order to evaluate the performance of the DSM data extracted from https://hoydedata.no/LaserInnsyn/, the inundation extent computed from the geometry file generated from the DSM was overlaid on the orthophoto that was obtained from https://www.norgeibilder.no/. Consequently, a computed water cover area was mapped on the orthophoto and evaluated. Before the geometry file was created in BLUEKENUE, primary data conversation from LAZ to ASCII have been processed in ArcMap. The ASCII is a point set and comma-separated file, which mainly contains XYZ coordinates. In order to link LiDAR data (LAZ data) to the mesh generation program (BLEUKNUE) and mathematical modeling (TELEMAC), a script was needed to convert the geometry data and create an *XYZ file that would be understood by each mesh algorithm. Lastools is a tool used to convert LAZ formatted data to LAS form. A LAZ format of 0.5 x 0.5 m resolution of a DSM which scanned an earth feature that appeared on 1st January 2014 was extracted from https://hoydedata.no/LaserInnsyn/ and converted to LAS format in lastools and further converted to a raster file that has 0.5 x 0.5 m cell dimension. This conversion was made by applying a spatial conversion tool of Arc Map, particularly the LAS dataset, to a raster program. Further, a sample tool from the extraction program in the spatial Analyst tools of Arc Toolbox was assigned to create *XYZ pointset file by using the nearest techniques.

Moreover, mesh generation for use in the TELEMAC -2D modeling requires high quality and dense unstructured meshes (Prodanovic, 2015). BLUEKNUE, software developed by the Canadian Hydraulics Centre National Research Council, is used to generate, interpolate, and define, with the BOTTOM variable of a computational mesh for a selected domain (Prodanovic, 2015). Fifty-six thousand three hundred and twenty-seven nodes (56327) and one hundred and eleven thousand four hundred and fifteen (111415) triangular elements of scalar mesh were generated from 1m default edge length with 1.2 growth edge ratio. The *XYZ file contains horizontal and vertical coordinates and represent the digital surface elevation of a selected area, a feature on earth surface used to interpolate scalar meshes (assigning of elevations) to the quality mesh which is further applicable in TELEMAC -2D simulation. Further, a Selafin object with a

BOTTOM variable was launched on the mesh domain and interpolated with the *XYZ file processed to create a binary format of a geometry file, which was further launched in a steering file. Selafin contains a BOTTOM variable used to identify TELEMAC computation for single roughness value input (BLUEKNUE).

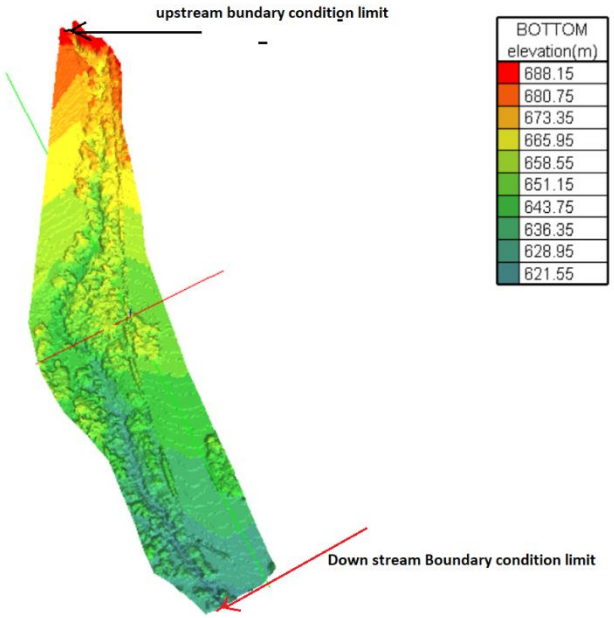

Figure 5-24:Geometry file (selafin) created from DSM data that contains a vegetation canopy

5.4.4.2 Boundary Condition File

In the case of parallel simulations applied for TELEMAC-2D in both the DEM and DSM, the same boundary condition options were created. A finite element mesh that consists of boundary segments was created in BLUEKNUE. For both scenarios, a prescribed flow rate equal to 0.898 m^3/s was applied at the upstream boundary limit. It has the same meaning as applying constant hydrography of 0.0898 m^3/s ordinate and simulation time along the abscissa. A prescribed elevation equal to 624 m, which describes elevation at a downstream boundary, is used to define a downstream segment.

5.4.4.3 Creating a Steering File

This file contains keywords that control hydrodynamic computation. The keywords include mathematical equations, physical parameters, solver types, and the initial condition used in TELEMAC simulation (Ata, 2018).

As defined in the previous section, two hydrodynamic computations were performed in each scenario; such that, a hydrodynamic calculation for the DEM and DSM was done by applying finite element and finite volume equations. Further, Strickler's law was used to define a friction parameter in all computational domains. Since model calibration was not done, single Strickler's roughness coefficient equal to 20, which translates from the 0.05 Manning coefficient, was defined as the 'FRICTION COEFFICIENT' keyword. Because TELEMAC-MASCARET requires an initial condition to compute the desired numerical scheme, an initial a condition of constant water depth equal to 0.001was set to initiate the mathematical computation. The propagation of water depth and velocity at each time step was solved by applying the extrapolation technique. In this case, both water depth and velocity at each simulation time are solved by modifying the initial value of the water depth or velocity at the start of the solving process (Ata, 2018).

In addition, linear triangle space discretization to velocity and water depth was used to specify a discretion used to compute a successful velocity and water depth. An advantage of this option is that it is most efficient in terms of memory and CPU time. A wave equation applied in the Saint-Venant equation was associated with the keyword FREE SURFACE GRADIENT COMPATIBILITY = 0.9. A mass conservative was applied to the advection of the velocity and water depth. This option is used to optimize a numerical scheme (Ata, 2018). A continuity correction that corrects velocity at downstream and a verifying continuity equation was applied to eliminate residual mass error that may appear a downstream boundary. Since Vekveselva is a steep-sloped river that oscillates, free surface is common and increases computation time, thus a wave equation is assigned to provide more stabilization. In both simulations (one simulation based on finite element and the other simulation on a finite volume equation) computed in both scenarios, the treatment of a tidal flat desires to application of specific treatment of dry cells; thus, tidal flats are detected, and the free surface gradient is corrected. Treatment of negative depths was done by flux control that ensures strictly positive depths.

For both scenarios and both hydrodynamic computations (one simulation based on finite element and the other simulation on a finite volume equation) for the DEM and DSM, a Courant number equal to 0.9 and NEWMARK TIME INTEGRATION COEFFICIENT equal to 0.5 was offered to compute flow parameters in the 5-hour simulation time. A Courant number equal to 0.9 is used to provide a variable time step, and NEWMARK TIME INTEGRATION COEFFICIENT equal to 0.5 gives the possibility to improve time integration (Ata, 2018). For a finite volume scenario, the

kinetic order was specified to define a finite volume scheme. Such an algorithm of finite volume scheme is explicit and means that the Courant number must be limited to 1(Ata, 2018).

5.4.4.4 Computer Specifications and Model Version for Vekveselva River TELEMAC-2D Modeling

The hydrodynamic simulations of the Vekveselva river in the DEM were performed in TELEMAC-2D version v8p0 parallel.

Table 5-6:Computer specification used for Vekveselva TELEMAC-2D simulation on both DEM and DSM

Component	**Information**
OS	64-bit Operating System, x64-based processor
Processor	Inter® Core ™ i7-7700 CPU @ 3.60GHz
RAM	32 GB
Parallel processes	Using 7 cores

6. RESULTS

The HEC-RAS 2D and TELEMAC-2D analysis for both case studies are presented. For the Surna river, statistical analysis tests were applied to determine the correlation between the parameters under consideration. Also, the models' performance for the Vekveselva river was assessed by overlapping the simulated inundation area on the orthophoto. Other factors such as simulation time, water surface profiles computed in both models, and comparison of mathematical equations were discussed.

6.1 Surna (mild and shallow) River Simulations' Result

For the Surna the river hydrodynamic simulations, the inundation extent for each simulation was extracted and a statistical comparison with the observed data was performed. Besides, the suitability of both models was evaluated in terms of degree fitness with the observed inundation extent. The duration of the computing hydrodynamics, the complexity of the models, and limitations in both models were also analyzed in this section. Moreover, a comparison of water surface elevation and velocity computed by both models was carried out.

6.1.1 Inundation Extent Results

As discussed in the Material and Methodology chapter (5), five simulations of unsteady flow conditions were performed to estimate the representative roughness coefficient of the Surna river and to compare the inundation extent results obtained from HEC-RAS 2D and TELEMAC-2D. Therefore, the inundation extent extracted from HEC-RAS 2D simulations performed by using 0.025, 0.03, 0.045, 0.05, and 0.06 Manning's coefficient, and the TELEMAC 2D modeling based on 16.67, 20, 22.22, 33.33 and 40 roughness coefficient of Strickler equation, were used to compare the simulated inundation extent with the observed water cover area. In HEC-RAS 2D, inundation boundary from hydraulic computation performed on 0.025, 0.03, 0.045, 0.05 and 0.06 Manning's roughness coefficients were exported from the RASMapper for further statistical analysis, which was carried out in Arc map software.

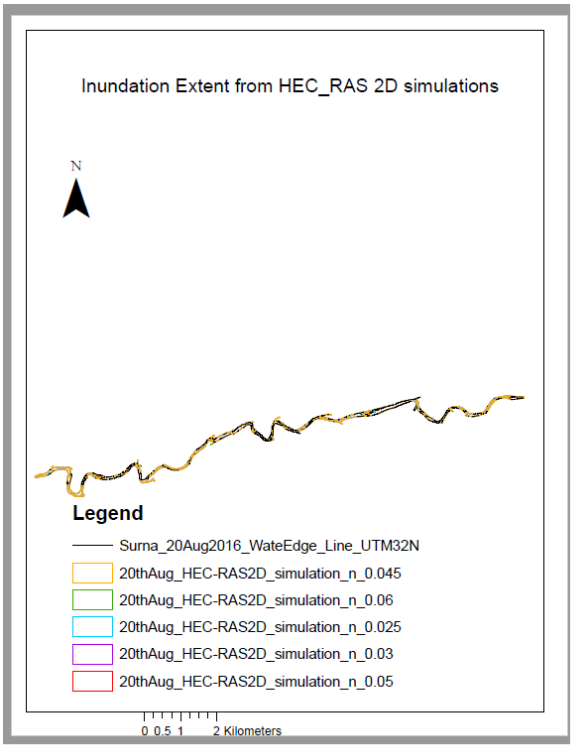

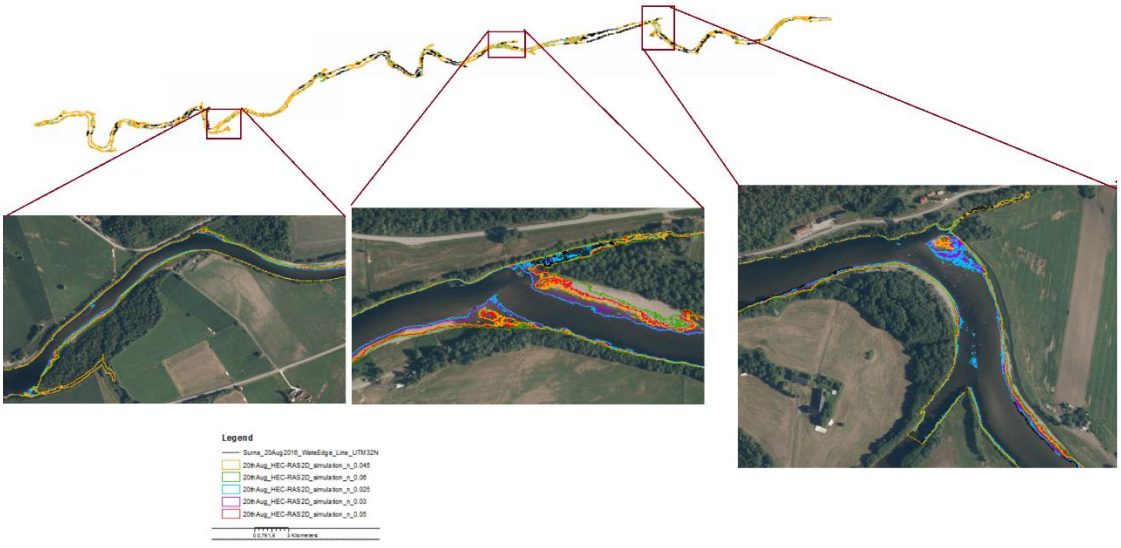

Figure 6-1: Inundation extent form HEC-RAS 2D simulations and observed water cover area. The black line represents bathymetry (observed waterline); light-blue, purple, orange, red and green colors show 20 August 2016 simulations performed on 0.025, 0.03, 0.045, 0.05 and 0.06 Manning's coefficient, respectively.

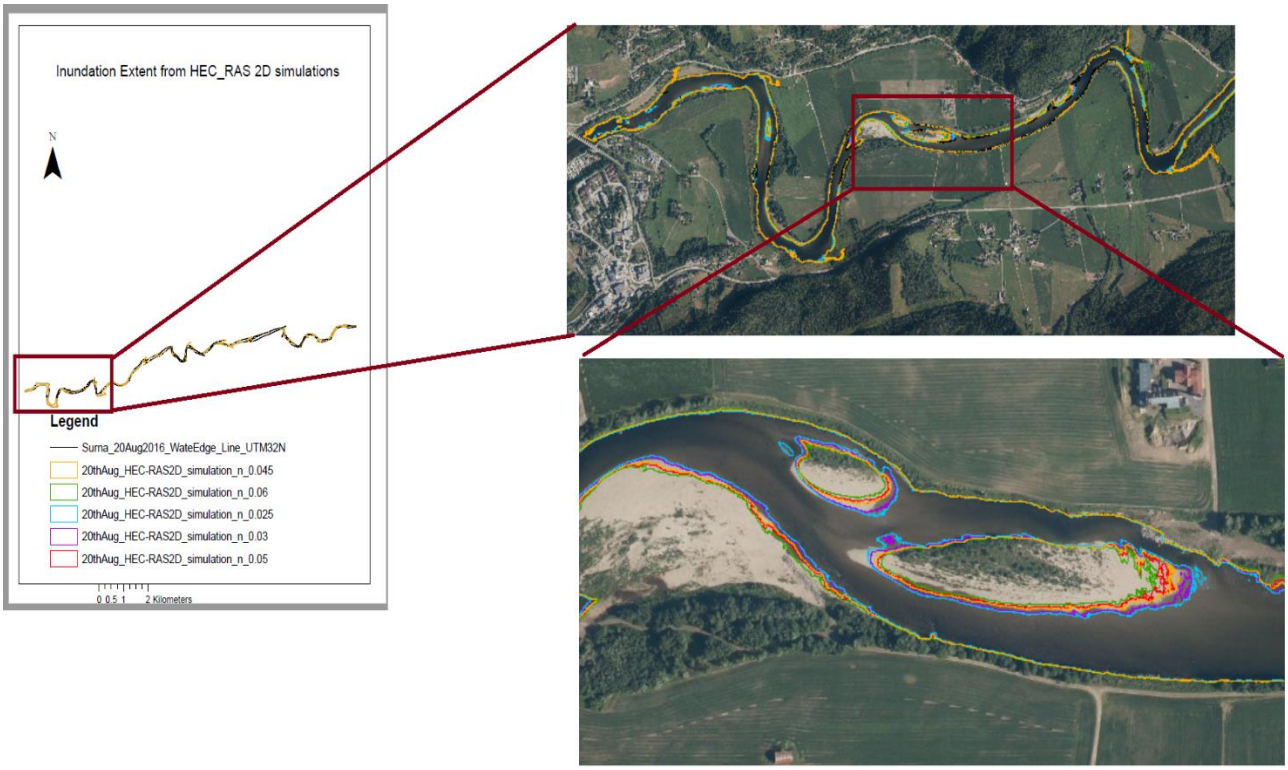

Figure 6-2: Inundation extent computed in HEC-RAS 2D. The black line represents bathymetry (observed waterline) light-blue, purple, orange, red and green colors shows that the 20th August 2016 simulations performed on 0.025,0.03, 0.05 and 0.06 Manning's coefficient, respectively.

On the other hand, the inundation boundaries' extraction from the TELEMAC-2D model was carried out by generating a single isoline of water depth. This process was performed in BLUEKENUE.

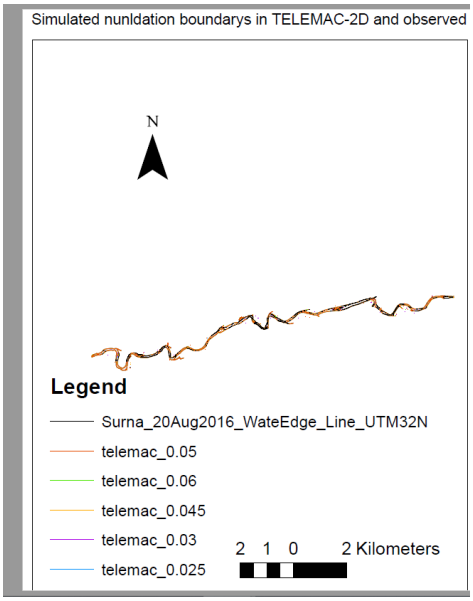

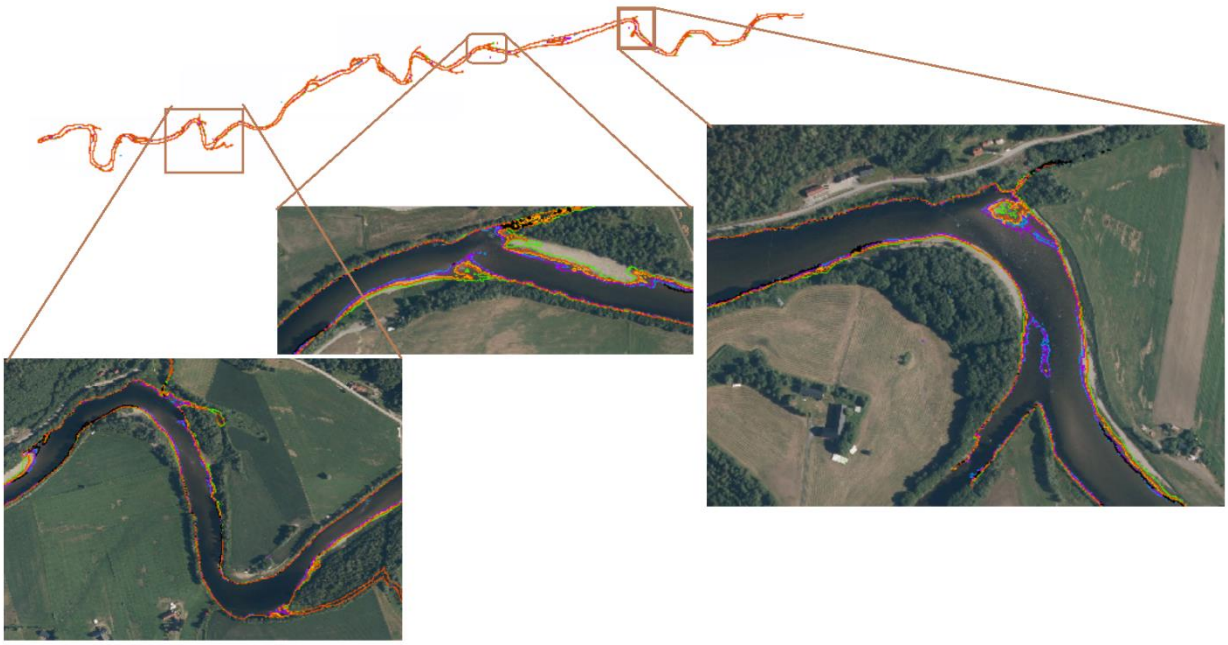

Figure 6-3:Inundation extent from TELEMAC 2D simulations and observed water cover. The black line represents bathymetry (observed waterline), light-blue, purple, orange, red and green colors show 20th August simulations performed on 0.025, 0.03, 0.05, and 0.06 manning's coefficient, respectively.

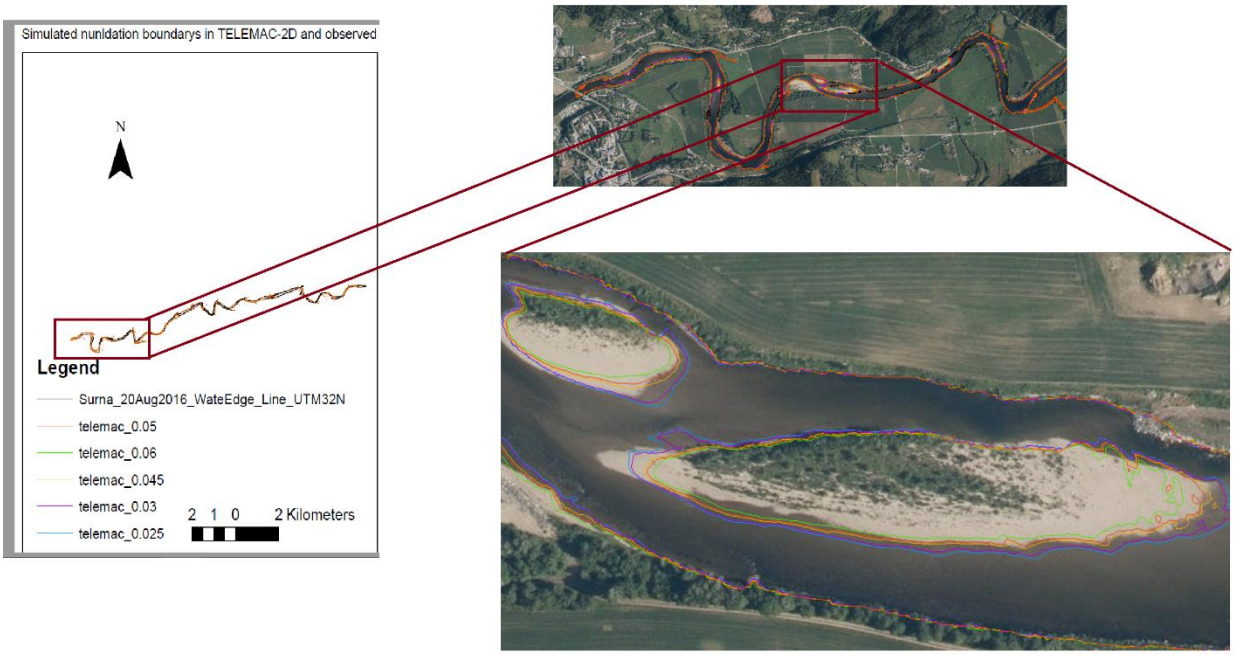

Figure 6-4: Inundation extent computed in TELEMAC-2D at downstream region. The black line represents bathymetry (observed waterline) light-blue, purple, orange, red and green colors shows that the 20th August 2016 simulations performed on 0.025, 0.03, 0.05 and 0.06 Manning's coefficient, respectively.

6.1.2 Statistical Comparison

Four HEC-RAS 2D simulations and TELEMAC-2D simulations performed on the same Manning's coefficient values were statistically compared to each other to get a representative channel roughness value and for evaluating the performance of both models. The examination of the accuracy of the models for a mild slope flow was carried out based on inundation extents computed in both HEC-RAS 2D and TELEMAC-2D models, and a comparison of the simulated results with bathymetry data (observed water cover area) by root mean square error (RMSE). In order to compute the RMSE values for each simulation, the river reaches were divided into 59 zones (sections), and the corresponding inundation area of each zones (sections) was calculated. Arc Map was used to compute the inundation areas that existed in each zones (sections).

$$RMSE = \sqrt{\frac{1}{N}\Sigma\left(O_j - s_j\right)^2} \qquad \textit{Equation 6-1}$$

Here O_j represents the observed inundation area at the j cross-section; S_j represents the simulated inundation area at the j cross-section; and N is the number of cross-sections. In the Surna river simulation case, N is equal to 59 as the river reach is divided into 59 zones.

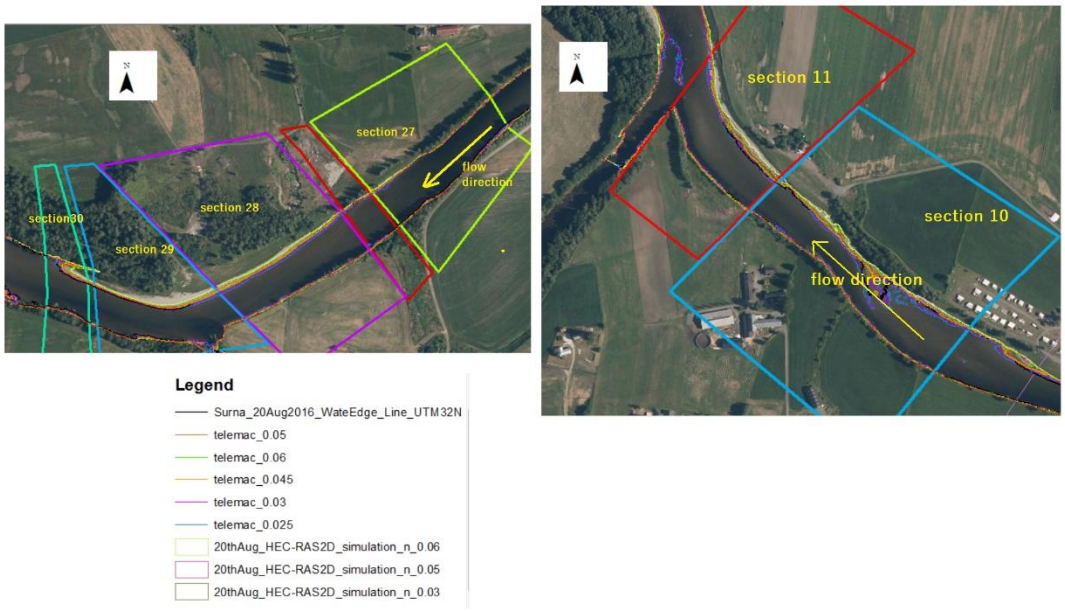

Figure 6-5: River sections

Table 6-1: RMSE values

Simulation	**$\sum (O_j - S_j)^2$ (m^4)**	**RMSE (m^2)**
20 August2016 HEC-RAS2D simulation on manning's coefficient value (n) = 0.025	439,237,847.8	2,728.499457
20 August2016 HEC-RAS2D simulation on manning's coefficient value (n)= 0.03	265,102,026.5	2,119.729862
20 August2016 HEC-RAS2D simulation on manning's coefficient value (n) = 0.045	129,158,196.9	1,479.568174 (minimum RMSE among HEC-RAS 2D simulations)
20 August2016 HEC-RAS2D simulation on manning's coefficient value (n) = 0.05	187,084,232.3	1,780.707498
20 August2016 HEC-RAS2D simulation on manning's coefficient value (n) = 0.06	430,938,391.2	2,702.598847

20 August2016 TELEMAC-2D simulation on roughness in Stickler equation = 16.67 or n = 0.06	240,077,222.0	2,017.20238
20 August2016 TELEMAC-2D simulation on roughness in Stickler equation = 20 or n =0.05	1229,124,104.0	4,564.27562
20 August2016 TELEMAC-2D simulation on roughness in Stickler equation = 22.22 or n = 0.045	102,757,368.6	1,319.715998 (Minimum RMSE among TELEMAC 2D simulations
20 August2016 TELEMAC-2D simulation on roughness in Stickler equation = 33.33 or n = 0.03	143,158,963.6	1,557.698017
20 August2016 TELEMAC-2D simulation on roughness in Stickler equation = 40 or n = 0.025	265,720,938	2,122.2028

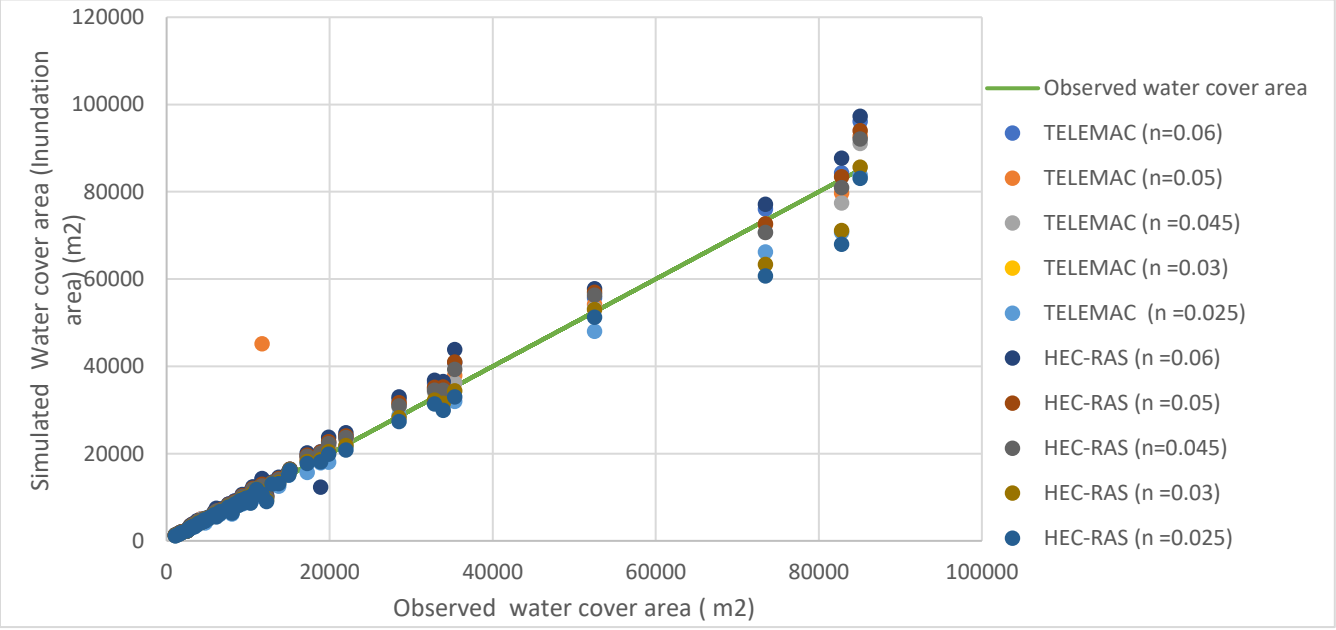

Figure 6-6: Simulated and observed water cover area. green line represents 1:1 and simulated water cover area (y-axis) drawn along with observed water cover area.

A result from the HEC-RAS 2D hydrodynamic modeling indicates that the HEC-RAS simulation of 0.045 Manning's coefficient gave the minimum RMSE value (best fit simulation), and Maximum RMSE generated is from inundation extent extracted from HEC- RAS 2D simulation of 0.025 Manning's coefficient. On the other hand, TELEMAC-2D simulation by applying 0.045 Manning's roughness coefficient (n) gave the minimum RMSE value and simulation on 0.05 gave the maximum. These show that represent roughness coefficient is equal to 0.045 based on both HEC-RAS 2D and TELEMAC modeling.

Further, there was a large area difference between inundation extents for those computed in HEC-RAS 2D. For instance, 21,500.84092 m^2, 16,053.7081m^2, 61,754.0282m^2 and 24,079.9836 m^2 inundation area differences were observed in between hydrodynamic modelling on n=0.06 and 0.05, n=0.05 and 0.045, n=0.045 and 0.03, n= 0.03 and 0.025 simulations, respectively (Table 6-2). However, hydrodynamic modeling in TELEMAC-2D gave a small difference among simulations performed on different roughness coefficients. For the Surna river TELEMAC-2D hydrodynamic computation, 2,096.1537 m^2, 4,8034.0988 m^2, 41,598.9426 m^2 and 18305.1776 m^2 inundation area differences was computed in between n =0.06 and 0.05, n=0.05 and 0.045, n=0.045 and 0.03, 0.03 and 0.025 simulations (Table 6-2).

In general, inundation results extracted from HEC-RAS 2D simulations were closer to the observed water cover area than those simulated in TELEMAC-2D. However, the HEC-RAS 2D simulation on 0.025 and 0.03 Manning's coefficients gave underestimated results. In the case of the total inundation area of fifty-nine river sections, HEC-RAS 2D hydrodynamic computation on 0.045 Manning's coefficient, which is the ratio of the simulated and observed inundation area, fitted best with the observed inundation area, and an overestimated inundation area computed on 0.05 and 0.06 Manning's coefficient in HEC-RAS. The same as HEC-RAS 2D, TELEMAC-2D simulation on 0.025, and 0.03 Manning's coefficient were under-estimated, and the rest of the simulations were over-estimated.

Table 6-2: Inundation area summation of fifty-nine sections

	$simulated\ inundation\ area = \sum_{j=1}^{59} inundation\ area\ at\ each\ section$		$\frac{simulated\ inundation\ area}{observed\ water\ cover\ area} *100$	
	HEC-RAS 2D (m^2)	TELEMAC-2D (m^2)	HEC-RAS 2D (%)	TELEMAC-2D (%)
Manning coefficient n=0.06	891,671.8538	880,138.0429	108.7685889	107.3616629
Manning coefficient n=0.05	870,171.0129	882,234.1966	106.1458571	107.6173575
Manning coefficient n=0.045	854117.3049	834,200.0978	104.1875816	101.7580258
Manning coefficient n=0.03	792,363.2766	792,601.1552	96.65465511	96.68367219
Manning coefficient n=0.025	76,8283.293	774,295.9776	93.71731238	94.4507562

To sum up, the lowest error between the simulated inundation area and bathymetry data was generated in TELEMAC- 2D simulation on 0.045 Manning's coefficient, and the maximum error (RMSE) was found in TELEMAC-2D simulation on 0.05 Manning's coefficient. Therefore, both HEC-RAS 2D and TELEMAC-2D modeling were consistent in that hydraulic roughness coefficient for the selected river channel was equivalent to 0.045 Manning coefficient. However, model calibration and validation, and more analysis by comparing water depth, flow velocity, and other measured hydraulic parameters are needed to get optimum value roughness for the simulated

river reach. Generally, the water cover area comparison by RMSE is also not enough for either screening the best model or for getting channel roughness.

6.1.3 Influence of Islands on Inundation Extent Prediction

Statistical comparing of the root mean square error (RMSE) measures the magnitude of variance between simulated and observed water cover areas in each river section. In such, that a low RMSE indicates that the simulated inundation extent tends to be close to the observed inundation area; whereas a large RMSE reflects that there is high variance between the observed and simulated water edge line. However, some sections that have a significant magnitude difference between the observed and simulated inundation areas can control the overall result. To overcome limitations in an RMSE comparison, analysis of the results at island cross-sections (zone), river bends, and the storage area can be necessary for meandering river modeling. Also, the way hydraulic models handle a water shore at bends and islands areas can decrease flood mapping performance and the accuracy of computed flow variables.

To check the influence of islands on hydrodynamic computation for the Surna river modeling and the performance of both models at islands, the RMSE value for four islands in the Surna river was evaluated.

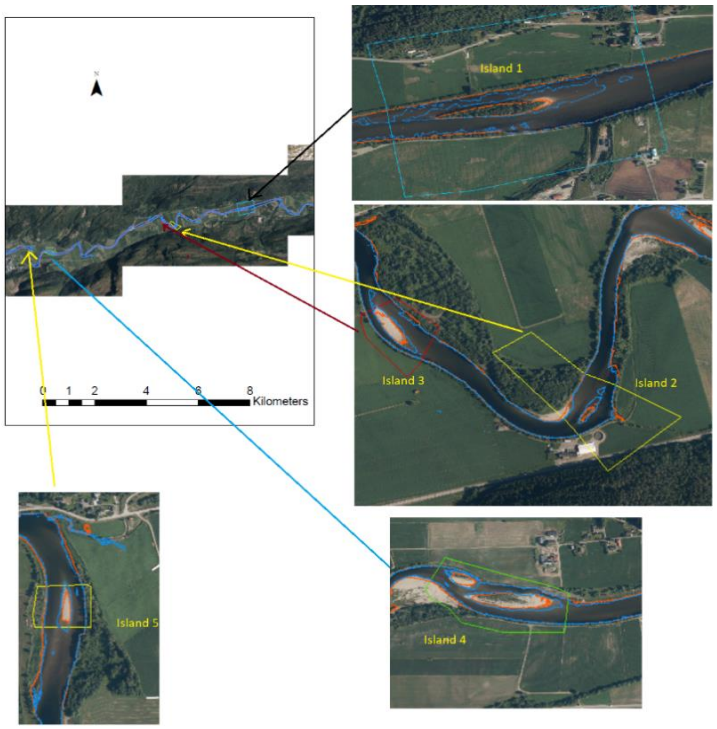

Figure 6-7: Islands selected for evaluating both hydrodynamic models performance at island sections

Table 6-3:RMSE at islands

Simulation name	$\boldsymbol{simulated\ inundation\ area = \sum_{j=1}^{5} inundation\ area\ at\ \ each\ section}$	**RMSE (m^2)**
20 August2016 HEC-RAS2D simulation on Manning's coefficient value = 0.06	68,306,864.27	3,696.129442
20 August2016 HEC-RAS2D simulation on Manning's coefficient value = 0.05	44,617,416.22	2,987.219986
20 August2016 HEC-RAS2D simulation on Manning's coefficient value = 0.045	31,768,661.2	733.792808
20 August2016 HEC-RAS2D simulation on Manning's coefficient value = 0.03	2,962,620.961	769.7559303
20 August2016 HEC-RAS2D simulation on Manning's coefficient value = 0.025	3,314,885.798	814.2340938

20 August2016 TELEMAC-2D simulation on Manning's coefficient value = 0.06	37,236,629.37	2,728.978907
20 August2016 TELEMAC-2D simulation on Manning's coefficient value = 0.05	15,926,188.88	1,784.723445
20 August2016 TELEMAC-2D simulation on Manning's coefficient value = 0.045	219,242,268.1	1,927.685308
20 August2016 TELEMAC-2D simulation on Manning's coefficient value = 0.03	5,873,805.101	1,083.863931
20 August2016 TELEMAC-2D simulation on Manning's coefficient value = 0.025	17,754,766.33	1,884.397321

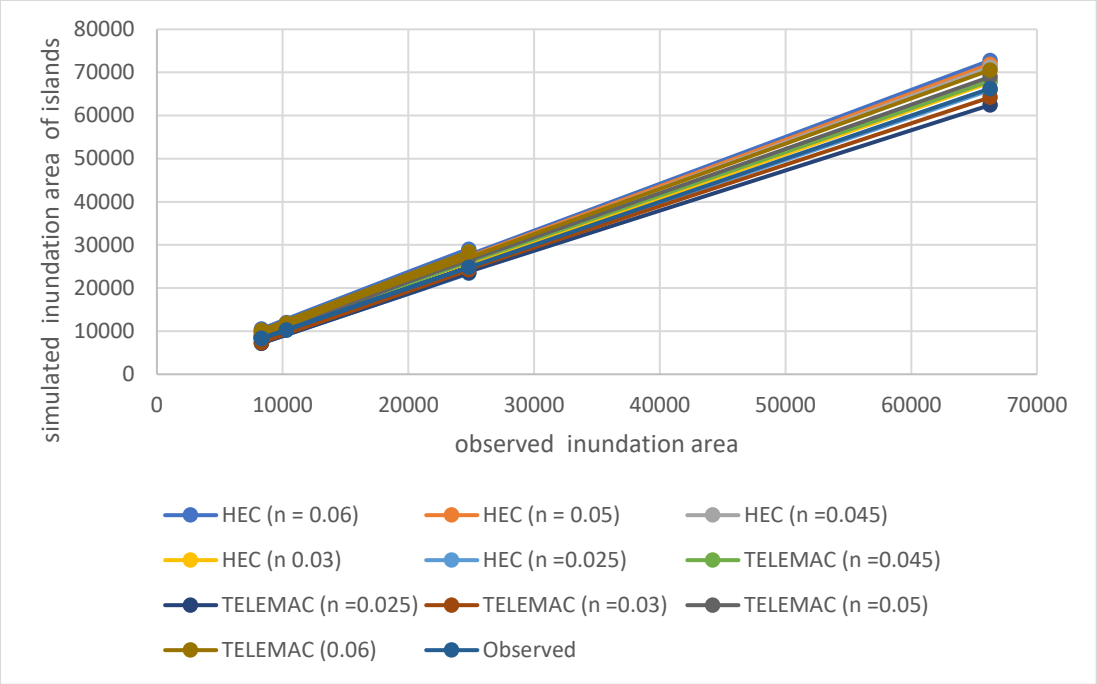

Figure 6-8: Simulated and observed water cover area at island zones. The best fitting simulation is that closest to the observed line.

As per the RMSE value from the above table, the RMSE results computed from observed and simulated inundation areas of five islands sections in the Surna river show that flood mappings computed in HEC-RAS 2D were better fit than TELEMAC-2D simulations. In contrast, hydrodynamic computation in HEC-RAS 2D on 0.045 roughness coefficient scored as the lowest RMSE value and the highest ration of the simulated inundation areas and observed water cover areas.

Generally, inundation results from HEC-RAS 2D and TELEMAC-2D simulations of the Surna river (meandering river and with islands) indicates that the accuracy of flood mapping at the islands zones is lower than modeling at the straight channel sections. In other words, the simulated inundation extents at the straight river zones are more fit with the observed inundation extent than the flood mapping at river's zones with its islands.

6.1.4 Comparison of Water Surface Elevation Computed in HEC-RAS 2D and TELEMAC-2D

In addition to comparing both models in terms of inundation area, a cross-sectional profile of the water surface elevation and water depth computed in HEC-RAS 2D and TELEMAC 2D by using

0.045 Manning's coefficient was assessed. Indeed, there was no measured water surface elevation and water depth for this study. However, analysis of a water surface elevation and water depth at the different river sections was processed to obtain the influence of bends, pools, and islands on the comparison models' accuracy. In addition, a comparison of terrain interpolated by RASMapper in HEC-RAS and BLUEKNUE of TELEMAC-MASCARET was made. Further, two river cross-sections at two river bends, two river cross-sections at two islands, and two river cross-sections at a straight river section were selected to analyze the influence of river morphology on the similarity of both models. The terms used in the figures below:

- HEC_0.045 = Water surface elevation computed in HEC-RAS 2D by using 0.045 Manning's coefficient
- TELEMAC_0.045 = Water surface elevation computed in TELEMAC- 2D by using 0.045 Manning's coefficient
- HEC_water depth (0.045) = Water depth simulated in HEC-RAS 2D by using 0.045 Manning's coefficient
- TELEMAC_water depth (0.045) = Water depth simulated in TELEMAC-2D by using 0.045 Manning's coefficient

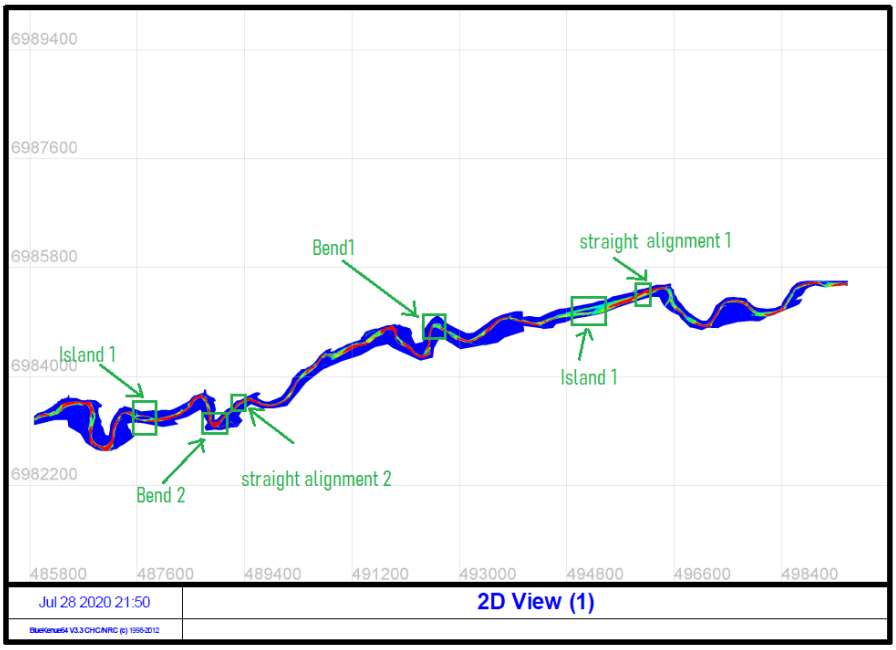

Figure 6-9:Selected river cross section for analyzing the influence of river morphology on hydrodynamic models

a. Cross section at bend 1

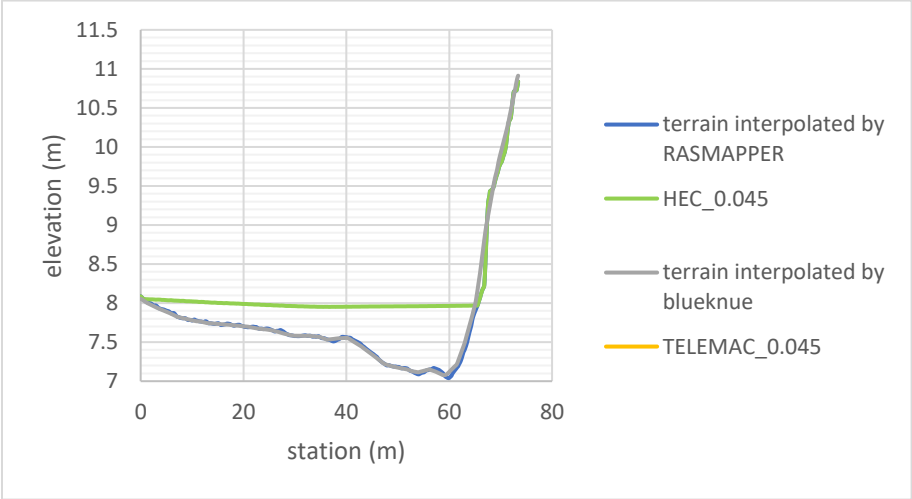

Figure 6-10: Water surface elevation at bend 1

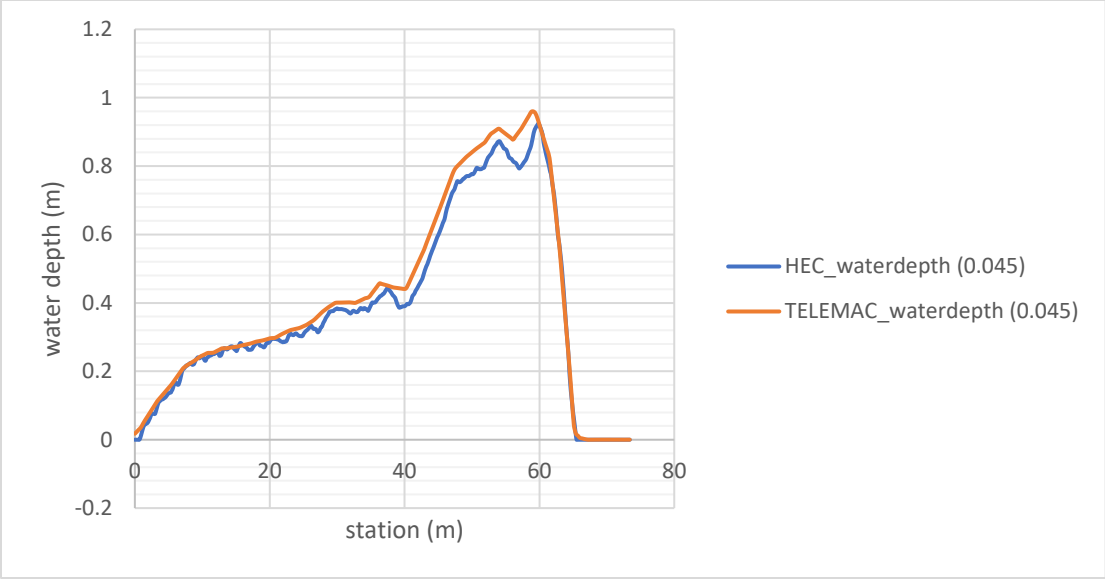

Figure 6-11: Water depth at bend 1

b. Cross section at bend 2

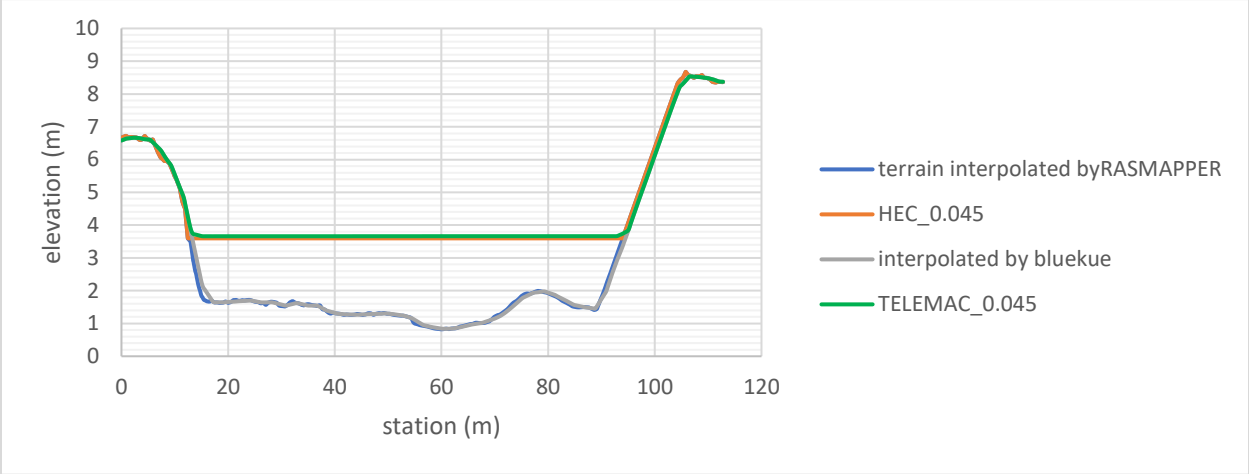

Figure 6-12:Water surface elevation at bend 2

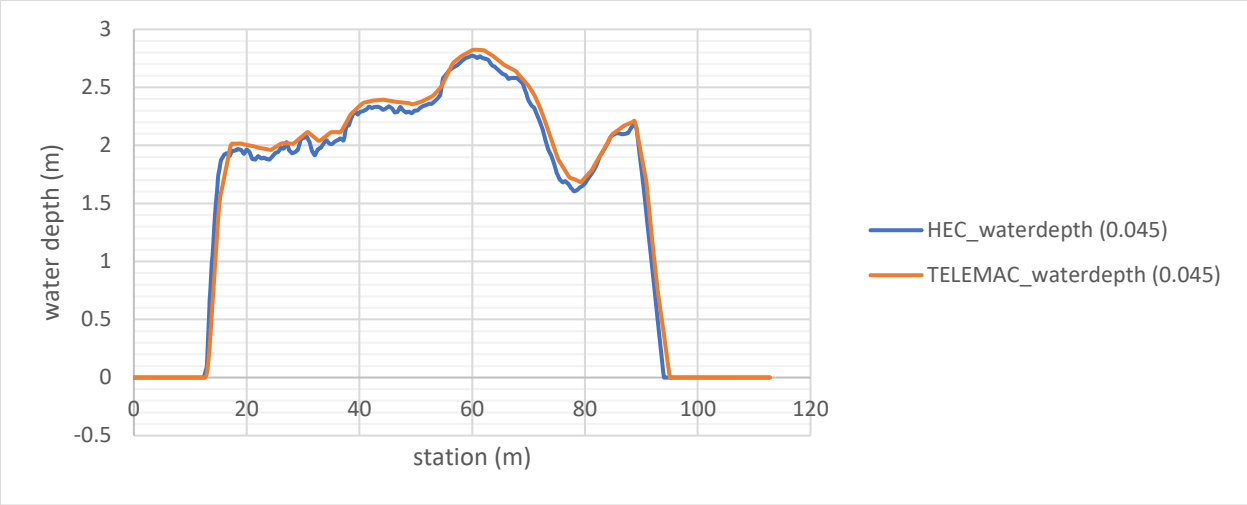

Figure 6-13: Water depth at bend 2

c. Cross section at island 1

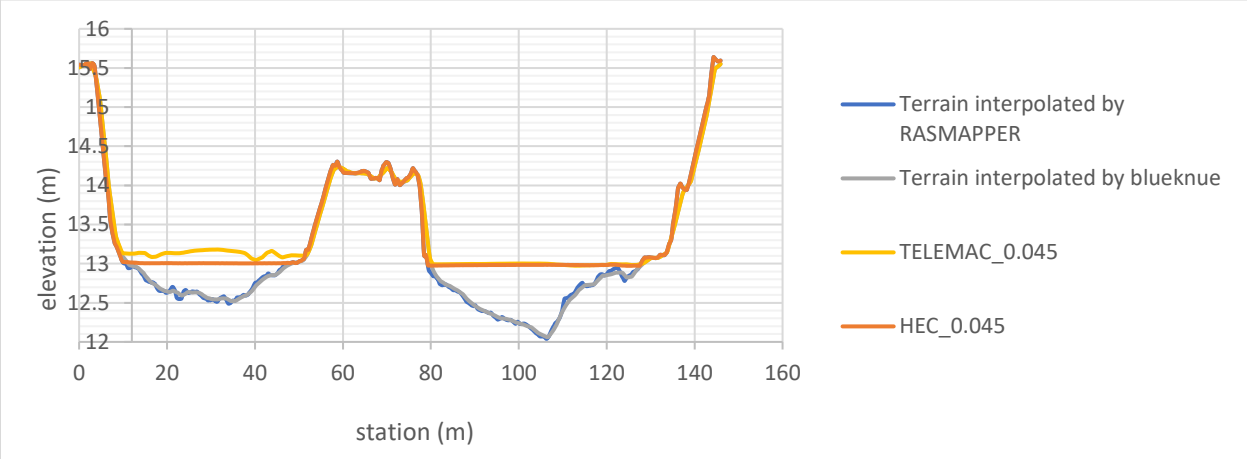

Figure 6-14: Water surface elevation at island 1

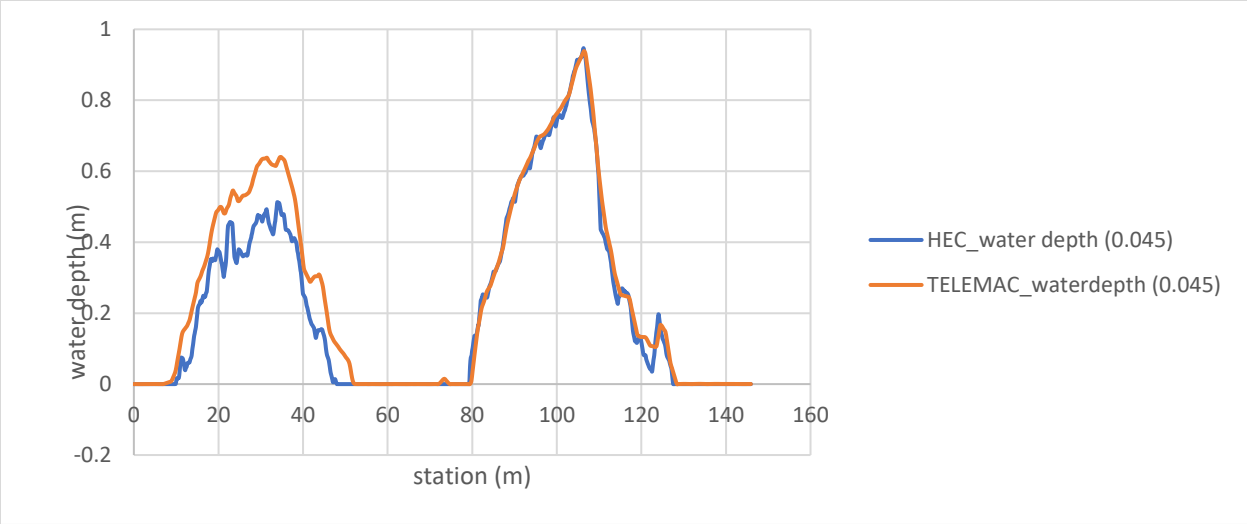

Figure 6-15: Water depth at island 1

d. Cross section at island 2

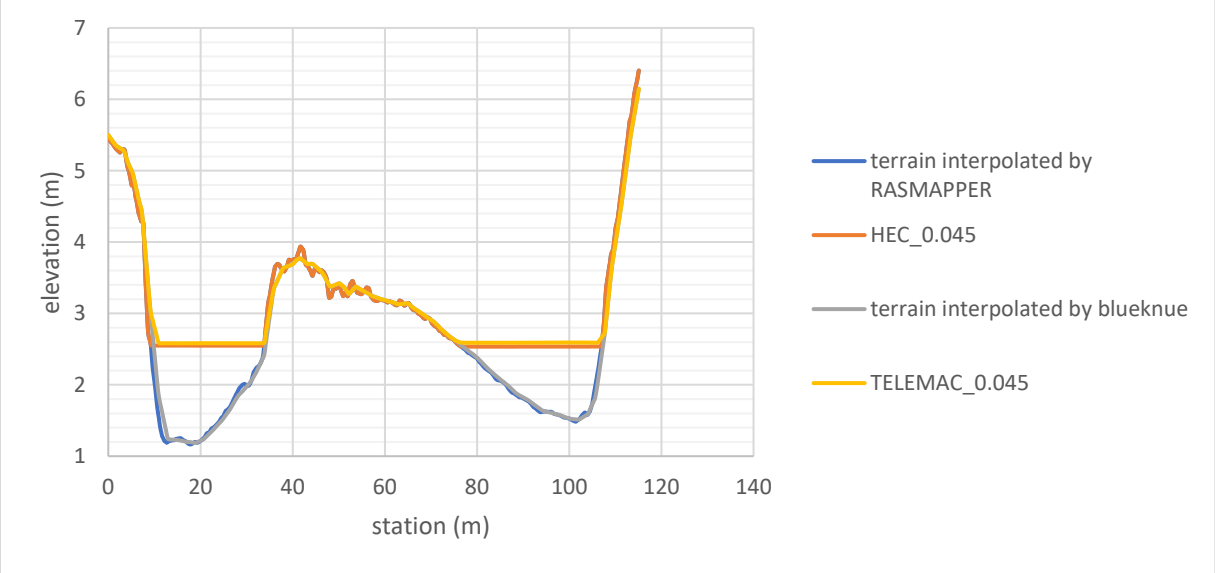

Figure 6-16: Water surface elevation at island 2

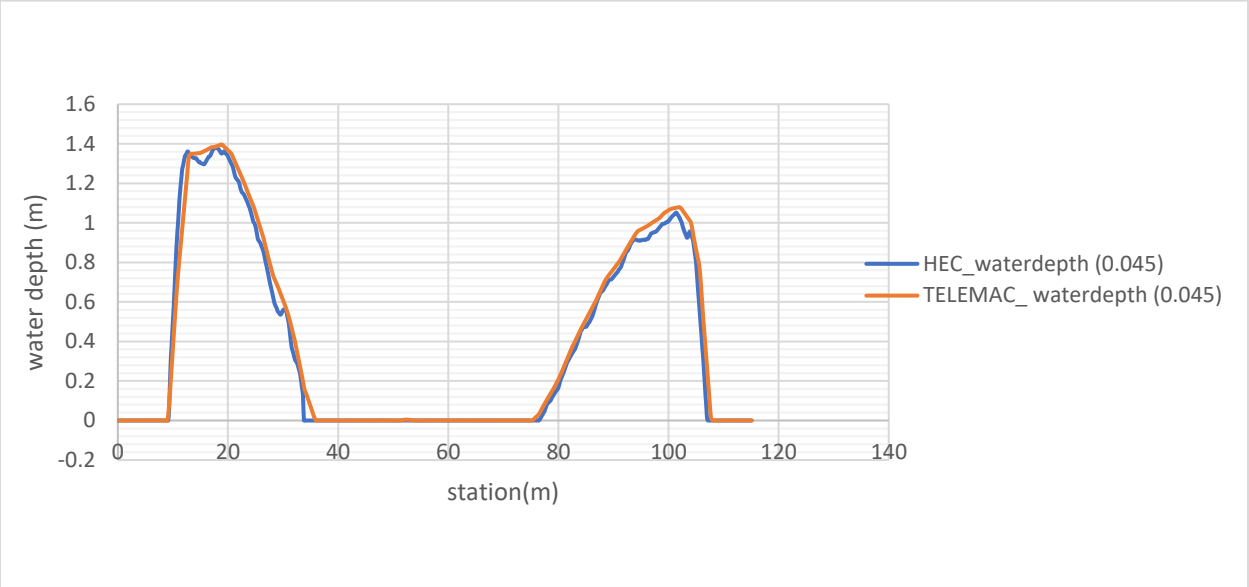

Figure 6-17: Water depth at Island 2

e. <u>Cross section at straight river alignment 1</u>

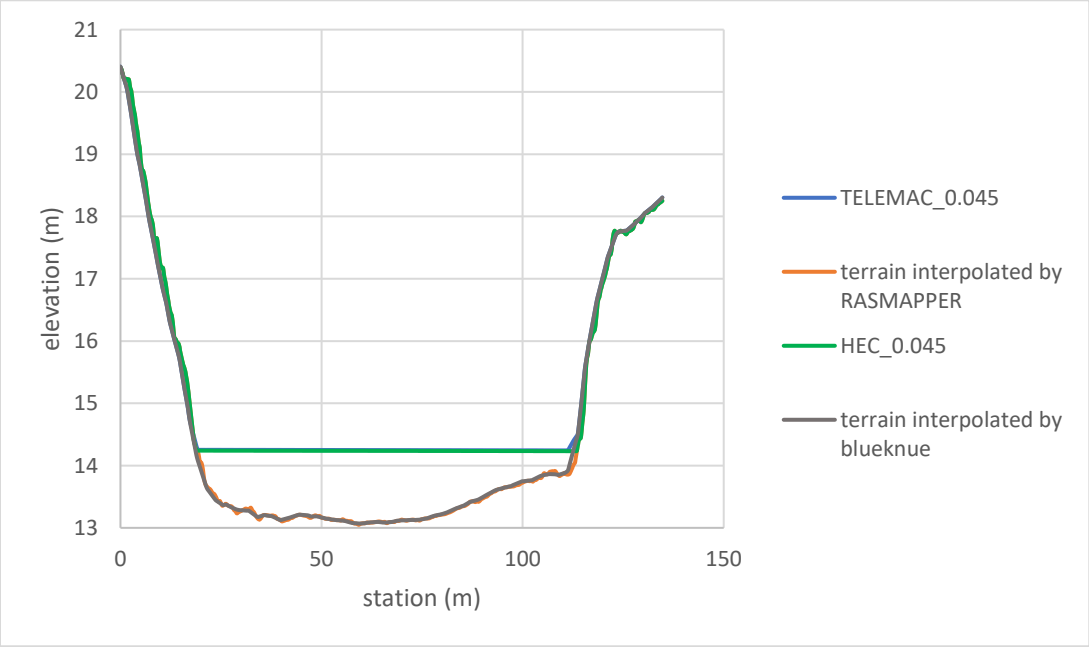

Figure 6-18:Water surface elevation at straight river alignment 1

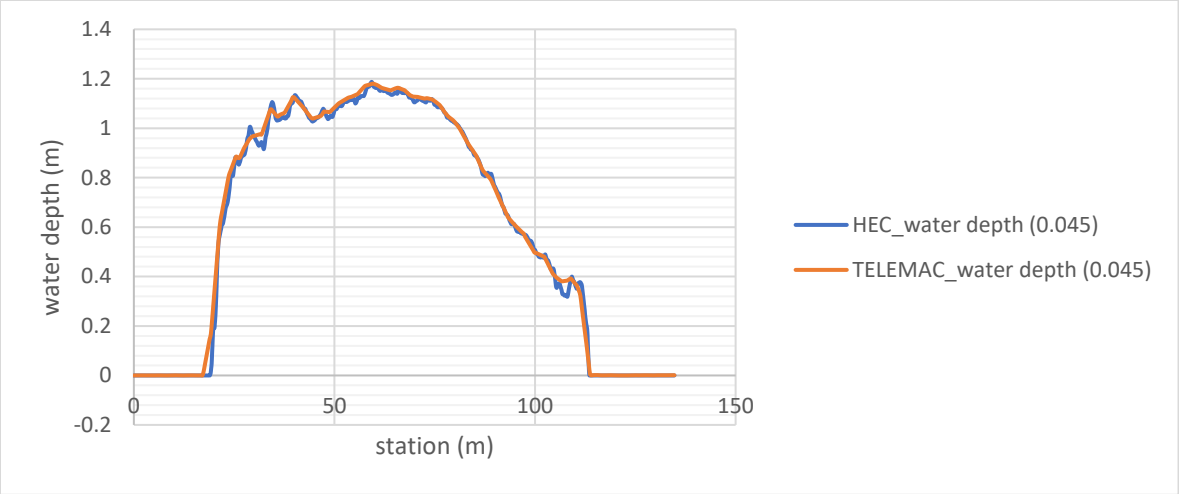

Figure 6-19: Water depth at straight river alignment 1

f. Cross section at straight river alignment 2

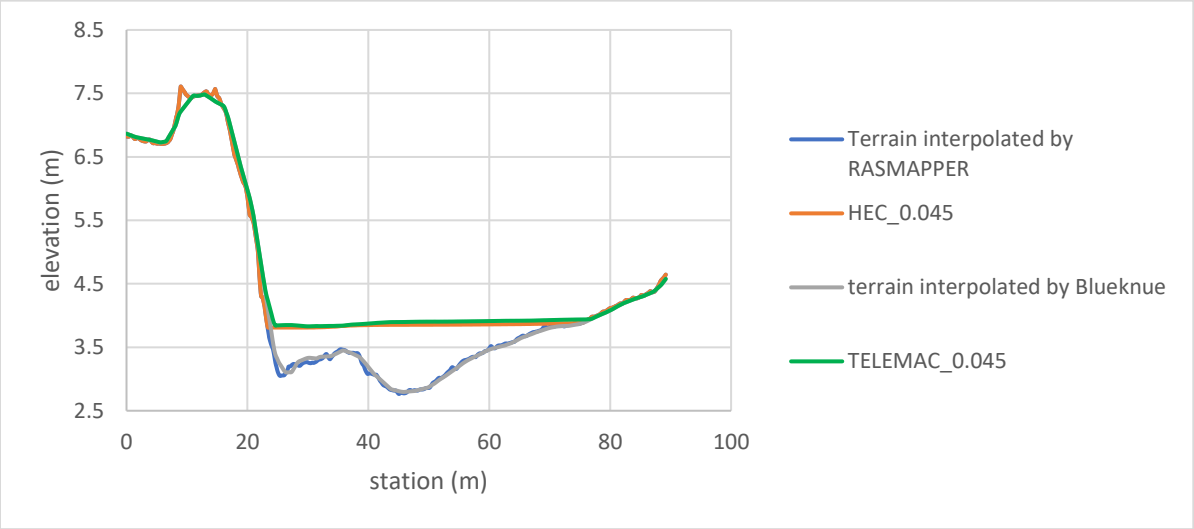

Figure 6-20: Water surface elevation at river straight alignment 2

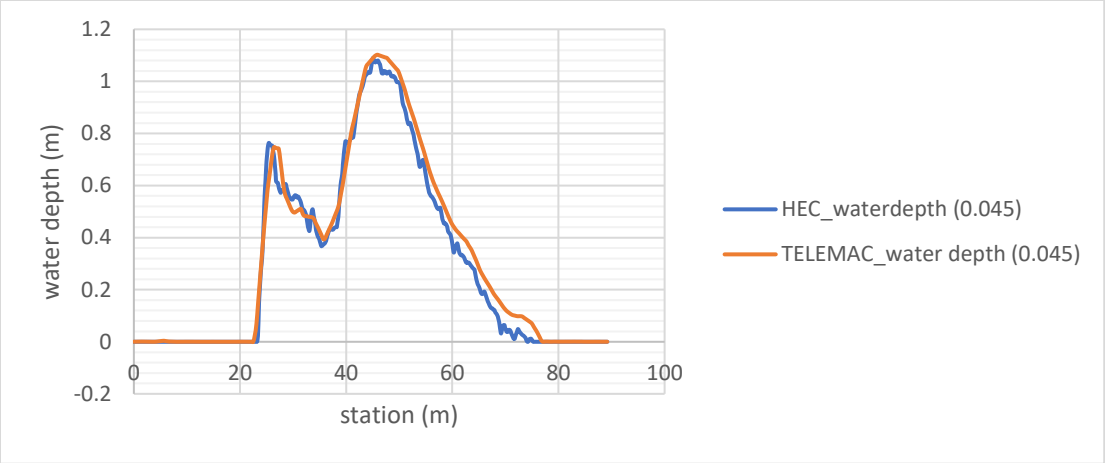

Figure 6-21: Water depth at straight river alignment 2

The results show a good agreement between water surface elevation, water depth and terrain interpolated by both packages, and minor differences at the island cross-sections. Such that both models need a calibrated set-up and an experimental governing equation at the island areas to handle the influence of tidal force in the hydrodynamic computations. In addition, TELEMAC-2D showed a minor higher water surface elevation value for the same roughness and flow event.

6.1.5 Comparison of Velocity Computed in HEC-RAS 2D and TELEMAC-2D

In addition to comparing simulated water surface elevation and inundation area, both models were compared to each other based on computed velocity. In this case, a simulated velocity from hydrodynamic computation in the Surna river by applying 0.045 Manning's roughness for both models was compared. As with the comparison of water surface elevation, the same cross-section location was selected for comparing velocity. The terms used in the figures below:

- HEC_veloctiy (0.045) = Flow velocity computed in HEC-RAS 2D by using 0.045 Manning's coefficient
- TELEMAC_ veloctiy (0.045) = Flow velocity computed in TELEMAC- 2D by using 0.045 Manning's coefficient

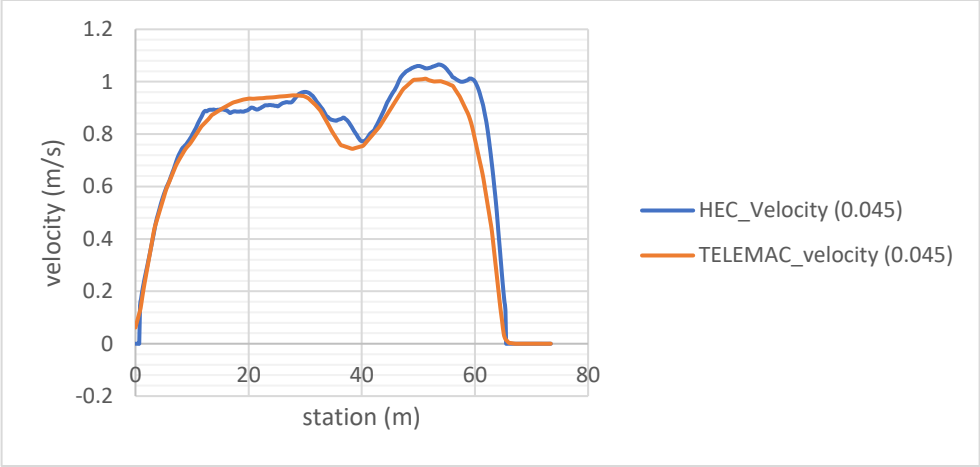

Figure 6-22: velocity at bend 1

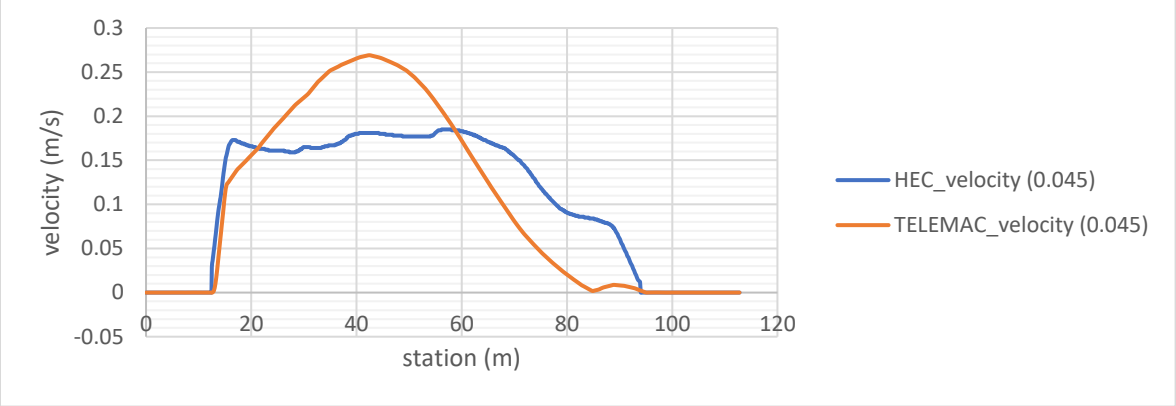

Figure 6-23: velocity at bend 2

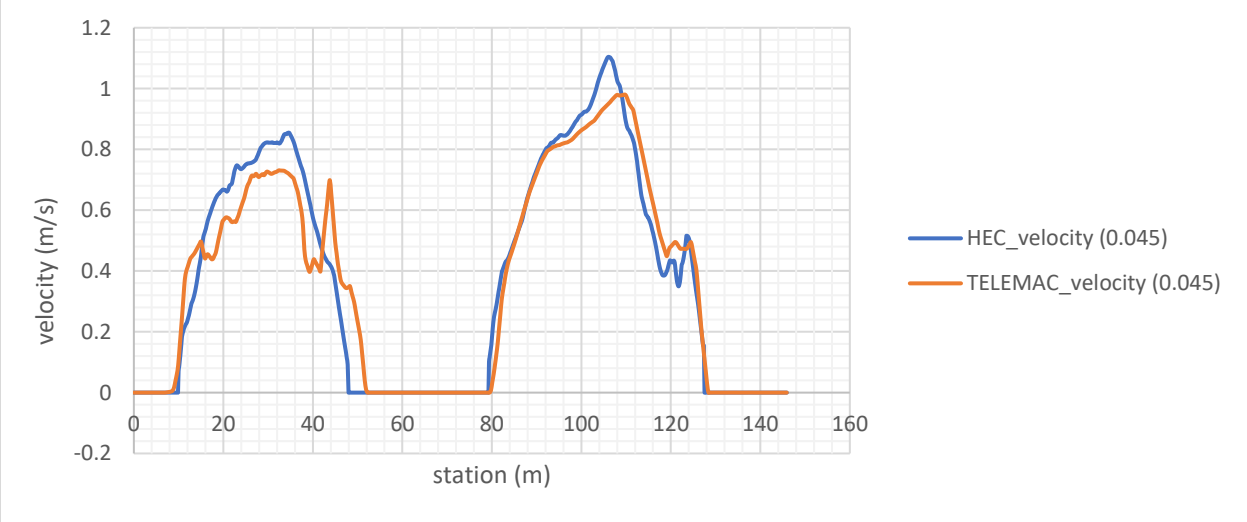

Figure 6-24: velocity at island 1

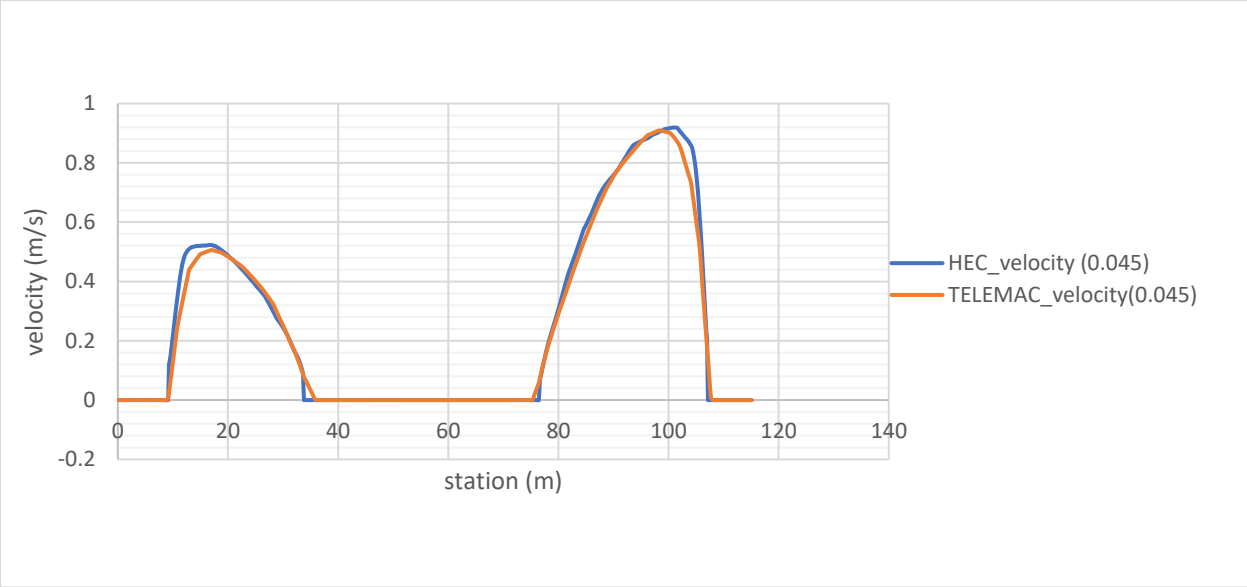

Figure 6-25: velocity at island 2

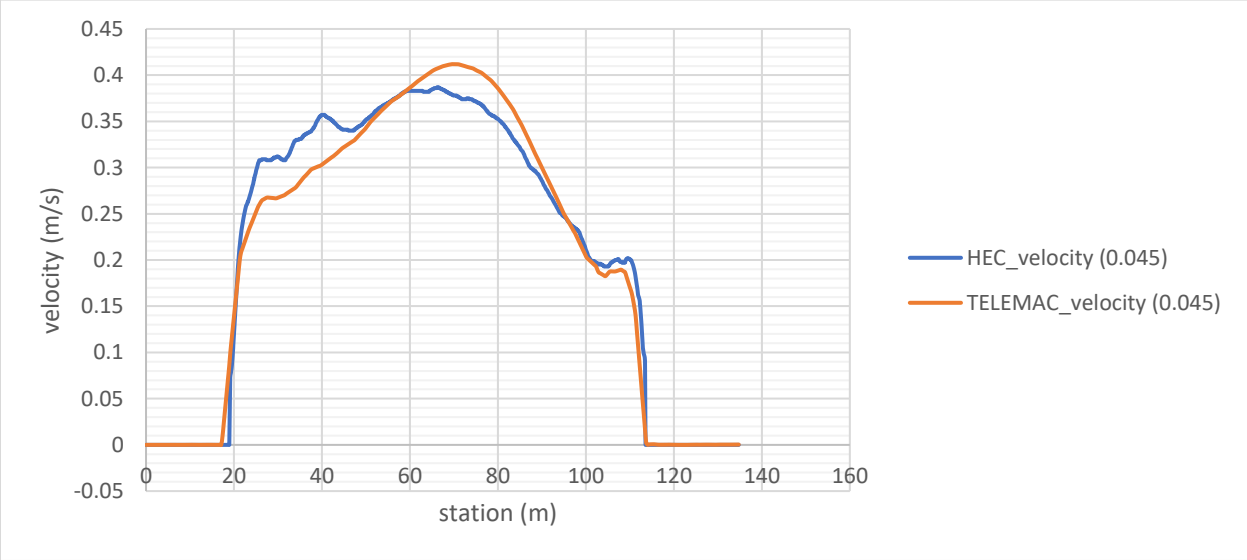

Figure 6-26: velocity at river straight alignment 1

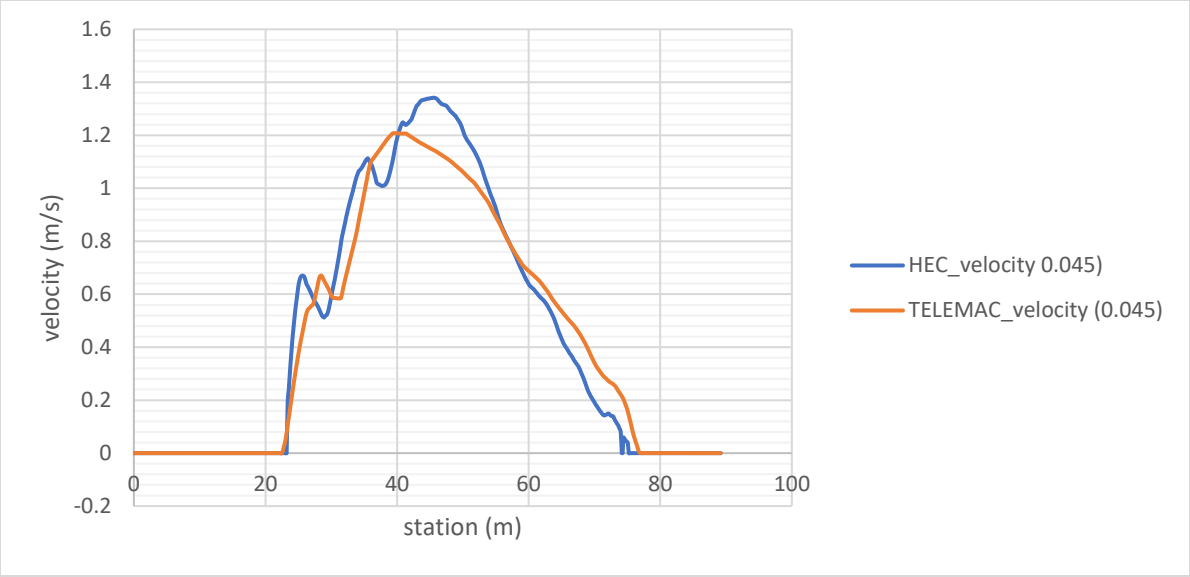

Figure 6-27: velocity at river straight alignment 2

The above graphs show that good agreement between cross-sectional velocity computed in HEC-RAS 2D and TELEMAC 2D was achieved at bend 1, bend 2 and island 2; and a minor difference (less than 0.17 m/s) occurred at island 1, straight alignment 1 and straight alignment 2. However, velocity profile shape simulated in HEC-RAS 2D was less fitting with that calculated in TELEMAC 2D, and at the 42.9 m station TELEMAC-2D estimated a 0. 27 m/s peak velocity and HEC-RAS 2D estimated 0.186 m/s.

6.1.6 Models Comparison Based on Simulation Time for Surna River Modeling

For the Surna river, since hydraulic computation in TELEMAC-2D was computed on a 17.17 km reach and 1.5 x1.5 m grid size, it took more than two weeks to perform a single simulation. Moreover, to save work simulation time, all simulations of the Surna the river modeling in TELEMAC-2D was performed by applying a 1-second simulation time. Indeed, computational time varies even in the simulation performed in one model; other factors such as the computer system, mesh sizes, and roughness value can also extend or decrease simulation time. To handle such conditions, HEC-RAS 2D and TELEMAC-2D simulation over a 24-hr duration by applying 0.05 Manning coefficient were performed on the same computer (processor).

Table 6-4: Simulation time for the Surna river modeling

Types of simulation	Simulation time	Remark
TELEMAC-2D simulation by applying FEM and constant time step	35hr: 45min: 4 seconds	Constant computation time step =1 sec
TELEMAC-2D simulation by applying FEM and variable time step	More than 2 weeks	Variable time step: Courant =0.5
HEC-RAS simulation by applying diffusion wave equation	182hr: 32min: 28 seconds	Variable time step: max courant =0.5, Minimum Courant = 2

6.2 Vekveselva (steep and shallow) River simulations' Result

This section of work aimed to extract results from HEC-RAS 2D and TELEMAC-2D model to evaluate the suitability of both models in hydrodynamic modeling for a steep river. Likewise, evaluating the accuracy of the digital surface model data and the digital elevation model obtained from https://hoydedata.no/LaserInnsyn/ was presented in this section. Also, a comparison of a finite element method (FEM) and finite volume method (FVM) in a steep river was included in this section, in order robust output data from the TELEMAC-2D simulation.

6.2.1 Evaluating of HEC-RAS 2D and TELEMAC-2D computations on Digital Elevation (DEM)

In this section, the suitability of both hydrodynamic models in the steep river is evaluated by applying simulated inundation areas on the orthophoto. An orthophoto, which is a geometrically corrected and projected image, was obtained from https://www.norgeibilder.no/ and used to represent the actual surface profile of the river and flood plain. Since both hydraulic computations in HEC-RAS 2D and TELEMAC-2D were performed on a DEM and DSM and corresponding simulations were needed in results' analysis; inundation extent, water surface elevation, water depth, velocity and interpolated terrain from both models were extracted.

6.2.1.1 Inundation Extent, Water Depth and Water Surface Elevation Results from HEC-RAS 2D Computations on Digital Elevation Model (DEM)

As mentioned in section (5.4.3.1.3), four hydraulic dynamics simulations were computed to achieve a suitable model set up and modifying terrain. In contrast, four simulations were applied to overcome the challenge from the discontinuities parameter results of steep slope hydraulic computation.

i. **Simulation1**: The first simulation (called simulation1) was a 5-hour simulation time on 0.5x0.5m mesh size. A 0.898 m^3/s of constant hydrography was applied at an upstream boundary condition with 0.03 energy grid line, and 0.03 friction slope was applied at downstream boundary condition.

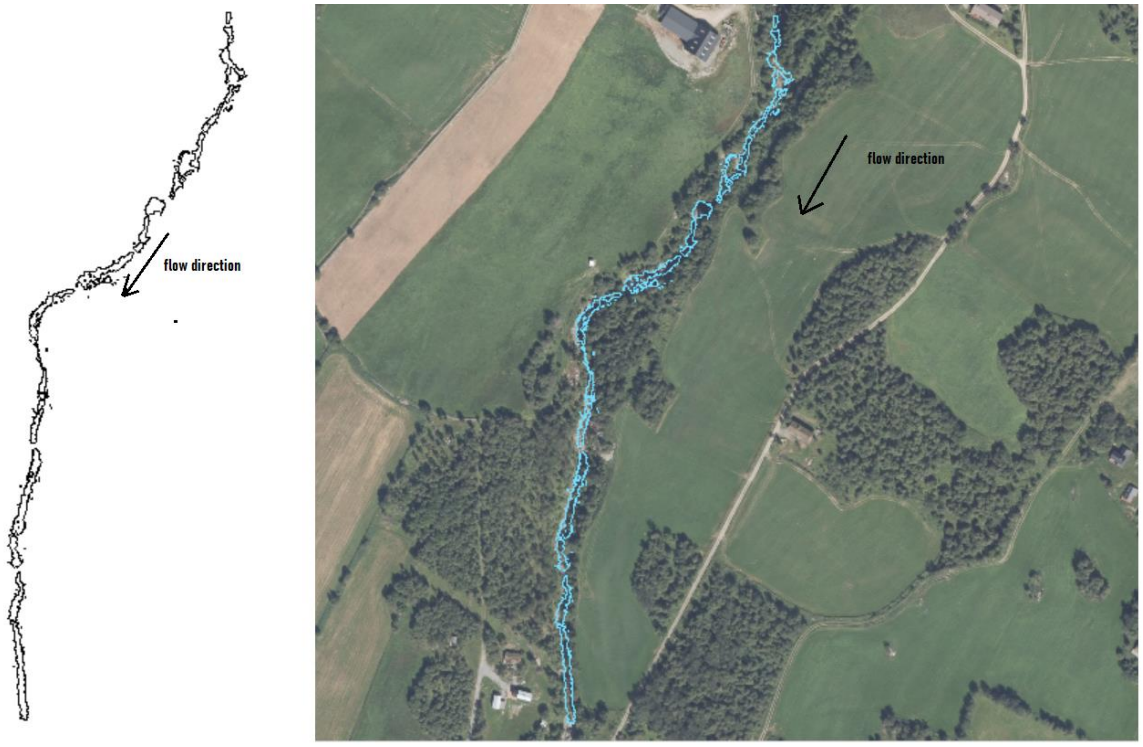

Figure 6-28:Inundation area extracted from simulation1 which was computed in HEC-RAS 2D modeling on a DEM. The left side represents the inundation area of simulation1 on a spreadsheet and the right side represents the inundation area overlap on an orthophoto obtained from https://www.norgeibilder.no/

The above inundation result shows that the simulated water edge was not continuous. As a result, the water surface elevation and the terrain slope where gapped simulated inundation extent occurred were assessed.

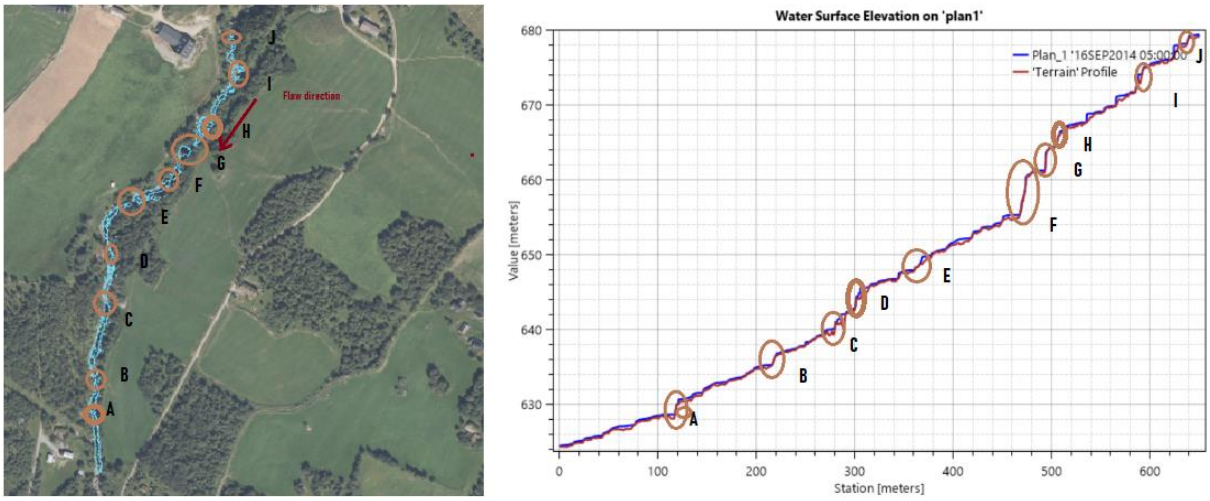

6-29:River sections where inundation area and water surface elevation discontinuities happened in simulation 2. The blue line on the water surface elevation graph represents water surface elevation and the brown line represents terrain elevation.

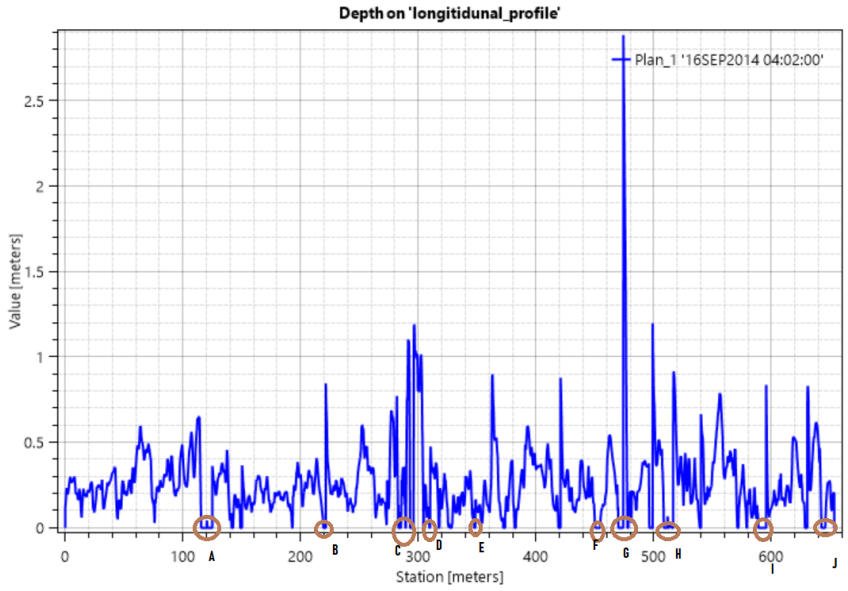

Figure 6-30:Water depth profile along with longitudinal river center line (longitudinal profile).

As far as described in figure (*6-29*; *Figure 6-30*), the simulated water surface line has gapped where the terrain slope is significantly changed. On the other hand, a peak water depth equal to 2.87 m was simulated.

Table 6-5: Slope value at selected points

Point/location	Slope (%)
A	37.92
B	27.14
C	32.59
D	42.94
E	13.18
F	65.54
G	25.45
H	36.05
I	47.19
J	30.02

ii. **Simulation 2**: this simulation's objective was to analyze the water surface profile, inundation area, and water depth by extending simulation time. The 24-hr simulation time was adjusted on the same geometry, mesh size, and boundary lines.

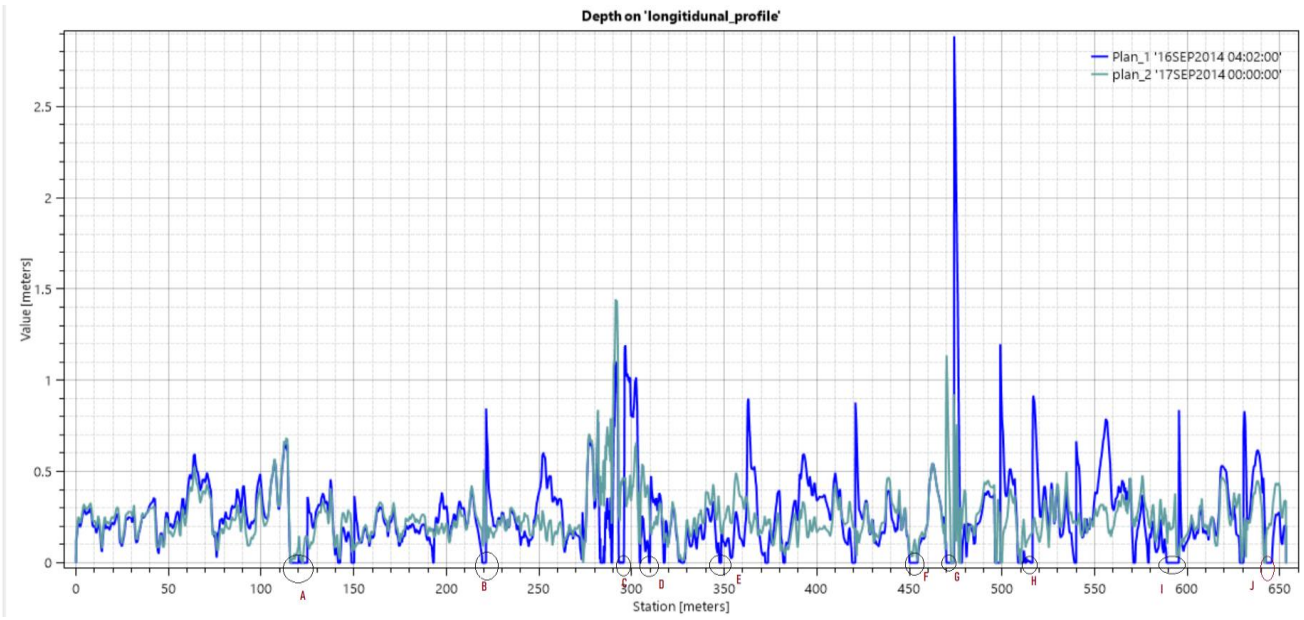

Figure 6-31: Longitudinal water depth profile along river centerline (longitudinal profile); blue colored line represents simulation 1's (5-hr simulation time) water depth; and the dark green colored line represents the simulation 2's water depth (24-hr simulation).

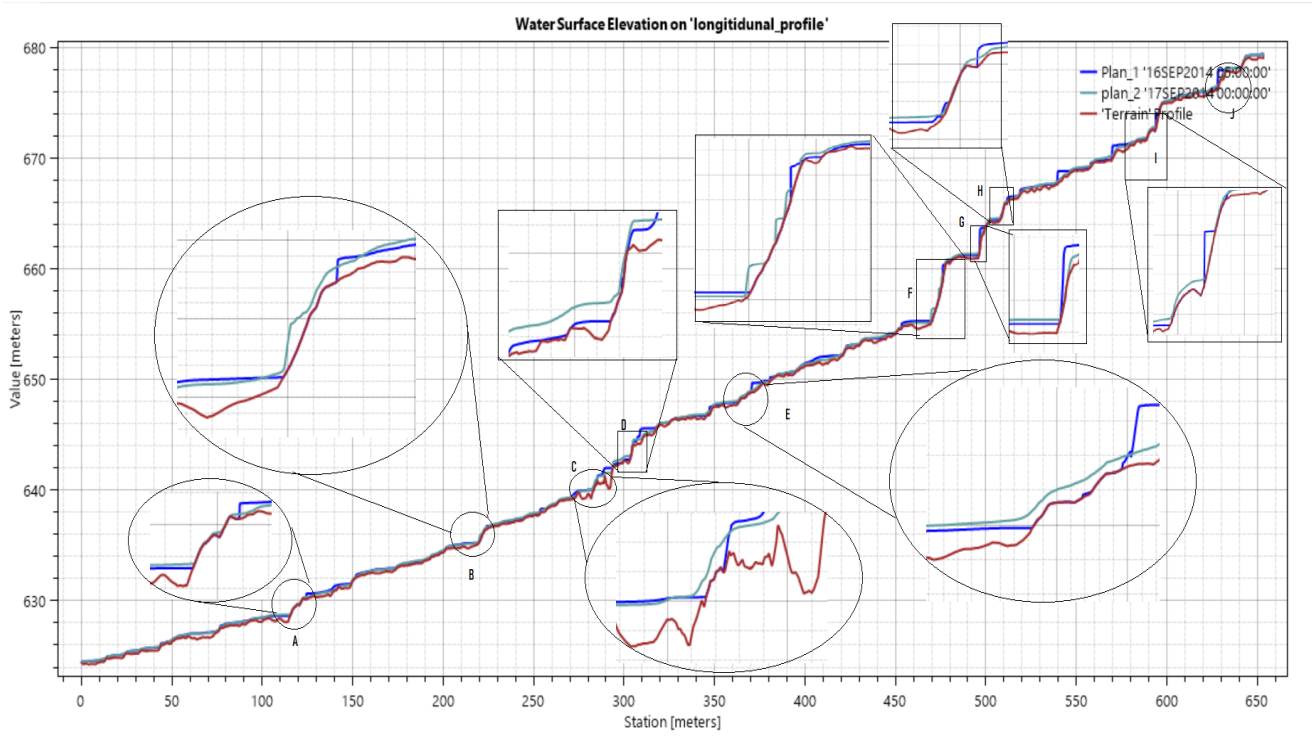

Figure 6-32:Longitudinal water surface elevation profile along river centerline (longitudinal profile). The blue colored line represents a simulation 1's (5-hr simulation time) water depth; and

the dark green colored line represents the simulation 2's water surface elevation (24-hr simulation).

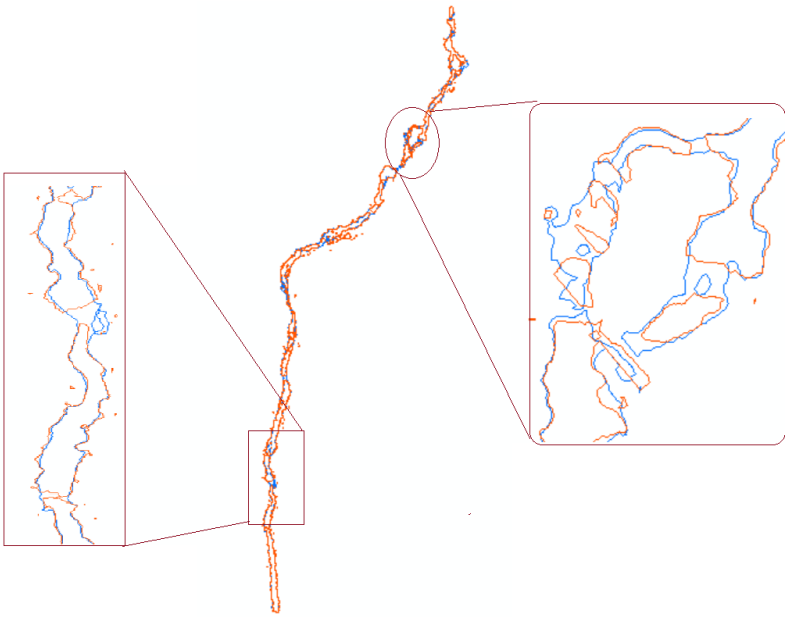

Figure 6-33:Inundation area extracted from simulation 2 which was computed in HEC-RAS 2D modeling on a DEM. The orange line represents a water edge extracted from the simulation 1(5-hr simulation time) and the blue line represents a water edge extracted from simulation 2 (24-hr simulation time).

To sum up, an extension of the simulation time from 5-hours to 24-hours reduced the number and extent of the gaps between the inundation areas. In contrast, extending the simulation time was limit the zero-water depth (water depth = 0) in the river centerline. Besides, these were troubles eliminated at low slope locations such as point B (27.14), C (32.59 % slope), and (E (13.18 % slope), and gaps decreased in points such as points D and F. Also, peak water depth at point 'G' was decreased from 2.87 m to 1.14 m, while a local peak at the 274 m station was increased.

iii. **Simulation 3:** a third trial to eliminate the cut-off inundation areas was carried out by decreasing an initial energy grid line and fraction slope. At this stage, both energy grid line and frictional slope decrease to 0.001, which makes flat slopes at the initial state of hydraulic calculation. The aim of this simulation analysis is to discover the influence of the initial friction

and energy grid line slope that are used at the downstream and upstream boundary conditions, respectively.

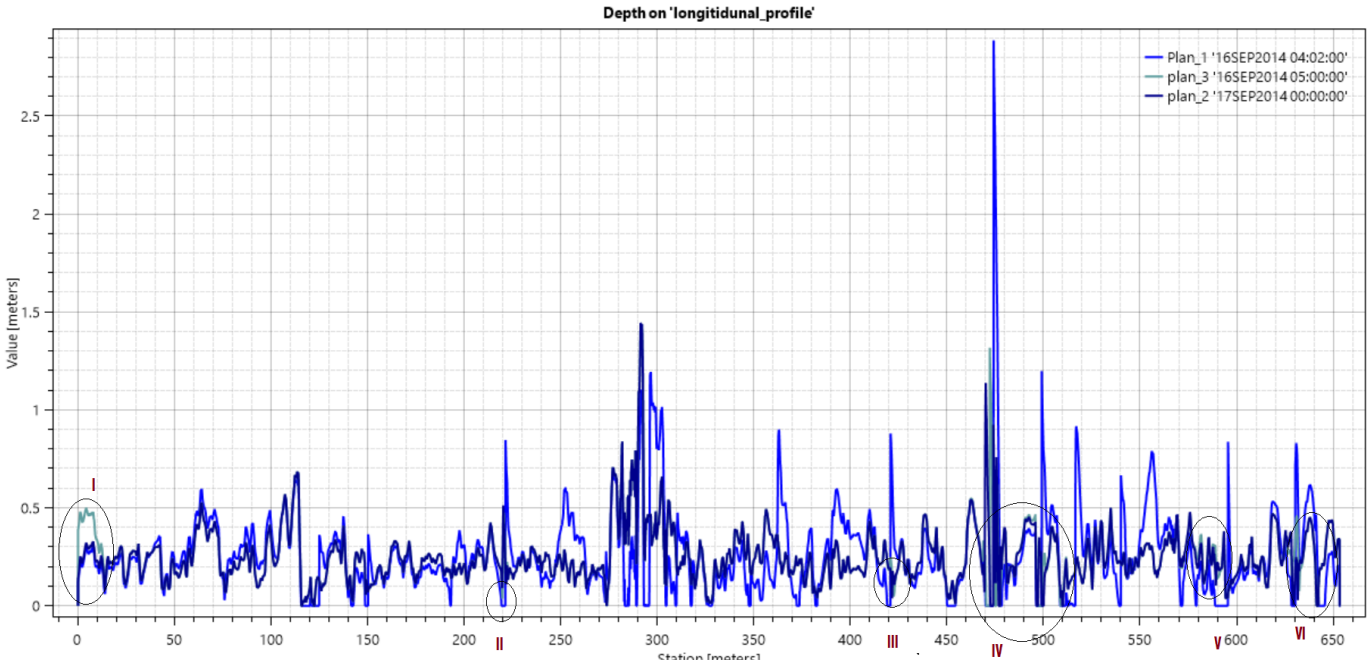

Figure 6-34:Longitudinal water depth profile along river centerline (longitudinal profile). The blue colored line represents simulation1 (5-hr simulation time, and 0.03 slope and energy grid line) water depth; the dark green colored line represents simulation of water depth (24-hr simulation time, and 0.03 slope and energy grid lines), and the blue-black colored line represents simulation 3 (5-hr simulation time and 0.001 slope and energy grid line).

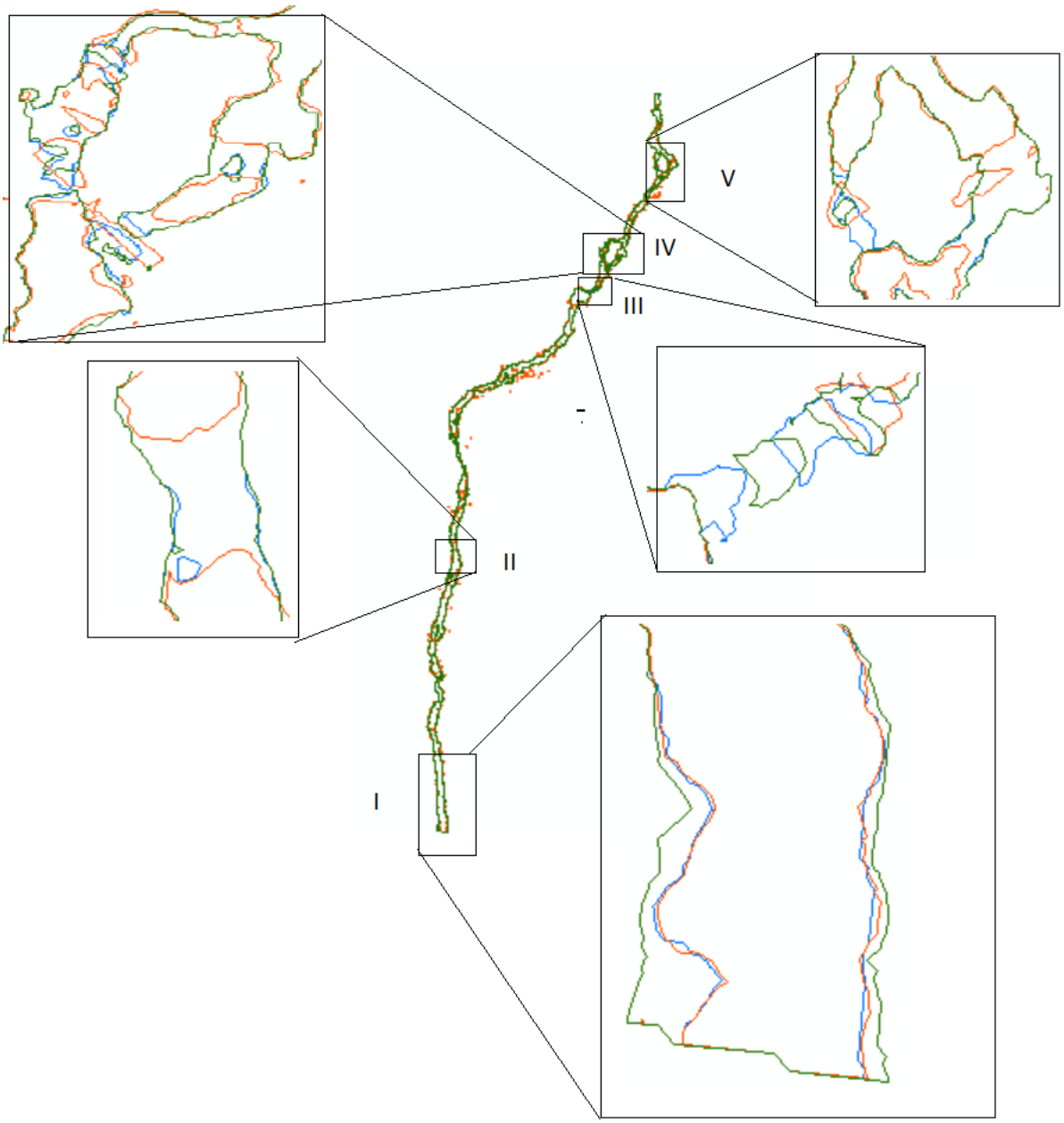

Figure 6-35: Inundation area extracted from simulation 3 which was computed in HEC-RAS 2D modeling on a DEM. The orange line represents a water edge extracted from simulation 1 (5-hr simulation time);the blue line represents a water edge extracted from simulation 2 (24-hr simulation time); and the green line represents a water edge extracted from simulation 3.

Water depth and inundation water edge extent from above figure (Figure 6-34; Figure 6-35)show that both the water depth and inundation extent of simulation 3 and simulation 2 are mostly the same. But a minor inundation extent difference occurred at the upstream reach, downstream, and

at the location where a high gradient occurred. In totally 2,704.148 m^2, 2,884.149 m^2 and 2,889.003 m^2 were simulated in simulation 1, simulation 2 and simulation 3, respectively. In contrast, a180 m^2 computed area difference occurred between simulation 1 and simulation 2; while only 4.854 m^2 of inundation area changed due to flattening of initial energy lines. A comparison of simulation 2 and 3 shows that a centimeter difference of water depth was simulated at the upstream reach. In contrast, changing the initial condition, energy grid line, and friction energy cannot address the significant impact in HEC-RAS modeling.

Simulation 4: this simulation plans to evaluate the model by smoothing mesh sizes to limit model instability. The HEC-RAS user manual advises that cell size should be based on a water surface gradient in selected area, where a large cell size could be appropriate for a flat slope. A steeper slope, where the water surface elevation and slope rapidly change and is localized, requires a smaller cell size to capture those changes (HEC-RAS 2D). Also, the HEC-RAS user manual defines that model instability can occur while the bed slope is higher than 10 %, where the vertical water pressure value is not equal with a multiple of the water unit weight and water depth. Following this theorem, in simulation 4 a refinement grid cell size of 0.2 x 0.2 m was drawn where a steep slope and inundation gap occurred. In principle, this hydrodynamic computation is aimed to decrease the change of the slope between consecutive grid cells, which is proposed to create a continuous water surface profile.

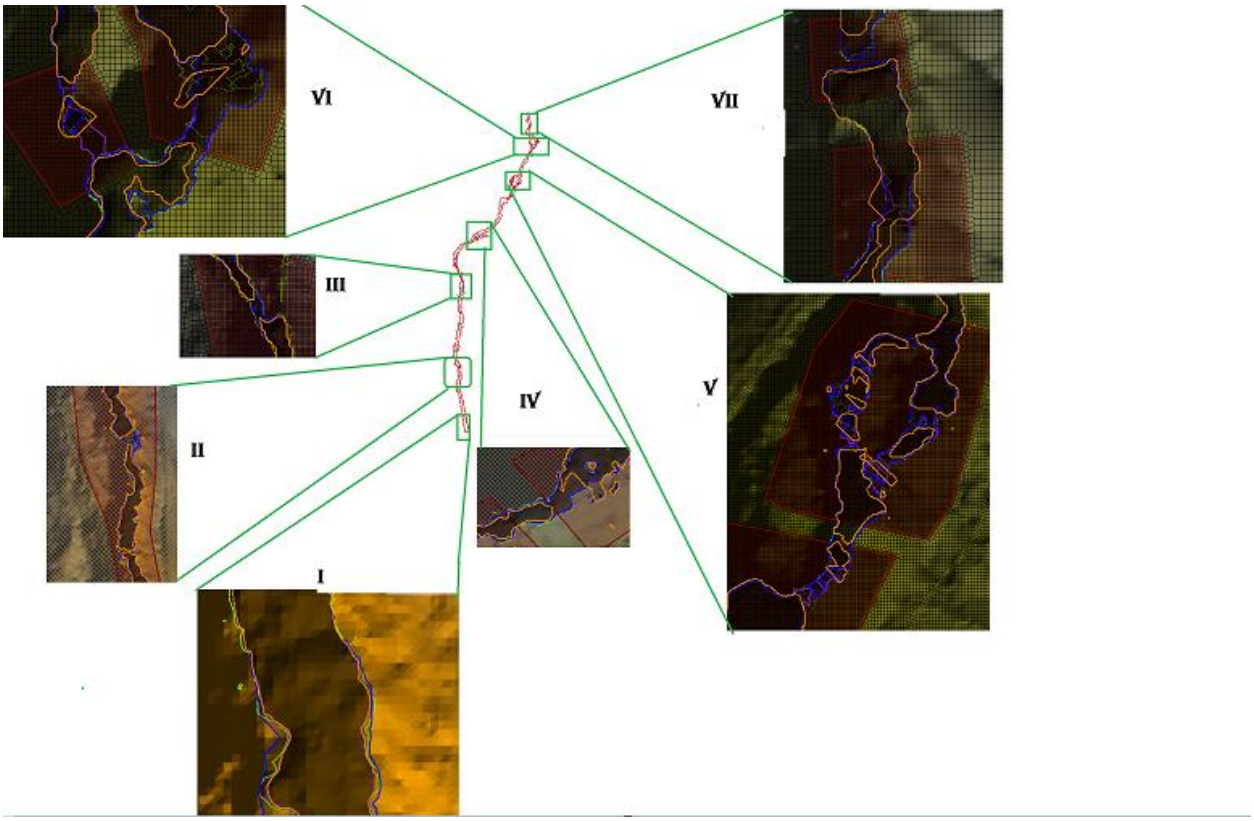

Figure 6-36:Inundation area extracted from simulation 4 which was computed in HEC-RAS 2D modeling on a DEM. The orange line represents a water edge extracted from simulation 1 (5-hr simulation time);the purple line represents a water edge extracted from simulation 2 (24-hr simulation time);the blue line represents a water edge extracted from simulation 3; and the green line represents a water edge extracted from simulation 4.

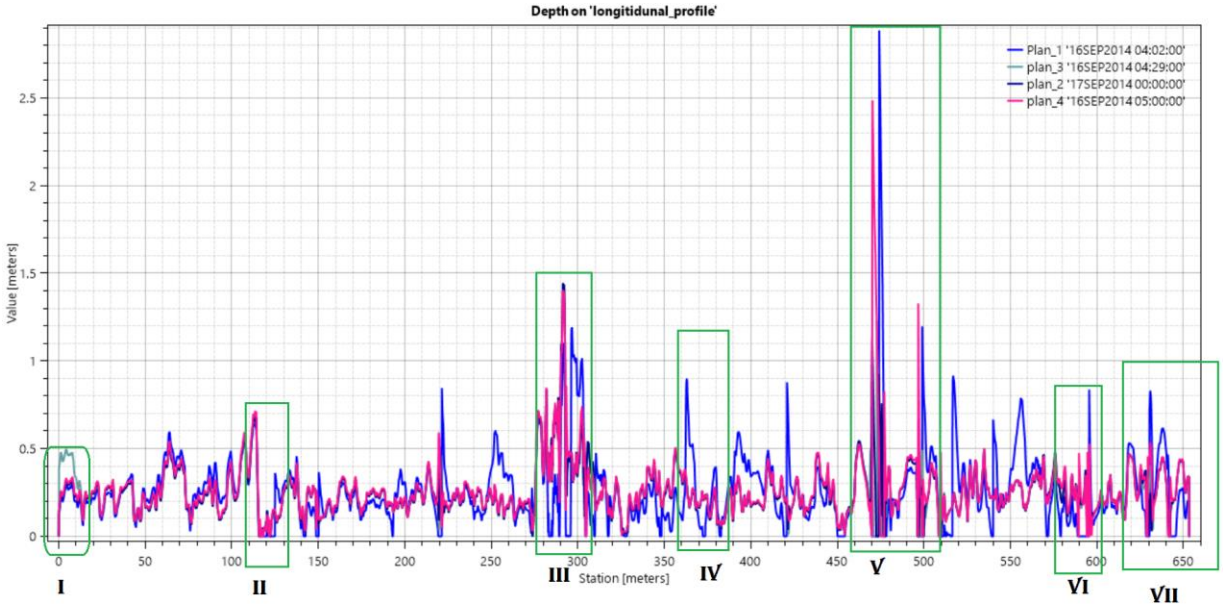

Figure 6-37: Longitudinal water depth profile along the river centerline (longitudinal profile). The blue colored line represents a simulation1 (5-hr simulation time, and 0.03 slope and energy grid line) water depth; the blue-black colored line represents a simulation 2 water depth (24-hr simulation time, and 0.03 slope and energy grid lines); and the dark-green colored line represents simulation 3 (5-hr simulation time and 0.001 slope and energy grid line) water depth; and the red line represents simulation 4 water depth.

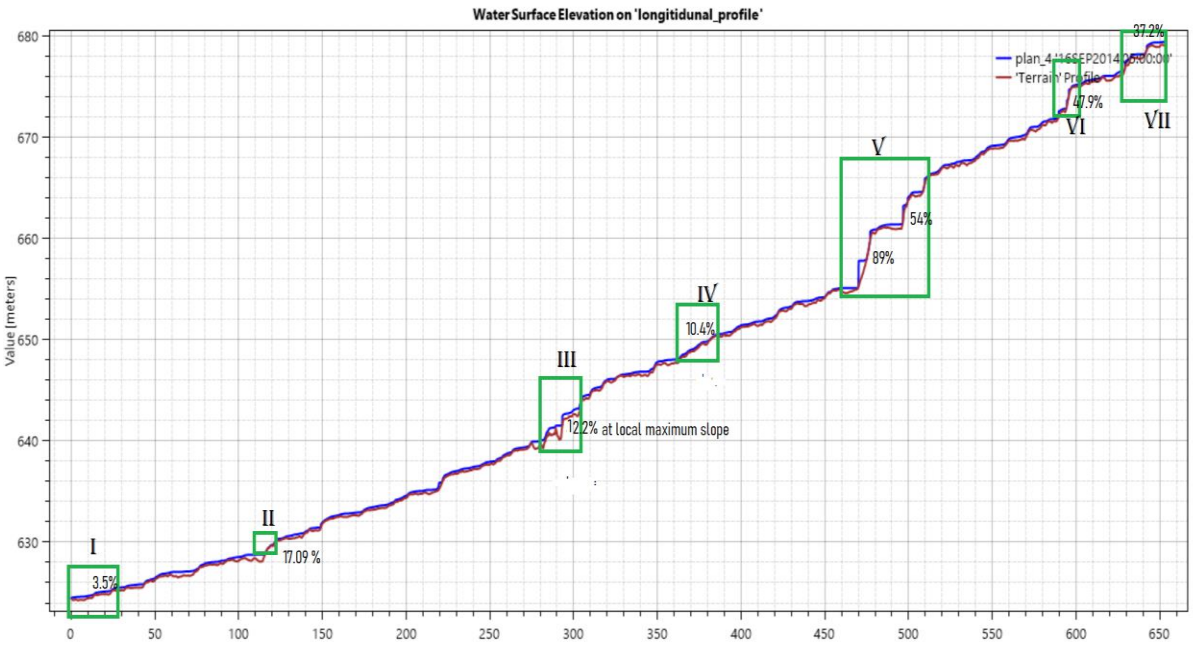

Figure 6-38: Water surface elevation and terrain profile. The red line represents a terrain profile and the blue line represents simulation 4.

As a result of an inundation extent (Figure 6-36), water depth profile (Figure 6-37) and terrain profile (Figure 6-38) extracted from simulation 4, the decreasing of the mesh size at discontinued inundation extent was not limited globally. However, refinement of mesh size solves inundation cut-off issues at lower slope river sections. For instance, water depth profile became non-zero at section I (slope = 3.5%), III (slope = 12.2%) and IV (slope = 10.4%). But model instability of cut-off and/ or zero water depth issues could not be handled by refining the grid size at high slope sections such as section II (slope = 17.09%), V (slope = 89% and 54%), VII (slope = 47. 9%) and VIII (slope = 37.2%).

To sum up, 2,972.06 m^2 of inundated area was simulated by simulation 4 and an inundation area estimated by refining the mesh grid size was estimated as the highest compared to previous simulations. Moreover, the HEC-RAS 2D modeling by applying the finite volume method and diffusion wave equation for the Vekveselva river (steep slope) was address a model instability.

6.2.1.2 Inundation extent, Water depth and Water Surface Elevation Results from TELEMAC -2D Computations on Digital Elevation Model (DEM)

As far as explained in section (5.4.4), Galerkin's finite element method (i.e. Saint-Venant equations; FEM) and finite volume algorithms were applied on an unstructured grid for the same case previously described in the HEC-RAS modeling for Vekveselva river based on DEM. Moreover, the suitability of TELEMAC-MASCARET was evaluated by overlapping a simulated inundation area on an orthophoto of the study area. For further analysis, water depth, water surface elevation, and simulated inundation area computed in FEM and FVM of TELEMAC-2D and HEC-RAS 2D were compared each other. Besides, the suitability of both models for steep river computation was evaluated based on simulation time.

6.2.1.2.1 Inundation Extent Simulated in TELEMAC-2D by Applying Finite Element Method (FEM) and Finite Volume Method (FVM)

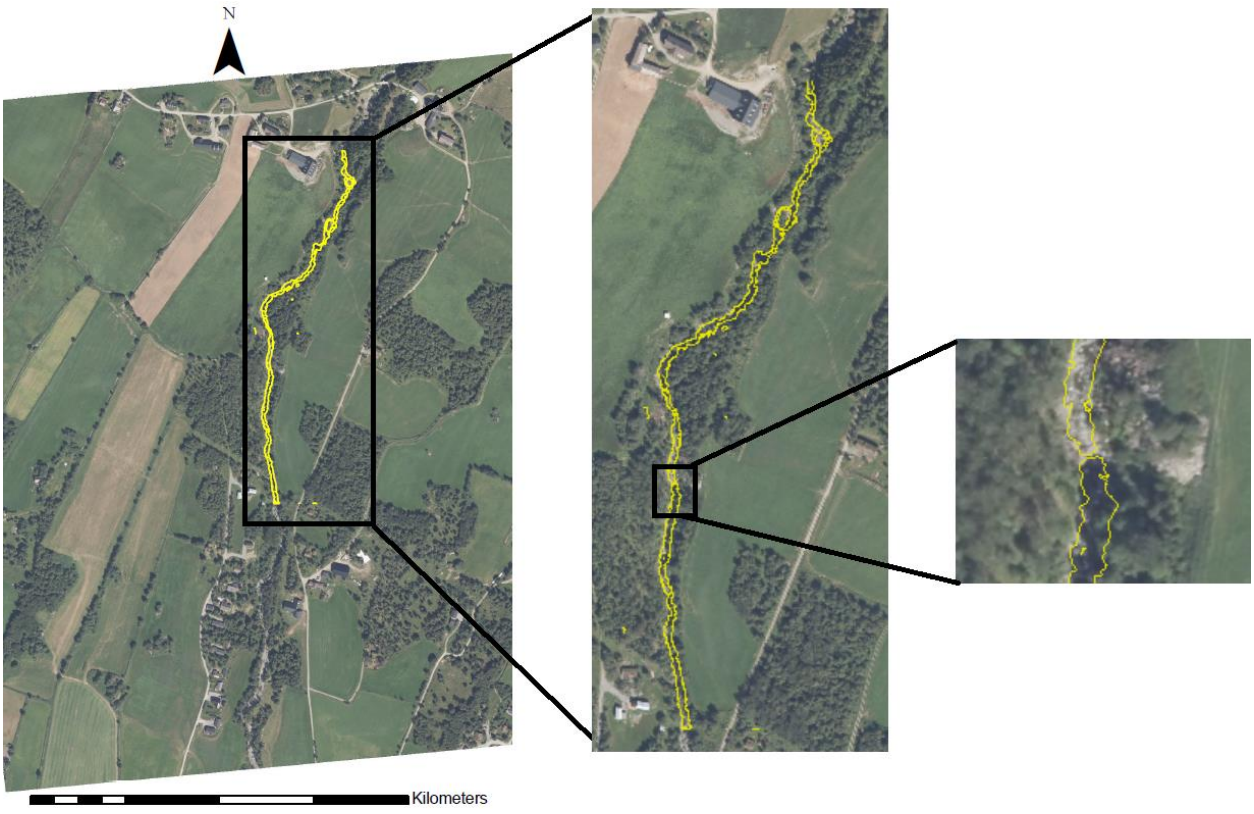

Figure 6-39:Simulated inundation area estimated by TELEMEMAC- 2D simulation with the finite element method (FEM) algorithm applied

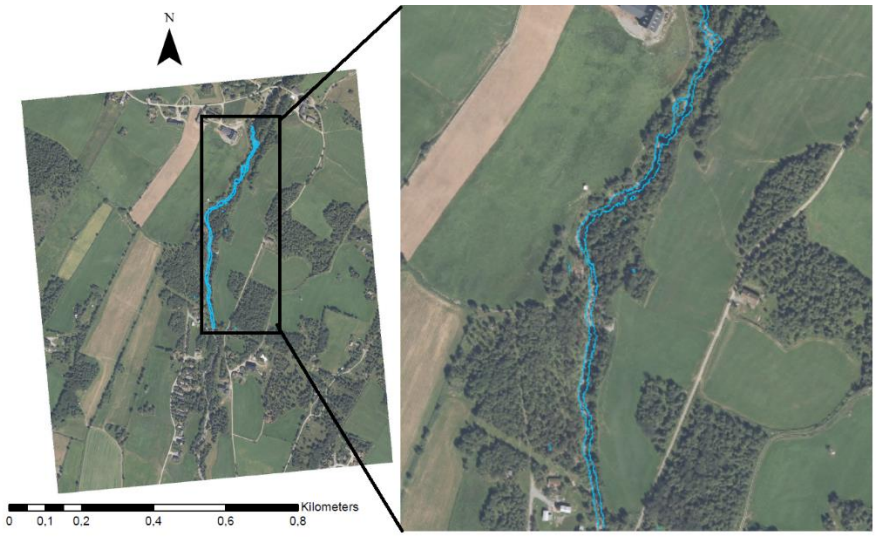

Figure 6-40: Simulated inundation area estimated by TELEMEMAC- MASCARET simulation with the finite volume method (FVM) algorithm applied

Inundation results computed by the TELEMAC-2D program indicate that the inundation cut-off or discontinuities were estimated in the finite element method (FEM). However, the continuous inundation extent was estimated while the finite volume method (FVM) was used for the computational equation.

Further analysis of the TELEMAC-2D simulation by applying the FEM and FVM was done by finding the water depth profile along the river centerline. A centerline (longitudinal) was drawn along the river's center line, and the water depth was computed at the stations of 0.05 m intervals. Also, a parallel comparison of theTELEMAC 2D simulation and HEC-RAS simulation was carried out. The results from the water depth profile along the centerline were determined to compare an agreement between the two models.

6.2.1.2.2 Water Depth Simulated in TELEMAC-2D by Applying Finite Element Method (FEM) and Finite Volume Method (FVM) and Comparison with Water Depth Simulated in HEC-RAS 2D

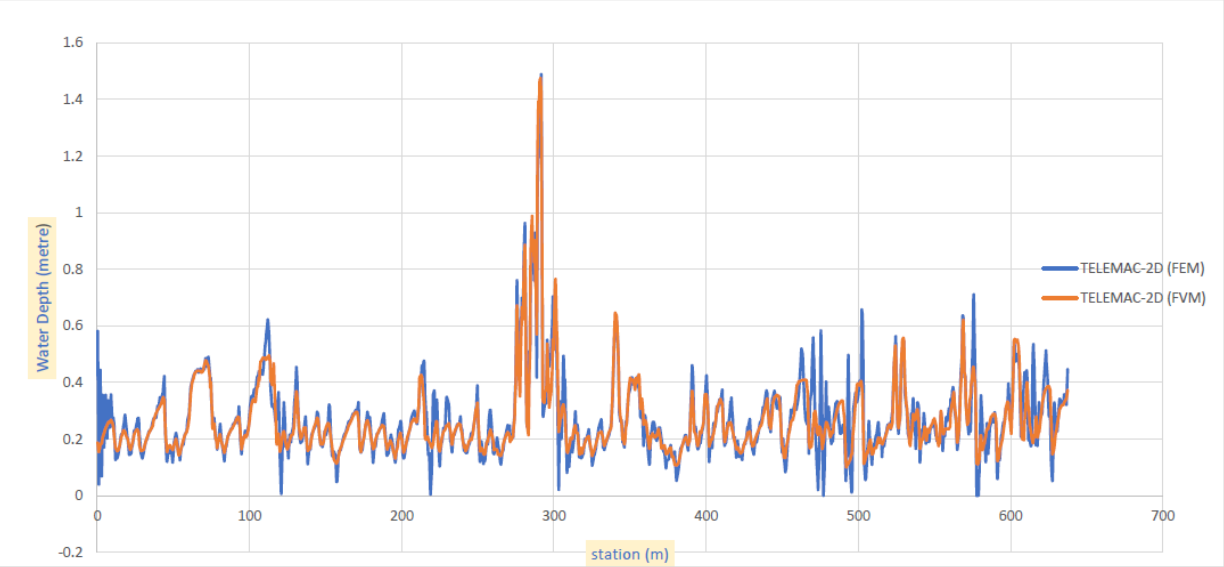

Figure 6-41: Relationship between water depth simulated in TELEMAC-2D by applying finite element method and finite volume method. The blue graph represents the water depth simulated by TELEMAC-2D based on the finite element method and the orange graph represents the water depth simulated by the finite volume method. The station starts from the downstream reach and ends at upstream reach.

A Water depth profile from above figure (Figure 6-41) indicates that a mostly smaller water depth was estimated in TELEMAC-2D modeling by using finite volume method than that of a finite element method. For the selected river centerline, a maximum 1.48945 m and minimum 0 m of water depth was calculated in TELEMAC-2D modeling by applying FEM and, a maximum 0.183471 m and minimum 0 m of water depth was calculated in TELEMAC-2D modeling by applying finite element of numerical scheme.

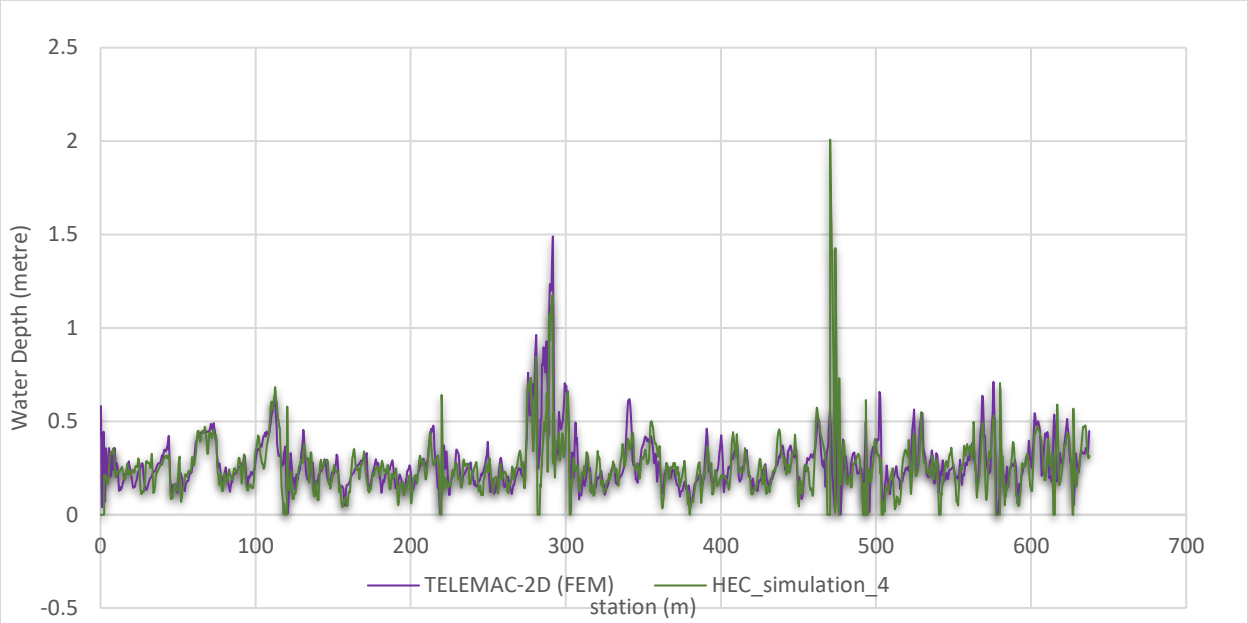

Figure 6-42: Relationship between water depth simulated in TELEMAC-2D by applying the finite element method equation and HEC-RAS 2D simulation 4. The green graph represents the water depth simulated by HEC-RAS 2D simulation 4 and the purple graph represents the water depth simulated by TELEMAC-2D by applying the finite element method. The station starts from the downstream reach and ends at the upstream reach.

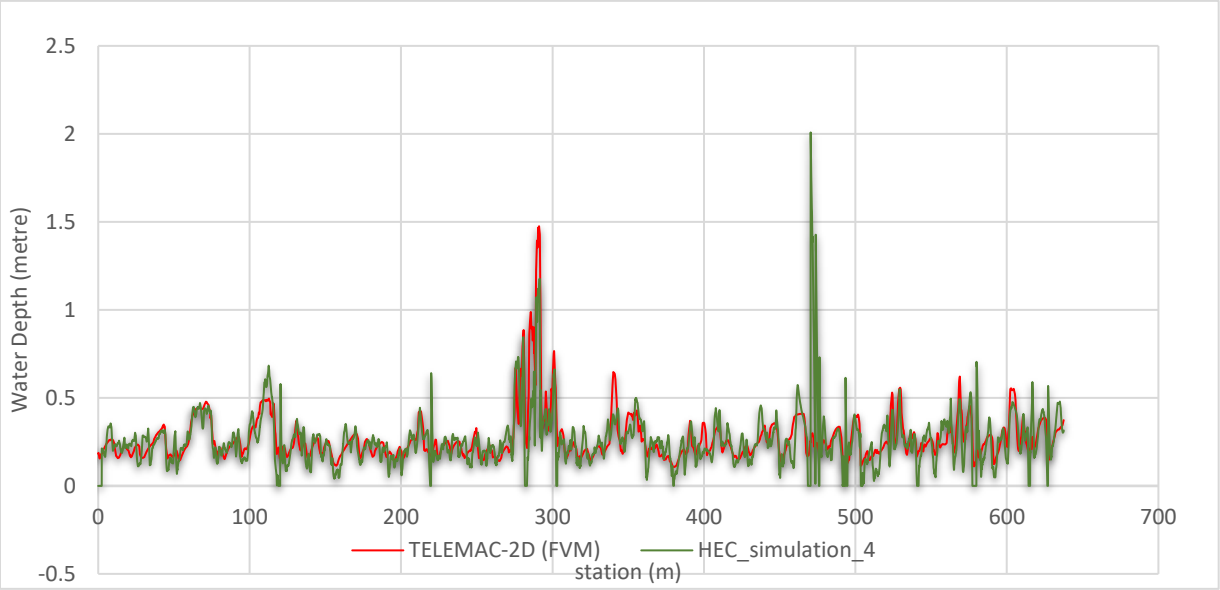

Figure 6-43: Relationship between water depth simulated in TELEMAC-2D by applying the finite element method equation and HEC-RAS 2D simulation 4 .The green graph represents the water

depth simulated by the HEC-RAS 2D simulation 4 and the red graph represents the water depth simulated by the finite volume method. The station starts from the downstream reach and ends at the upstream reach.

The result of the TELEMAC and HEC-RAS 2D comparison in terms of water depth profiles along river center line (longitudinal profile) is presented in above figures (Figure 6-42 and Figure 6-43). The result shows that good agreement between TELEMAC- 2D and HEC-RAS 2D computations on the steep river was reached when a hydrodynamic simulation of TELEMAC -2D was performed by applying finite element method. However, an agreement between HEC-RAS and TELEMAC-MASCARET based on finite element and finite volume equations is validated when further analysis is performed on the calibrated model setup and the observed data.

6.2.1.3 Models Comparison Based on Simulated water depth and Velocity Along River Cross-section

In order to analyze the agreement between the models in terms of a cross-sectional profile of hydraulic parameters, a similarity of water depth and velocity calculated in HEC-RAS 2D and TELEMAC-2D assessed. Two river cross-sections was selected to analysis the similarity of water depth and velocity simulated in both models. terms used in figures below:

Water depth_HEC = water depth simulated in HEC_RAS 2D

Water depth_TELEMAC (FEM) = water depth simulated in TELEMAC-2D by applying finite element scheme

Water depth_TELEMAC (FVM) = water depth simulated in TELEMAC-2D by applying finite volume scheme

Velocity_HEC = velocity simulated in HEC_RAS 2D

Velocity_TELEMAC (FEM) = velocity simulated in TELEMAC-2D by applying finite element scheme

Velocity_TELEMAC (FVM) = velocity simulated in TELEMAC-2D by applying finite volume scheme

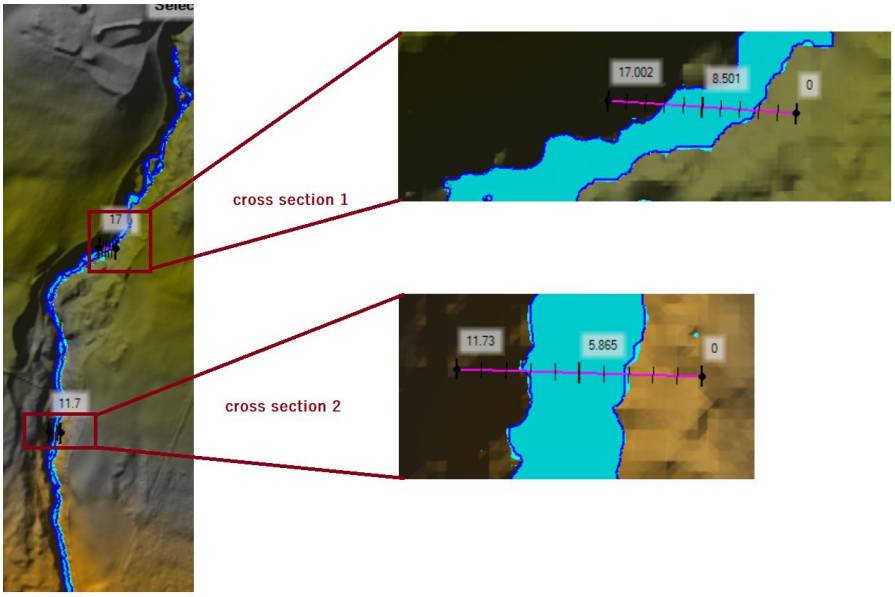

Figure 6-44: Selected river cross section for analyzing an agreement between velocity and water depth simulated by models

Cross-section 1

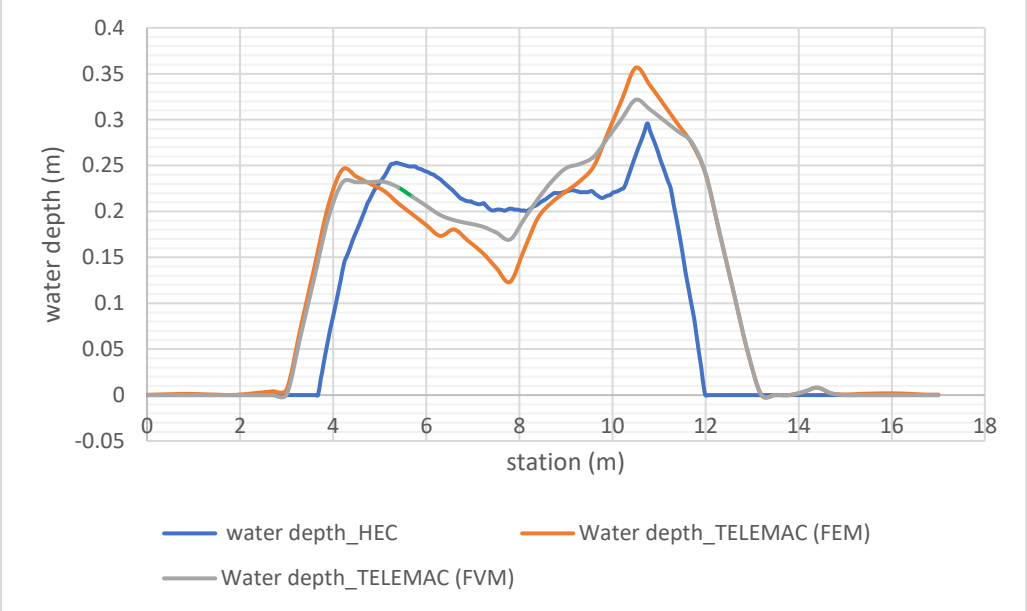

Figure 6-45: Water depth profile at cross-section 1

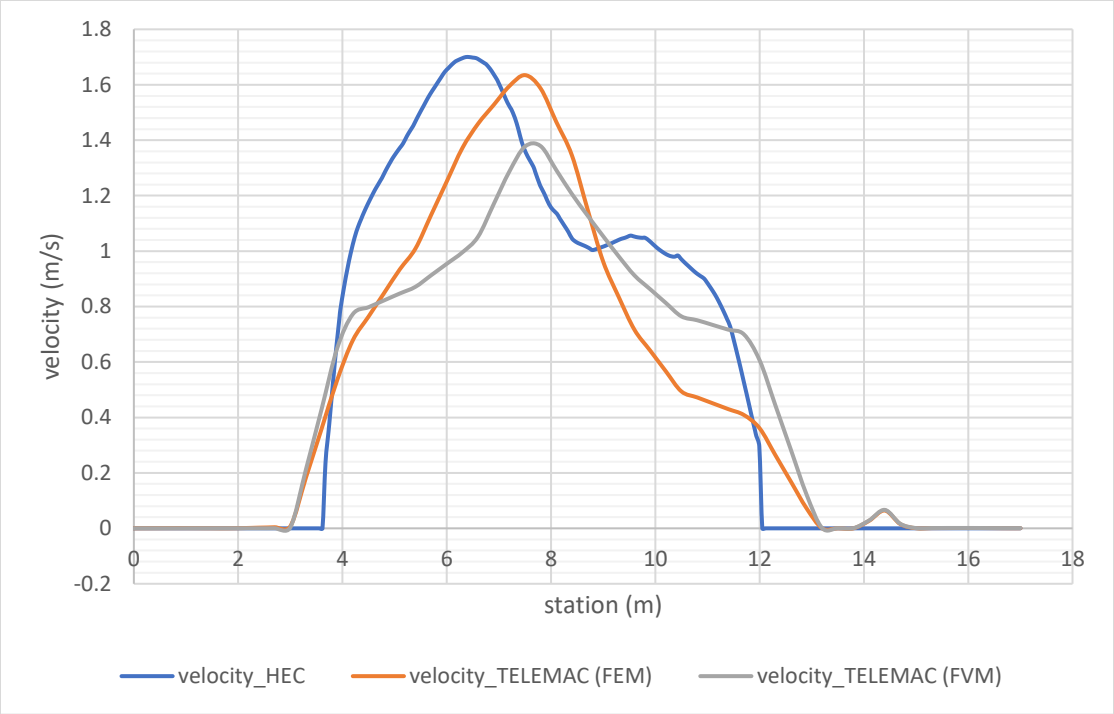

Figure 6-46: Velocity profile at cross-section 1

Cross-section 2

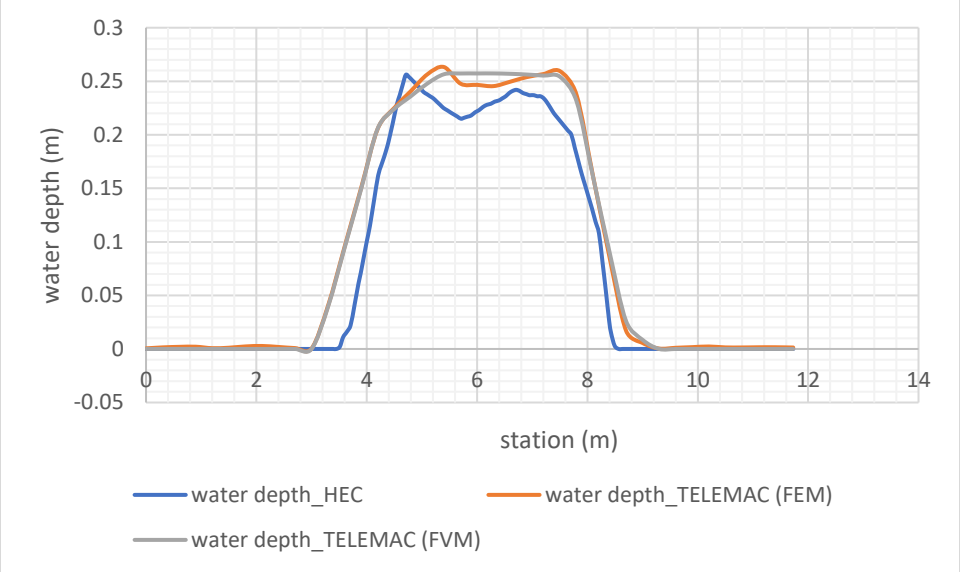

Figure 6-47: Water depth profile at cross-section 2

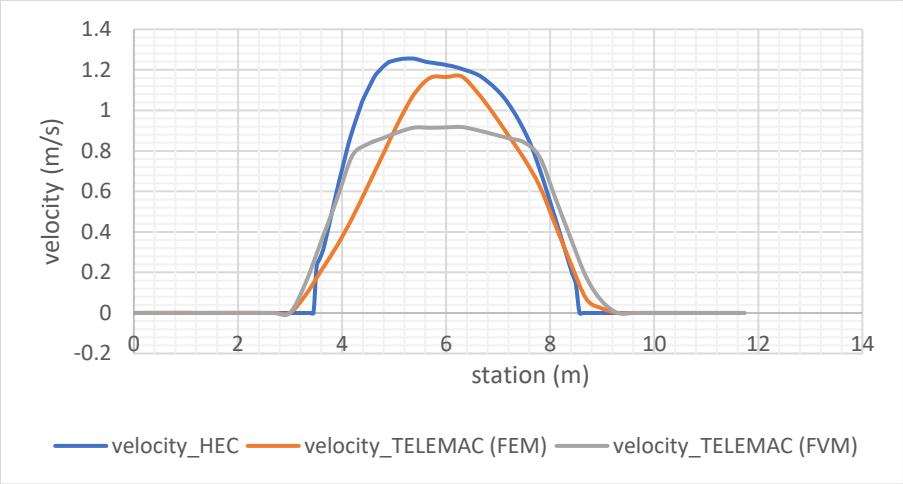

Figure 6-48: Velocity profile at cross-section 2

The above graphs (Figure 6-45; Figure 6-46; Figure 6-47 and Figure 6-48) show that a better agreement was achieved between water depth calculated in HEC-RAS 2D by applying the diffusion wave equation and in TELEMAC-2D by applying FEM and FVM than velocity computed in both models. However, calibration validation and observed data are needed to identify the best model and numerical scheme appropriate for steep river simulation.

6.2.1.4 Models Comparison Based on Simulation Time in Vekveselva River Modeling by Applying DEM

Simulation time is become important when hydrodynamic models compute a long reach of a river with a small mesh grid size. To check the simulation time for TELEMAC-2D computation by applying finite element and finite volume methods, hydrodynamic modeling of both equations was carried out on a computer with a 64-bit operating system, x64-based processor and 32 GB RAM. In addition, both simulations were computed on seven parallel processors.

Table 6-6:Simulation time of TELEMAC-2D modelling for Vekveselva river

Types of simulation	**Simulation time**
TELEMAC-2D simulation by applying FEM	0hr:31min :15 seconds
TELEMAC-2D simulation by applying FVM	16 hr:10 min: 32 seconds

For Vekveselva, TELEMAC- MASCARET modeling by applying a finite volume equation took more simulation time than the finite element method. The reason is that applying of finite volume

scheme for computing governing equation is interrogated over a volume of a cell. Furthermore, using a finite volume method makes simulation more realistic due to a piece-wise linear variation in Saint-Venant equation determines accuracy and complexity (CFD, 2019). In this mathematical integration method, there is a hydraulic computation balance flux across the boundary of each volume. However, finite element method is generally known as Galerkin's method is governs hydraulic computation by integrating Saint-venant equation over elements of weight function (CFD, 2019) (Sauvaget et al., 2000).

6.2.2 Evaluating of HEC-RAS 2D and TELEMAC-2D Computations on a Digital Surface Model (DSM)

Another hydrodynamic computation done for the Vekveseva river is that incorporating 3-D classified data from photogrammetry which includes features exist on the earth surface. As far as explained in section 5.4.3.2, a DSM based on LiDAR information extracted from https://hoydedata.no/LaserInnsyn/ was used for both HEC-RAS 2D and TELEMAC-2D computation. In the Vekveselva case, vegetations existing in the flow area are included in the hydrodynamic computation. The DSM, which incorporates vegetations, and used for creating a computational grid, can cause model instability. Previous studies indicate that the quality of the DSM data generated by LiDAR is a primary issue when the data is used for hydrodynamic computation (Morgan et al., 2016). For instance, the impact of high vegetation on lower height vegetation is the main issue in green LiDAR generating. BLUEKENUE (a tool used to generate mesh for TELEMAC) and HEC-RAS geometric data tools that create non-structured meshes need high-quality LiDAR data for generating a proper mesh. Therefore, smooth cell size and high investigation in mesh generation must be needed to create a significant computational mesh. As far as possible ,the quality of LiDAR data extracted from https://hoydedata.no/LaserInnsyn/ was evaluated based on overlaying the inundation extent that was computed in HEC-RAS 2D and TELEMAC 2D with Orthophoto extracted from https://www.norgeibilder.no/.

6.2.2.1 Results from HEC-RAS 2D Simulation Based on Digital Surface Model

As described in section 5.4.3.2.2, three simulations were performed to evaluate the suitability of the performance of HEC-RAS software modeling in a steep river and to examine the quality of LiDAR data extracted from https://hoydedata.no/LaserInnsyn/.

i. **Simulation 1:** as described in section 5.4.3.2.2, a hydrodynamic computation with a5-hour simulation time and 0.5 x0.5 m mesh size was performed to analyze the suitability of the DSM obtained from https://hoydedata.no/LaserInnsyn/. An inundation area extracted from simulation 1 shows that the simulated water edge was not continuous (Figure 6-49: section a and c). Moreover, a false blockage incorporated in the geometric data changes a flow line alignment. In other words, flow streams miss the river centerline, and the river channel is dried (Figure 6-49: section b).

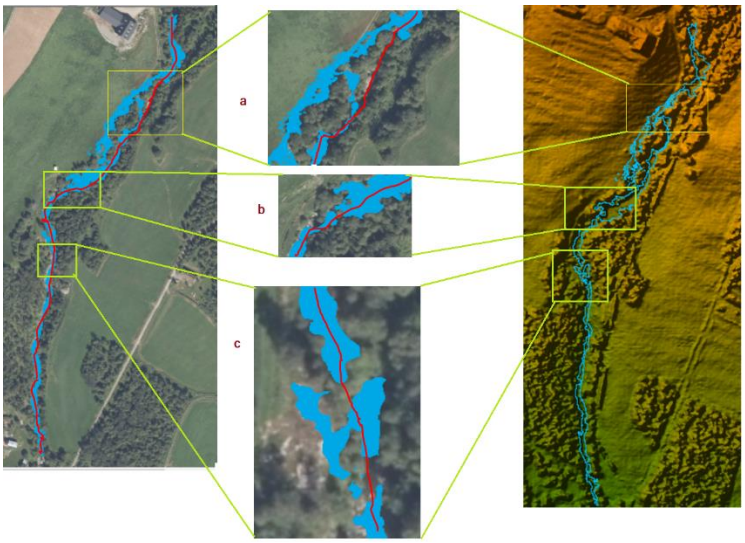

Figure 6-49: Inundation area extracted from simulation 1 which was computed in HEC-RAS 2D modeling on a DSM. The red line represents the river center line.

ii. **Simulation 2:** on the other hand, further analysis was done by decreasing the computational grid cell size and flattening the energy grid line at the initial state. However, a more gapped inundation extent was simulated, and flow streamlines missed the river channel.

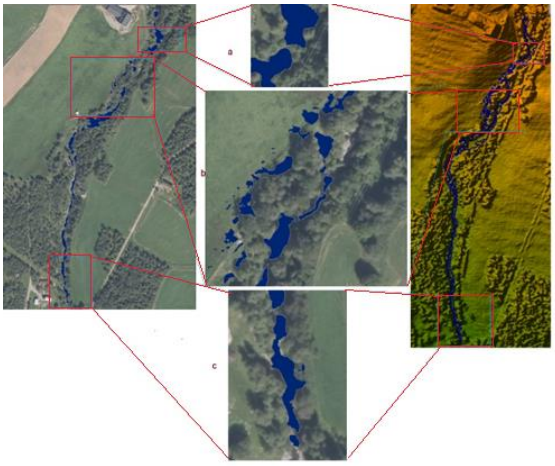

Figure 6-50:Inundation area extracted from simulation 2 which was computed in HEC-RAS 2D modeling on a DSM

iii. **Simulation 3:** As discussed in section 5.4.3.2.2, terrain modified by removing a false blockage appeared in the river channel, and a modified 2D flow area was created by interpolating the river cross-section.

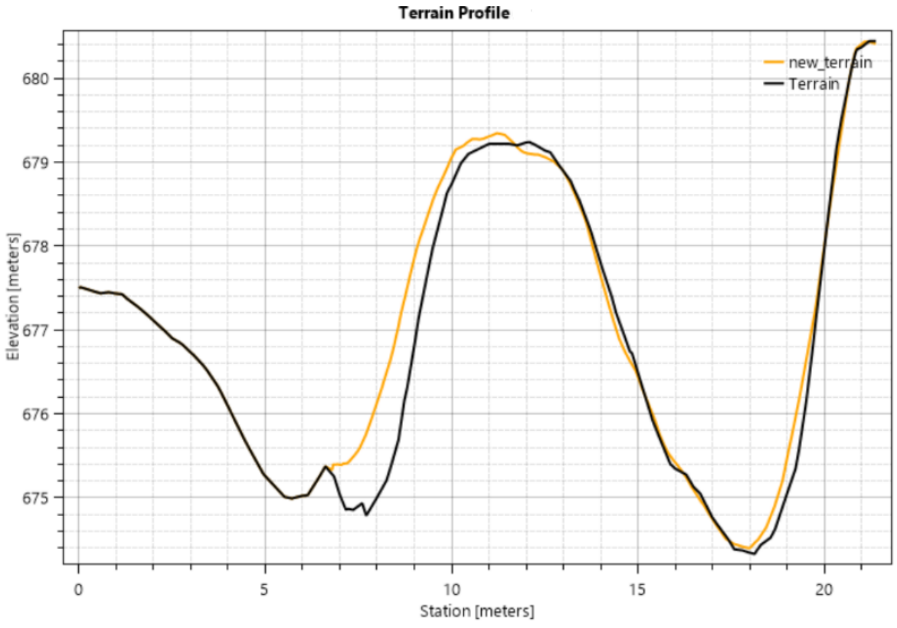

Figure 6-51: Cross-sectional river profile at 83 m from upstream boundary. A black line represents an elevation of original terrain interpolated from the DSM, and an orange colored line represents the elevation profile of the modified terrain.

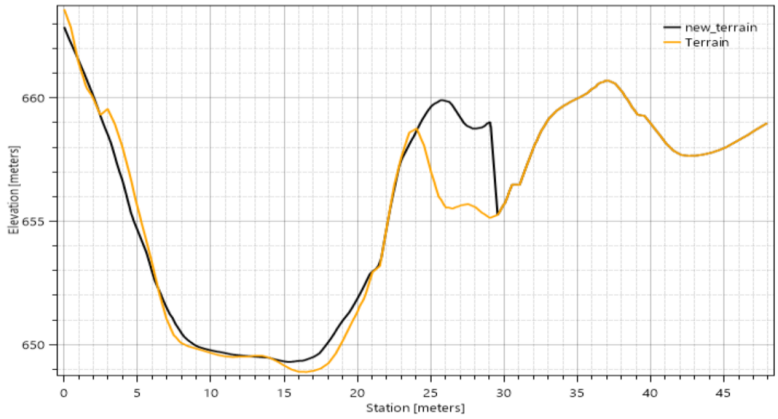

Figure 6-52: Cross-sectional river profile at 245 m from upstream boundary. An orange line represents an elevation of the original terrain interpolated from the DSM, and an black line represents the elevation profile of modified terrain.

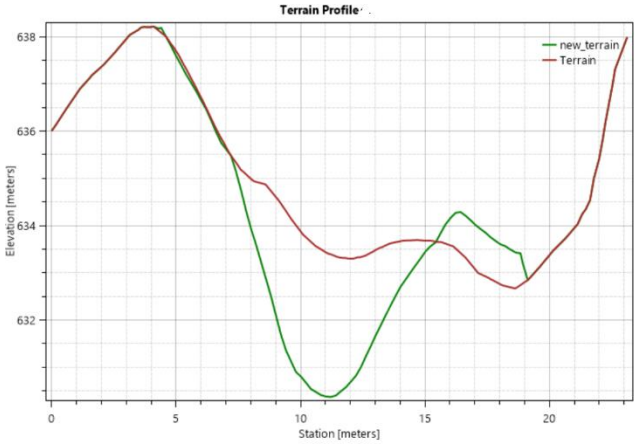

Figure 6-53: Cross sectional river profile at 87.6 m from downstream boundary. The red line represents an elevation of original terrain interpolated from the DSM, and a green-colored line represents the elevation profile of modified terrain.

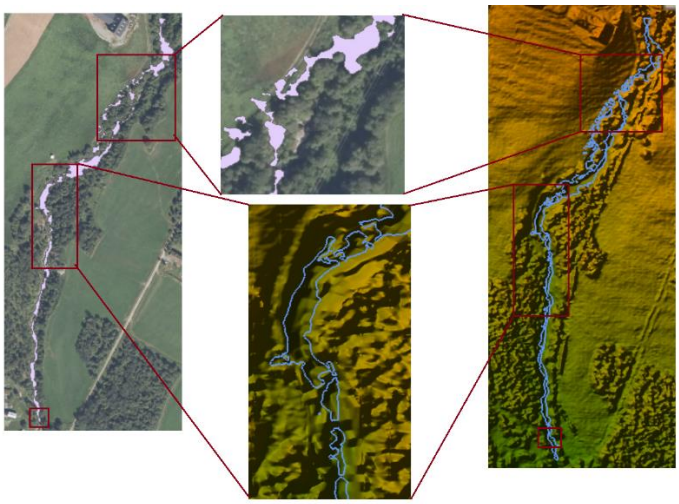

Figure 6-54: Inundation area extracted from simulation 3 which was computed in HEC-RAS 2D modeling on a DSM

As a result of an inundation extent (Figure 6-54) extracted from simulation 3, decreasing the mesh size and modifying the terrain by a removing blockage did not achieve a non-gapped inundation area. However, an inundation area of 4,035.64482 m^2 was computed in simulation 1. While 3,656.377655m^2 inundation area was simulated in simulation 2 and a minimum inundation area (3,535. 905375 m^2) was computed in simulation 3.

6.2.2.2 Results from TELEMAC-2D Simulation Based on a LiDAR Derived Digital Surface Model

A LiDAR obtained from https://hoydedata.no/LaserInnsyn/ was applied in both models to evaluated the efficiency of hydrodynamic modeling on DSM data. The same as with TELEMAC-2D modeling for the Vekveselva river on a LiDAR derived DEM (section 6.2.1.2) , finite element and finite volume schemes were applied and model stability was evaluated based on the simulated water depth and inundation extent.

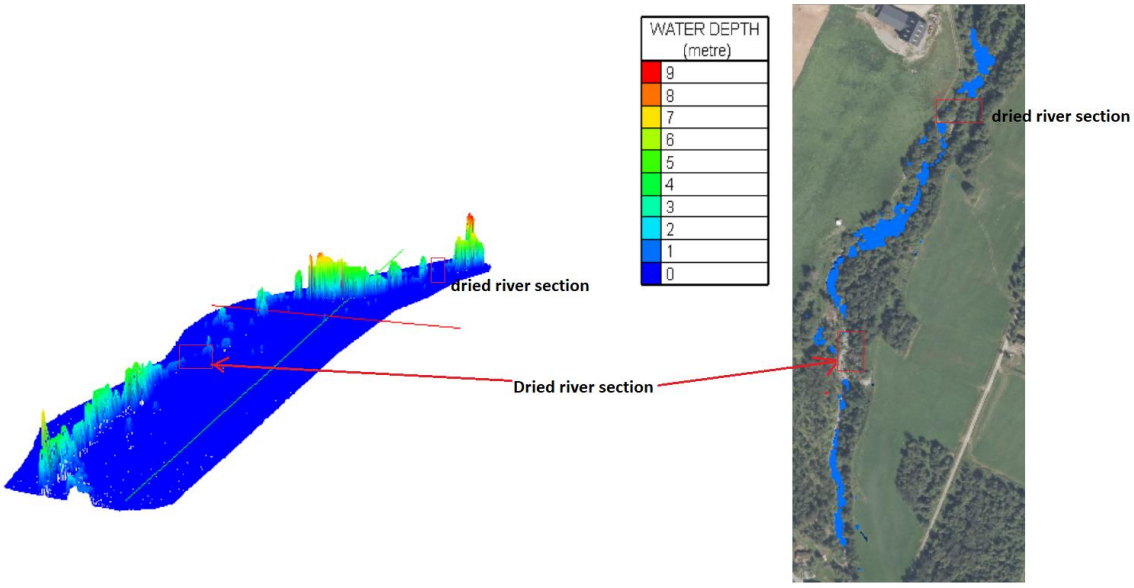

Figure 6-55: Water depth and inundation extent from the Vekveselva river TELEMAC modeling by applying FEM on the DSM; Left-hand side: 3-D view of water depth viewed on BLUEKENUE; and right-hand side: inundation area overlapped on an orthophoto of the Vekveselva river.

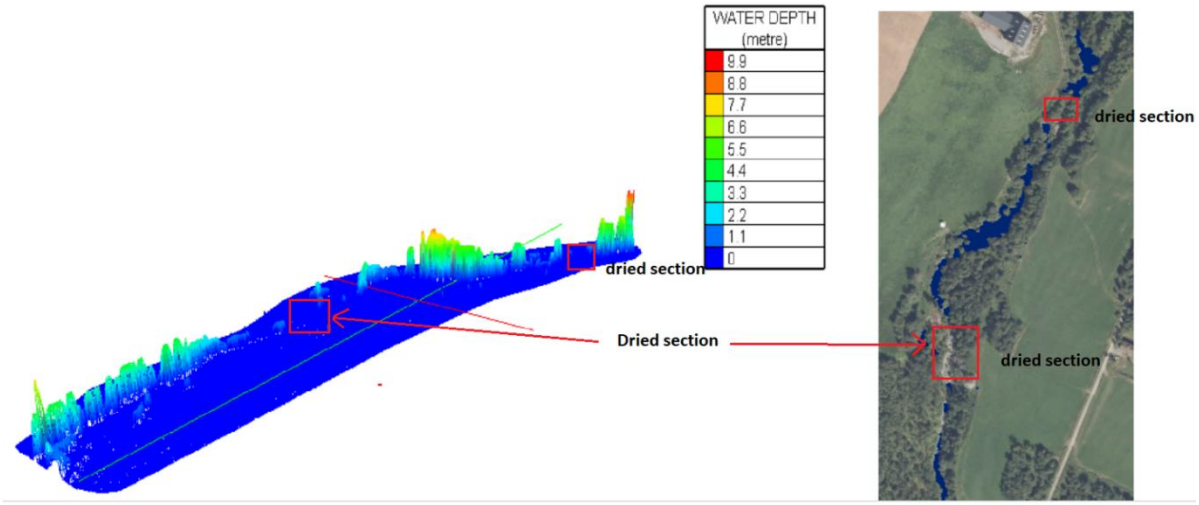

Figure 6-56: Water depth and inundation extent from the Vekveselva river TELEMAC modeling by applying FVM on the DSM; Left-hand side: 3-D view of water depth viewed on BLUEKENUE and right-hand side: inundation area overlapped on an orthophoto of the Vekveselva river.

An application of two numerical schemes, the finite element method and finite volume method, in TELEMAC 2D modeling on a DSM terrain was calculate large dried river sections. Also, most of simulated water depth in a river is more than 3 m, that is not a reasonable water depth for steep river that has 0.898 m^3/s flow rate.

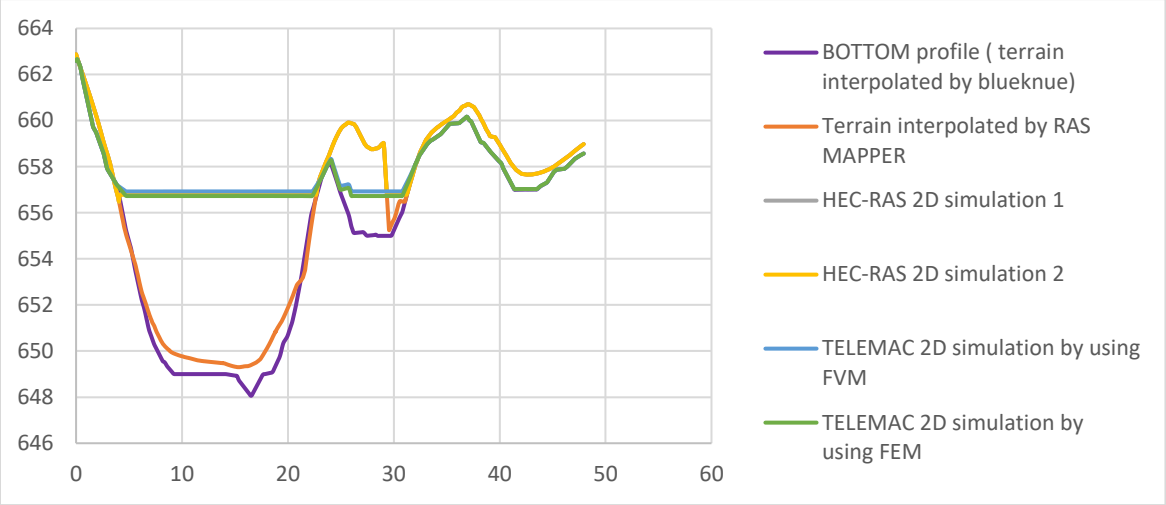

Figure 6-57: Cross-sectional water surface elevation simulated in HEC-RAS 2D and TELEMAC-2D by applying FEM and FVM on DSM

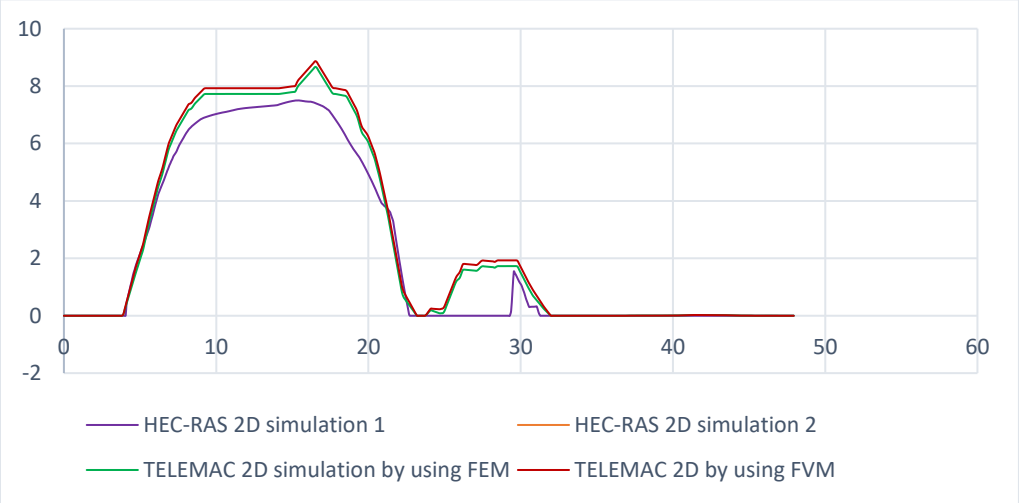

Figure 6-58: Cross-sectional water depth simulated in HEC-RAS 2D and TELEMAC-2D by applying FEM and FVM on DSM

A cross-sectional water depth profile simulated in both models indicates that more than 6.5 m water depth is estimated between 10 m to 18 m stations. In fact, high water depth is unexpected in such a tiny river, which has no structures that can block water, and a low flow rate.

In addition, TELEMAC-2D modeling based on the FEM method was estimate a 2,565.579519 m^2 water covered area, and a 2,682.38443 m^2 inundation area was estimated by FVM.

In general, the DSM data obtained from https://hoydedata.no/LaserInnsyn/, which was derived by using 0.5 m resolution, was not sufficient for hydrodynamic computation in both models.

7. DISCUSSION

This study aimed to evaluate HEC-RAS and TELEMAC-MASCARET for hydrodynamic computation of a mildly sloping and steeply sloping river, and then examine the efficiency of red and green LiDAR data in the hydrodynamic computations. Further, the study includes the efficiency of numerical equations in the computation of hydrodynamic models. Different simulations were computed in each scenario to recognize the critical issues in both models and the given topographic data of the corresponding river.

The study's outcome can be used to guide the readers to choose a good model based on the morphology of a river and related factors identified in the results chapters. Indeed, this study was focused on a 2-D numerical modeling version of both models. The major advantages offered by the 2-D approach, as compared to the 1-D modeling technique, are high accuracy of the simulated result, confirming fewer assumptions, and the realism guaranteed by an enhanced graphical presentation of simulated results. Also, 2D gives detailed knowledge of flood fields, particularly floodplains, which was the primary way that the models involved in this study were evaluated.

In fact, the evaluation of both models performed in both rivers, where the water would flow mainly within the channel rather than in the flood plain, was highly dependent on the simulated water cover area. The models also did not testify with different discharge. The sensibility of the models on inclusive hydraulic structures was not considered, and models did not testify for large discharge values. For instance, hydrodynamics simulations for the Vekveselva river were computed by using 0.898 m3/s, which is a very shallow water depth and even could not cover the main channel. For the Surna river, where both models were evaluated based on the degree fitness with the observed inundation area, a sensibility of the inundation extent focused on the roughness coefficient. It did not consider the impact of topographic uncertainty and the coarseness of geometric grid sizes on inundation extents. However, the impact of terrain interpolation by RAS Mapper of the HEC-RAS and BLUEKNUE of TELEMAC-MASCARET were correlated based on riverbed elevation. Besides, an agreement of both models was evaluated by comparing simulated water surface elevation as well as created terrain in both models; and both models mostly calculate the same cross-sectional water surface profile and interpolated precise river channel elevation profiles.

In general, the suitability of both models for the Surna river (mild slope) was evaluated by applying different roughness and evaluating the simulated inundation extent on observed inundation extent. Indeed, the single roughness value applied for all river sections, which is not true in real world, and a decision of evaluation was mostly inundation dependent. In fact, one model give better performance in simulation of inundation extent and may be poor in other hydraulic parameters estimation(Pinos & Timbe, 2019). Similarly, both models' performance at critical points, such as at bends and shore areas, was evaluated by using observed and simulated inundation extent (section 6.1.4). However, all HEC-RAS 2D simulations for the Surna river were performed using a variable time step; whereas TELEMAC-2D simulations were computed on a constant simulation time step.

For the Vekveselva river, both models' suitability for the steep river was evaluated based on two numerical schemes (namely finite element and finite volume methods) to examine the efficiency of red and green LiDAR in hydrodynamic simulations. Indeed, the models' set-up was not calibrated, and the models' output was not validated. Applying uncalibrated roughness coefficient is a source of uncertainty. Even though the Manning roughness coefficients in the channel have a significant impact on the estimation of water levels and inundation extent, this aspect was excluded in the performance assessment. However, the suitability of the models was evaluated based on overlaying simulated inundation extent on orthophoto of the river and by checking dryness in the river. As result of this, the HEC-RAS 2D modeling on the steep river by using DEM and DSM was generate a gapped inundation extent; also, the channel dried out at points where the bed slope abrupted. However, the TELEMAC-2D modeling by applying FVM for the steep river on the DEM was estimate a continuous inundation extent and had a good fit on the river alignment on the orthophoto (Figure 6-40). However, modeling on DSM models computed unrealistic inundation extent and water surface elevation such that simulated inundation extent did not fit river alignment on Orthophoto, and some sections have zero water depth (Figure 6-55 and Figure 6-56).

In order to achieve the study goal, factors such as the impact of the slope, simulation time, the digital surface model, refinement of the meshes and numerical equation were identified for discussion in this study.

7.1 Impact of River Steepness in Hydrodynamic Modeling by Using LiDAR Derived DEM

In essence, both HEC-RAS and TELEMAC-MASCARET are programmed to compute hydraulic parameters for shallow river and many users can find numerical instability problems of unsteady analysis, and particularly unsteady flow computation in a dynamic and steep river (Ata, 2018; G. W. Brunner & CEIWR-HEC, 2016). However, it often possible to the handle the models' uncertainty. For instance, the HEC-RAS and TELEMAC v8p0 user manuals advise users to smooth the mesh size for a steep river and an abrupt change of bed slope situation(Ata, 2018) (G. W. Brunner & CEIWR-HEC, 2016). In addition, a user can slightly modify bathymetry or terrain to overcome the model instability, or a very steep bank can be replaced by a vertical wall (Ata, 2018). Gary Brunner, a senior hydraulic engineer in the U.S. Army Corps of Engineers and HEC-RAS developer, mentioned that increasing of the roughness coefficient, base flow, or running the model as a mixed regime (such as to incorporate super and subcritical flow computation) can address more HEC-RAS stability (G. W. Brunner, 2008). In such a case, the model allows both supercritical and subcritical flow conditions to overcome instability. On the other hand, TELEMAC-MASCARET invites a user to set up proper numerical schemes and solve severe water surface oscillation and long simulation time(G. W. Brunner & CEIWR-HEC, 2016).

In nature, a river slope is a continuous parameter, and slope changes can be abrupt, such as a steep-pool situation or can form a waterfall, which is encountered often in steep rivers. However, an incremental slope was used to identify an impact river of slope on hydrodynamic models' suitability.

The results output from a hydrodynamic simulation in steep rivers shows that HEC-RAS's instability occurred. HEC-RAS modeling in the steep river estimated a gapped inundation extent (Figure 6-36; Figure 6-39). A discrete inundation extent was formed at points where a bed slope gradient abrupt changed, and numerical instability occurred at a location where the river slope was higher than thirteen percent. The HEC-RAS user manual supports this result because the true derivation of the energy equation computed vertical pressure head(G. Brunner & Bonner, 2010).

$$H_P = d\cos\emptyset \qquad \textit{Equation 7-1}$$

H_p, d and Ø represent vertical pressure, water depth and river channel bed angle, respectively. Based on this equation, steep bed elevation gives less than 1 cos(Ø) which can produce an error in

water depth estimation. To support the above theorem, Lee et al., 2019 defined a steep-sloped channel, where an energy line slope is more than five to six percent by using a gradually varied flow equation, momentum balance assumptions are no longer satisfied. In addition, instability of the model at a steep slope was recovered by increasing the simulation time. By this approach, an extending simulation time allows a model to generate a continuous inundation extent and a troubled water surface is eliminated at lower slope locations (Figure 6-32). However, extending the simulation time did not generate a continuous inundation for all river sections. Another simulation performed by decreasing energy the line and friction slope in a model set up, show that a significant change of simulated water depth (Figure 6-34) and inundation extent did not achieve except near the boundary conditions (Figure 6-35). Additional further computation was made by creating a smaller mesh size at critical points. This technique allows a model to compute a water surface in the nearer consecutive cells. However, refinement of mesh size could not solve instability issues for all river sections, but the model computed a reasonable water surface and inundation areas at the lower slope.

On the other hand, finite element and finite volume techniques were applied in TELEMAC -2D simulation to identify suitable numerical schemes for modeling steep rivers. Indeed, TELEMAC-2D modeling by applying the finite element method gave a gapped inundation extent (Figure 6-39). However, utilizing the finite volume method stabilized the model and gave a non-discrete (un gapped) inundation extent (Figure 6-40). In the finite volume method, the Saint-Venant equation is integrated over a volume or cell, assuming a piece-wise linear variation of the dependent variables (u, v, w, p, T). Again, the piece-wise linear variation determines both the accuracy and the complexity. Using these integrations, the models essentially balance fluxes across the boundaries of the individual volumes (CFD, 2019) . This method orders a model to compute hydraulic parameters based on a flux, rather than dealing with mesh geometry as in the finite element method (CFD, 2019). In fact, hydraulic computation based on the finite volume method requires long computation time, but fluxes have more physical significance (CFD, 2019).

In general, among the three scenarios for the Vekveselva river simulation, namely HEC-RAS 2D simulation of using wave diffusion, TELEMAC-2D simulation by applying the finite element method and TELEMAC-2D simulation by applying finite volume method, the application of finite volume scheme in TELEMAC-2D performed well.

7.2 Application of Digital Surface Model Data Derived from LiDAR in a Hydrodynamic Simulation

Two-dimensional (2-D) modeling requires the geometric characterization of the selected domain to generate a reliable inundation extent and other hydraulic parameters. The precision of digital topography, expressed in terms of vertical accuracy and resolution, can generate high-quality terrain data, and can well perform in hydrodynamic modeling. Notably, in high dense vegetation areas, high-resolution topographic data is needed to estimate adequate flow parameters. An airborne LiDAR technology, among other topographic collection systems, can derive precise and relevant topographic data. However, this source of topographic data cannot generate a proper river morphology, especially when a river channel is covered by vegetation canopy and other features, where continuous and topographic slope change is frequent. Indeed LiDAR data obtained from https://hoydedata.no/LaserInnsyn/ has a high resolution (0.5 x 0.5 m). However, these data have a limitation in data classification, where 99.08 % of points are classified as ground and the rest as a water body, no points are classified for vegetation. In addition, the river surface of this data not cleaned.

As a result of HEC-RAS 2D and TELEMAC -2D simulations, a DSM derived from LiDAR was create strange in model, and the data was insufficient to generate proper flow parameters and was unable to generate a continuous inundation extent (section 6.2.2.1 and 6.2.2.2). The regenerating DSM data by cleaning channel surface (removing false blockage) is needed to deliver a successful DSM for hydraulic modeling. In addition, manual measurements to getting additional elevation data at unfiled features and where the surface changes are may be recommendable.

Theoretically, LiDAR is generate high quality and precise data which can accurately represent the topography of the earth surface (Bodoque et al., 2016). However, LiDAR based data may not contain important details from a hydraulic point of view, because of its systematic sampling procedure (Bodoque et al., 2016). There is much room for improvement in the representation of many elements of LiDAR-derived DSMs, despite the high density of points represented. For example, LiDAR-derived DSMs are unable to reflect thin structures, like levees or continuous walls, which are an obstacle to water. Also, they do not allow small features such as small

vegetation and canals to be represented, possibly because such information has not been captured correctly (Bodoque et al., 2016).

7.3 Comparison Between Models Related to Inundation Area, Water Depth and Velocity

The sensitivity of the flood mapping result is a function of the applied numerical scheme and default used in the model's parameters. The performance of both models and the representing roughness value of the computation domain was evaluated based on RMSE, which calculates an error between the simulated inundation area and the observed inundation area. Five different roughness values were applied in both models, and both models estimated a 0.045 Manning's roughness for the selected computational domain. However, an inundation area simulated in TELEMAC- 2D based on 0.045 Manning's coefficient gave the lowest RMSE (Table 6-1). On the other hand, HEC-RAS 2D modeling based on 0.045 Manning's coefficient gave best fit with the observed inundation area at the islands zones (Table 6-3). In general, both models performed well at a straight river alignment zone, and the low performance of two models was scored at the bends and islands zones.

On the other hand, HEC-RAS 2D and TELEMAC 2D modeling on the mild slope river showed that they had good agreement on the estimating the water depth and terrain, interpolated by both packages and minor differences at the island zones. Thus, both models need a calibrated set-up and experimentational governing equation at island zones to handle the influence of tidal forces in hydrodynamic computations (section 6.1.4). However, TELEMAC-2D shows a minor higher water surface elevation value for the same roughness and flow event. A minor water difference occurred in the water depth when both models applied were on the steep river and mostly the same water depth was estimated when a finite element and volume method was applied in TELEMAC-2D (Figure 6-45 and Figure 6-47). However, regarding steep river modeling, it is difficult to generalize due to model instability in HEC-RAS 2D and TELEMAC 2D with the finite element scheme.

In regards of the comparison of the simulated velocity of the mildly sloping river, similar cross-section velocity profiles were estimated at bends, islands, and straight river zones. A minor velocity difference was estimated in both modes at the straight river alignment and island area; and relatively, HEC-RAS 2D calculated a higher velocity than TELEMAC-2D (section 6.1.5). However, a significant difference occurred when both models were applied to compute the velocity

of the steep river. In contrast, the hydraulic modeling of TELEMAC-2D based on finite volume for the steep river estimated a calm flow (low velocity) than HEC-RAS 2D computation based on diffusion wave equation and TELEMAC-2D based on finite element approach.

7.4 Comparison of Models Based on Simulation Time

In general, the application of the finite volume method to integrate a governing equation over cells of the TELEMAC-MASCARET simulation takes a long simulation time; whereas applying the finite element method for the TELEMAC-MASCARET simulation on a mildly sloping and meandering river take a short time when compared with that of modeling in HEC-RAS and TELEMAC-MASCARET with finite volume method. In fact, simulated hydraulic parameters computed in finite element and finite volume methods are similar when TELEMAC -MASCARET was applied for modeling the mildly sloping river and non-frequently changed surface features. Further, many studies advise a finite element numerical equation for hydraulic analysis of mildly sloping rivers.

It is the same for the steep river; hydraulic computation of TELEMAC-MASCARET by applying the finite volume method takes a long simulation compared to HEC-RAS and TELEMAC-MASCARET modeling based on the finite element method. Hydrodynamic modeling based on applying the finite volume numerical scheme in TELEMAC-MASCARET takes the shortest time among the three approaches. Indeed, the outcome of this study identifies TELEMAC-2D modeling based on the finite volume method that gave the most stable modeling.

7.5 Comparison of Models Based on ease to Set Up

The hydrologic Engineering Center's (HEC) River Analysis System (HEC-RAS) software is integrated software and is comprised of a graphical user interface (GUI) that can be easy for new users. The software consists of programs for analysis simulations, storing data, and managing data. The model comprises well organized and easily understandable graphical and tabular reports. The software also contains a program that efficiently computes inundation extents.

On the other hand, TELEMAC-MASCARET is a non-graphical user interface (GUI) software that needs additional programs to access pre- and post-processing data. The user of a program must build a configuration of the computation that is comprised in the TELEMAC-MASCARET system. It can greatly benefit anyone who wants to modify specific subroutines and apply a different governing equation; and it has functional models for the user wants to a control

computational configuration on themselves. However, it needs basic knowledge of Fortran and computer programming. Also, TELEMAC-2D has a limitation on computing supercritical flow. In addition, models can not directly simulate inundation areas, and the user must extract the water cover area from the flow parameters.

8. CONCLUSION

Hydrodynamic simulations were carried out to evaluate the performance of HEC-RAS and TELEMAC-MASCARET on mildly sloping and steep rivers. In addition, both models were applied for the steep river to examine the efficiency of red and green LiDAR data in hydrodynamic simulations.

The results obtained from the mildly sloping Surna river, modeling show that both models estimated 0.045 Manning's coefficient, and both models could be used to determine hydraulic parameters in mildly sloping rivers. Based on the observed inundation extent, both models performed well at a straight river zone, but gave a low performance at the bends and the islands zones. In regards to the statistical evaluation, the inundation area simulated in TELEMAC-MASCARET provides a lower RMSE than that simulated in the HEC-RAS, Even though HEC-RAS performed well at the islands zones; which indicates the models could satisfactorily handle the influence of tidal force in hydrodynamic computations.

The HEC-RAS modeling for the steep river estimated a gapped inundation extent. The result shows that a discrete inundation extent was formed at points where a bed slope gradient abruptly changed, and numerical instability occurred at a location where the river slope was higher than thirteen percent. Similarly, the TELEMAC-MASCARET with finite element application on steep river simulated a gapped water cover extent. However, an application of the finite volume method in TELEMAC-MASCARET performed well.

An application of the LiDAR-based digital surface model in HEC-RAS 2D and TELEMAC -2D show that the DSM obtained from the Norwegian authority, https://hoydedata.no/LaserInnsyn/, was insufficient to generate proper flow parameters and was unable to generate a continuous inundation extent. In addition, this paper identifies that inaccuracy in DSM topographic data leads a model to estimate a fake flow blockage and fake deep-water level.

For the mildly sloping river, both models are in good agreement when estimating water depth and velocity. Minor differences were calculated at the island zones. In general, HEC-RAS estimated slight lower water depth and slightly higher velocity compared to the water depth and velocity calculated in TELEMAC-MASCARET for the same roughness and flow event. With regards to the steep river, both models calculated water depth with minor difference. An application of finite

element and finite volume methods in TELEMAC-MASCARET calculated mostly the same water depth.

Comparing with HEC-RAS, the application of the finite volume method in TELEMAC-MASCARET requires a longer simulation time, and TELEMAC-MASCARET modeling by applying the finite element method takes the shortest simulation time. Furthermore, HEC-RAS is a well-organized model and easy to use. In contrast, TELEMAC-MASCARET is a non-graphical user interface (GUI) that a user must control computational configuration by themselves.

9. RECOMMONDATION AND FUTURE WORKS

Suggestions for future studies of Surna river:

- In this study, hydraulic modeling was performed without calibration. Therefore, a future study must include calibration and validation.
- The performance of both models was evaluated based on the single roughness coefficient for all river sections that practical not correct. Future studies must apply different roughness coefficient throughout the river section.
- Suitability of both models was evaluated based on a single flow rate, and future study must flood plain hydraulics.
- In addition to comparing simulated and observed inundation extent, simulated water depth and flow velocity calculate in both models must include in the future study.
- 3-D analysis have to carried out to analysis an influence of river bend in hydraulic modeling.

In addition to suggestion given in Surna river modeling, following recommendations were labeled form the Vekveselva river modeling.

- This study recognizes that a topographic data obtained form https://hoydedata.no/LaserInnsyn/, namely Trøndelag del2 3pkt 2014, is not ready for hydraulic modeling and future study must look for the way that features on river surface can be removed from topographic data.
- Future studies for the Vekveselva river modeling must consider geomorphology, deposition and transportation of sediments.
- This study was performed based small discharge. However, Vekvselva river, which subject to flooding, must run the models with big discharges.

Moreover, the following suggestions were recommended from HEC-RAS and TELEMAC-MASCARET.

- TELEMAC-MASCARET V8P0 version has a limitation during compute supercritical flow, and owners should allow it.
- It is not possible to direct extract reliable inundation extent form TELEMAC-MASCARET, a program coder should include inundation extent in outputs.

- A programmer of BLUEKENUE should allow channel mesh tool which possibly allow a user for refining meshes.
- This study recognize that HEC-RAS is instability for high slope river modeling. Therefore, HEC-RAS programmer must allow the model for steep river modeling.

REFRERENCE

Abdullah, A. F., Vojinovic, Z., Price, R. K., & Aziz, N. A. A. (2012). A methodology for processing raw LiDAR data to support urban flood modelling framework. *Journal of Hydroinformatics*, *14*(1), 75–92. https://doi.org/10.2166/hydro.2011.089

Aberle, J., & Smart, G. M. (2003). L'influence de la structure de rugosité sur la résistance à des écoulements en fortes pentes. *Journal of Hydraulic Research*, *41*(3), 259–269. https://doi.org/10.1080/00221680309499971

Alcrudo, F. (2002). A state of the art review on mathematical modelling of flood propagation. *EC Contract EVG1-CT-2001-00037 IMPACT Investigation of Extreme Flood Processes and Uncertainty: Proceedings of the First IMPACT Project Workshop, Wallingford, UK, May 2002 (CD-ROM)*, 1–22. http://www.impact-project.net/cd/papers/print/008_pr_02-05-16_IMPACT_Alcrudo.pdf

Alfredsen, K., & Lidar, G. (n.d.). *LiDAR and use of drones LiDAR and Drone mapping*.

Amadio, M., Rita Scorzini, A., Carisi, F., Essenfelder, H. A., Domeneghetti, A., Mysiak, J., & Castellarin, A. (2019). Testing empirical and synthetic flood damage models: The case of Italy. *Natural Hazards and Earth System Sciences*, *19*(3), 661–678. https://doi.org/10.5194/nhess-19-661-2019

Anonnser.nu. (n.d.). *Surna*. http://www.laxfiske.nu/fiske/fishing?location=/norway/more_romsdal/surna&locale.cmd=change&newlocale=en_UK

Arc Map. (2020). *What is a LAS dataset?* https://desktop.arcgis.com/en/arcmap/10.3/manage-data/las-dataset/what-is-a-las-dataset-.htm.

AS, H. & S. (n.d.). *Sedimenteringsdam Vekveselva*. https://hoelogsonner.no/prosjekt/sedimenteringsdam-vekveselva/

Ata, R. (2018). *Telemac2d*.

Bates, P. D., Horritt, M. S., Smith, C. N., & Mason, D. (1997). Integrating remote sensing observations of flood hydrology and hydraulic modelling. *Hydrological Processes*, *11*(14),

1777–1795. https://doi.org/10.1002/(sici)1099-1085(199711)11:14<1777::aid-hyp543>3.0.co;2-e

Bhandari, M., Nyaupane, N., Mote, S. R., Kalra, A., & Ahmad, S. (2017). Various hydraulic models have developed globally to estimate flood events to enhance decision-making, damage protection, and mitigation measurement (49). Some models can perform for 1-D,2-D, and 3-D hydraulic analysis. Some of them can only- compute for 1. *World Environmental and Water Resources Congress 2017: Hydraulics and Waterways and Water Distribution Systems Analysis - Selected Papers from the World Environmental and Water Resources Congress 2017*, 292–303. https://doi.org/10.1061/9780784480625.027

Bodoque, J. M., Guardiola-Albert, C., Aroca-Jiménez, E., Eguibar, M. Á., & Martínez-Chenoll, M. L. (2016). Flood damage analysis: First floor elevation uncertainty resulting from LiDAR-derived digital surface models. *Remote Sensing*, *8*(7). https://doi.org/10.3390/rs8070604

Brunner, G., & Bonner, V. (2010). *HEC River Analysis System (HEC-RAS) Version 4.1 January 2010*. *January*, 411. http://oai.dtic.mil/oai/oai?verb=getRecord&metadataPrefix=html&identifier=ADA289522

Brunner, G. W. (2008). Calibration of Unsteady Flow Models. *L-10 (188-04)/May-2008*, *10*(May), 1–42. http://www.nws.noaa.gov/oh/hrl/modelcalibration/6. Hydraulic Model Calibration/3.4 L-10 Calibration.pdf

Brunner, G. W. (2016). *HEC-RAS River Analysis System, 2D Modeling User's Manual Version 5.0. CPD-68A*, 1–171. www.hec.usace.army.mil

Brunner, G. W., & CEIWR-HEC. (2016). *HEC-RAS River Analysis System User's Manual. US Army Corps of Engineers–Hydrologic Engineering Center*. *January*, 1–790. https://www.hec.usace.army.mil/software/hec-ras/documentation/HEC-RAS 5.0 Users Manual.pdf

Casas, A., Benito, G., Thorndycraft, V. R., & Rico, M. (2006). The topographic data source of digital terrain models as a key element in the accuracy of hydraulic flood modelling. *Earth Surface Processes and Landforms*, *31*(4), 444–456. https://doi.org/10.1002/esp.1278

CFD. (2019). *Finite Element vs Finite Volume*. AutoDesk.Help. https://knowledge.autodesk.com/support/cfd/learn-explore/caas/CloudHelp/cloudhelp/2014/ENU/SimCFD/files/GUID-12A9AED8-2047-4D3A-BC80-82BE9CF47517-htm.html#:~:text=The main advantage as well,not so with finite elements.

Chow, V. Te. (1959). Open-Channel Hydraulics McGraw-Hill Book Company. *New York*, 507–510.

Cone, J. (1998). Principles of Geographical Information Systems by Peter A. *New Zealand Geographer*, *54*(2), 56–57. https://doi.org/10.1111/j.1745-7939.1998.tb02089.x

Cooper, M. (2010). Advanced Bash-Scripting Guide An in-depth exploration of the art of shell scripting Table of Contents. *Okt 2005 Abrufbar Uber Httpwww Tldp OrgLDPabsabsguide Pdf Zugriff 1112 2005*, *2274*(November 2008), 2267–2274. https://doi.org/10.1002/hyp

Dusty Robinson, P. (2018). *Benefits of 2D Modeling for River Hydraulics*. https://www.ayresassociates.com/benefits-of-2d-modeling-for-river-hydraulics/

Edf. (2000). *TELEMAC-2D validation document v5.0*. *July*.

Engvik, T. (2011). *Bunntransport i Vekveselva*. 72.

Ettritch, G., Hardy, A., Bojang, L., Cross, D., Bunting, P., & Brewer, P. (2018). Enhancing digital elevation models for hydraulic modelling using flood frequency detection. *Remote Sensing of Environment*, *217*(August), 506–522. https://doi.org/10.1016/j.rse.2018.08.029

Geography, G. (n.d.). *DEM, DSM & DTM Differences – A Look at Elevation Models in GIS*. https://gisgeography.com/dem-dsm-dtm-differences/

Hicks, F. E., & Peacock, T. (2005). Suitability of HEC-RAS for Flood Forecasting. *Canadian Water Resources Journal*, *30*(2), 159–174. https://doi.org/10.4296/cwrj3002159

Hirabayashi, Y., Mahendran, R., Koirala, S., Konoshima, L., Yamazaki, D., Watanabe, S., Kim, H., & Kanae, S. (2013). Global flood risk under climate change. *Nature Climate Change*, *3*(9), 816–821. https://doi.org/10.1038/nclimate1911

Hirt, C. (2016). *Encyclopedia of Geodesy*. *June 2016*, 0–6. https://doi.org/10.1007/978-3-319-

02370-0

Horritt, M. S., & Bates, P. D. (2001). Predicting floodplain inundation: Raster-based modelling versus the finite-element approach. *Hydrological Processes*, *15*(5), 825–842. https://doi.org/10.1002/hyp.188

Hoydedata.no. (n.d.). https://hoydedata.no/LaserInnsyn

Julzarika, A., & Harintaka. (2019). DEM, which is widely used for hydrodynamic modeling, is removing existing objects on earth surface. In other words, DEM has equivalent meaning with a representation of 3D spatial value on bare earth (43). Indeed, these objects can control flood parameters. *International Archives of the Photogrammetry, Remote Sensing and Spatial Information Sciences - ISPRS Archives*, *42*(4/W16), 319–325. https://doi.org/10.5194/isprs-archives-XLII-4-W16-319-2019

Kayyun, T. S., & Dagher, D. H. (2018). Potential Sediment within a Reach in Tigris River. *International Journal of Hydraulic Engineering*, *7*(2), 22–32. https://doi.org/10.5923/j.ijhe.20180702.02

Kivva, S., Zheleznyak, M., Pylypenko, O., & Yoschenko, V. (2020). Open Water Flow in a Wet/Dry Multiply-Connected Channel Network: A Robust Numerical Modeling Algorithm. *Pure and Applied Geophysics*, *177*, 3421–3458. https://doi.org/10.1007/s00024-020-02416-0

LAS Point Cloud Format. (n.d.). https://www.usna.edu/Users/oceano/pguth/md_help/html/las_format.htm

las2las. (n.d.). https://rapidlasso.com/lastools/las2las/

Lee, J. S., Lee, S. O., Gray, D. D., & Hong, S. H. (2019). Visualization of Specific Energy for Open Channel Flow in Three Dimensions. *KSCE Journal of Civil Engineering*, *23*, 2541–2549. https://doi.org/10.1007/s12205-019-2171-y

Lidar vs Radar. (n.d.). https://www.thedrive.com/article/16916/lidar-vs-radar-pros-and-cons-of-different-autonomous-driving-technologies

Manual, R. (2010). Blue Kenue. *Organization*, *August*.

Matthew Hickox, P. (2019). *What is Computational Fluid Dynamics/3D Hydraulic Modeling?* Ayres. https://www.ayresassociates.com/what-is-computational-fluid-dynamics-3d-hydraulic-modeling/

Meneses, N. C., Baier, S., Geist, J., & Schneider, T. (2017). Evaluation of green-LiDAR data for mapping extent, density and height of aquatic reed beds at Lake Chiemsee, Bavaria-Germany. *Remote Sensing*, *9*(12). https://doi.org/10.3390/rs9121308

Merwade, V. (2009). *Effect of Topographic Data, Geometric Configuration and Modeling Approach on Flood Inundation Mapping*. 223009379_Effect_of_Topographic_Data_Geometric_Configuration_and_Modeling_Approach_on_Flood_Inundation_Mapping

Mino, T., Tanaka, Y., Sakamoto, M., & Fujita, T. (2006). Development of praline derived chiral aminophosphine ligands for palladium -catalyzed asymmetric allylic alkylation. *Yuki Gosei Kagaku Kyokaishi/Journal of Synthetic Organic Chemistry*, *64*(6), 628–638. https://doi.org/10.5059/yukigoseikyokaishi.64.628

Molinari, D., De Bruijn, K. M., Castillo-Rodríguez, J. T., Aronica, G. T., & Bouwer, L. M. (2019). Validation of flood risk models: Current practice and possible improvements. *International Journal of Disaster Risk Reduction*, *33*(November), 441–448. https://doi.org/10.1016/j.ijdrr.2018.10.022

Molinari, D., Scorzini, A. R., Arrighi, C., Carisi, F., Castelli, F., Domeneghetti, A., Gallazzi, A., Galliani, M., Grelot, F., Kellermann, P., Kreibich, H., Mohor, G., Mosimann, M., Natho, S., Richert, C., Schroeter, K., Thieken, A., Zischg, A. P., & Ballio, F. (2020). Flood inundation modelling: A review of methods, recent advances and uncertainty analysis. *Natural Hazards and Earth System Sciences*, *February*, 1–32. https://doi.org/10.5194/nhess-2020-40

Morgan, A., Olivier, D., Nathalie, B., Claire-Marie, D., & Philippe, G. (2016). High-resolution Modelling with Bi-dimensional Shallow Water Equations Based Codes - High-Resolution Topographic Data Use for Flood Hazard Assessment over Urban and Industrial Environments. *Procedia Engineering*, *154*, 853–860. https://doi.org/10.1016/j.proeng.2016.07.453

Neachell, E. (2014). Book Review - Environmental flows: Saving rivers in the thrid millennium. *River Research and Applications*, *30*(January), 132–133. https://doi.org/10.1002/rra

Olivier, M., Sébastien, E., Pierre, A., Benjamin, D., & Michel, P. (n.d.). Bottom friction formulations for free surface flow modeling. *Recherche*.

Pinos, J., & Timbe, L. (2019). Performance assessment of two-dimensional hydraulic models for generation of flood inundation maps in mountain river basins. *Water Science and Engineering*, *12*(1), 11–18. https://doi.org/10.1016/j.wse.2019.03.001

Pinos, J., Timbe, L., & Timbe, E. (2019). Evaluation of 1D hydraulic models for the simulation of mountain fluvial floods: A case study of the santa bárbara river in Ecuador. *Water Practice and Technology*, *14*(2), 341–354. https://doi.org/10.2166/wpt.2019.018

Podhorányi, M., Unucka, J., Bobál', P., & Říhová, V. (2013). Effects of LIDAR DEM resolution in hydrodynamic modelling: Model sensitivity for cross-sections. *International Journal of Digital Earth*, *6*(1), 3–27. https://doi.org/10.1080/17538947.2011.596578

Populus, J. (2019). *Use of Lidar for coastal habitat mapping*. http://www.coastalwiki.org/wiki/Use_of_Lidar_for_coastal_habitat_mapping

Prodanovic, P. (2015). QGIS as a pre-and post-processor for TELEMAC: mesh generation and output visualization. *Proceedings of the XXII TELEMAC-MASCARET Technical User Conference October 15-16, 2030, October 2015*, 83–90.

Rahman, a, Zulkarnain, M., & Dinand, a. (2006). Digital surface model (DSM) construction and flood hazard simulation for Development Plans in Naga City, Philippines. *GIS Development*, 1–15. http://eprints.utm.my/1078/

Rickenmann, D., & Recking, A. (2011). Evaluation of flow resistance in gravel-bed rivers through a large field data set. *Water Resources Research*, *47*(7). https://doi.org/10.1029/2010WR009793

Rosgen, D. L. (1994). C A T E N A A classification of natural rivers. *Catena*, *22*, 169–199. https://wildlandhydrology.com/resources/docs/Stream Classification/Rosgen_1994_A_Classification_of_Natural_Rivers.pdf

Saurabh Singh. (2013). *Confused Between DEM, DTM and DSM*. http://www.gisresources.com/confused-dem-dtm-dsm/

Sauvaget, P., David, E., Demmerle, D., & Lefort, P. (2000). Optimum design of large flood relief culverts under the A89 motorway in the Dordogne-Isle confluence plain. *Hydrological Processes*, *14*(13), 2311–2329. https://doi.org/10.1002/1099-1085(200009)14:13<2311::AID-HYP31>3.0.CO;2-F

Selméus, L. (2018). *Dynamic modelling of bathing water quality with biodegradation of Escherichia coli in TELEMAC-3D*.

Seyoum, S. D., Vojinovic, Z., Price, R. K., & Weesakul, S. (2012). Coupled 1D and Noninertia 2D Flood Inundation Model for Simulation of Urban Flooding. *Journal of Hydraulic Engineering*, *138*(1), 23–34. https://doi.org/10.1061/(ASCE)HY.1943-7900.0000485

ShahiriParsa, A., Noori, M., Heydari, M., & Rashidi, M. (2016). Floodplain zoning simulation by using HEC-RAS and CCHE2D models in the Sungai Maka river. *Air, Soil and Water Research*, *9*, 55–62. https://doi.org/10.4137/ASWR.S36089

Shamkhi, M. S., & Attab, Z. S. (2018). EKnowing proper roughness coefficient values is the challenge and challenging thing in the flow computation natural river (59). Many researchers have been found in various formulas for estimating flow-resistance, but no one gets a standard equation (59). . *Wasit Journal of Engineering Sciences*, *6*(3), 90–97. https://doi.org/10.31185/ejuow.vol6.iss3.107

Sturm, C., Zhang, Q., & Noone, D. (2010). An introduction to stable water isotopes in climate models: Benefits of forward proxy modelling for paleoclimatology. *Climate of the Past*, *6*(1), 115–129. https://doi.org/10.5194/cp-6-115-2010

Sulebakk, V. (2017). *Identification and analysis of step-pool morphometry*. *May*, 90. http://hdl.handle.net/11250/2506125

Tamiru, A., & Rientjes, T. H. M. (2005). *Effects of Lidar Dem Resolution in Flood Modelling : a Model Sentitivity Study for the City of Tegucigalpa , Honduras*. *January 2005*, 168–173.

Telemac. (1999). *Mesh Interface*. *April*.

Teng, J., Jakeman, A. J., Vaze, J., Croke, B. F. W., Dutta, D., & Kim, S. (2017). Flood inundation modelling: A review of methods, recent advances and uncertainty analysis. *Environmental Modelling and Software*, *90*(April), 201–216. https://doi.org/10.1016/j.envsoft.2017.01.006

Theses, M., & Sharkey, J. K. (2014). *Trace: Tennessee Research and Creative Exchange Investigating Instabilities with HEC-RAS Unsteady Flow Modeling for Regulated Rivers at Low Flow Stages*. https://trace.tennessee.edu/utk_gradthes/3183

Usman, K. R. (2019). *Safe Rivers – Identification of critical locations along steep watercourses during flood events*. 119. http://hdl.handle.net/11250/2624540

Values, N. (n.d.). *2 The (Galerkin) Finite Element Method*. 31–80.

Vojinovic, Z., Seyoum, S. D., Mwalwaka, J. M., & Price, R. K. (2011). Effects of model schematisation, geometry and parameter values on urban flood modelling. *Water Science and Technology*, *63*(3), 462–467. https://doi.org/10.2166/wst.2011.244

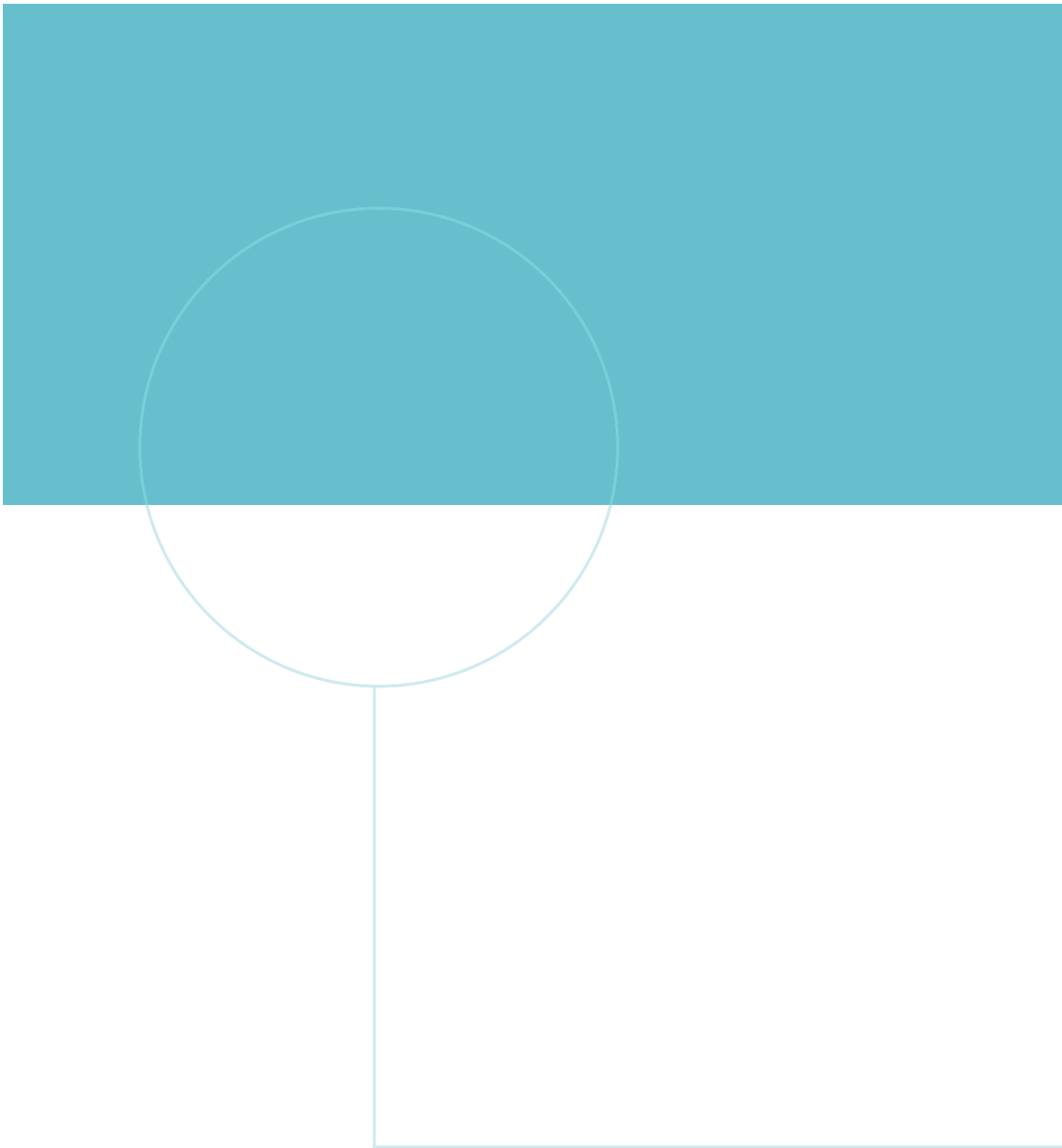

NTNU

Norwegian University of
Science and Technology